nature immunology

ARTICLES

https://doi.org/10.1038/s41590-022-01163-9

Check for updates

Mechanisms of innate and adaptive immunity to the Pfizer-BioNTech BNT162b2 vaccine

Chunfeng Li[1], Audrey Lee[1], Lilit Grigoryan[1], Prabhu S. Arunachalam[1], Madeleine K. D. Scott[1,2], Meera Trisal[1], Florian Wimmers[1], Mrinmoy Sanyal[3], Payton A. Weidenbacher[3], Yupeng Feng[1], Julia Z. Adamska[1], Erika Valore[1], Yanli Wang[1], Rohit Verma[1], Noah Reis[1], Diane Dunham[4], Ruth O'Hara[5], Helen Park[6], Wei Luo[7], Alexander D. Gitlin[8,9], Peter Kim[3,10], Purvesh Khatri[1,2], Kari C. Nadeau[4,11,12] and Bali Pulendran[1,9,13] ✉

Despite the success of the BNT162b2 mRNA vaccine, the immunological mechanisms that underlie its efficacy are poorly understood. Here we analyzed the innate and adaptive responses to BNT162b2 in mice, and show that immunization stimulated potent antibody and antigen-specific T cell responses, as well as strikingly enhanced innate responses after secondary immunization, which was concurrent with enhanced serum interferon (IFN)-γ levels 1 d following secondary immunization. Notably, we found that natural killer cells and CD8$^+$ T cells in the draining lymph nodes are the major producers of this circulating IFN-γ. Analysis of knockout mice revealed that induction of antibody and T cell responses to BNT162b2 was not dependent on signaling via Toll-like receptors 2, 3, 4, 5 and 7 nor inflammasome activation, nor the necroptosis or pyroptosis cell death pathways. Rather, the CD8$^+$ T cell response induced by BNT162b2 was dependent on type I interferon-dependent MDA5 signaling. These results provide insights into the molecular mechanisms by which the BNT162b2 vaccine stimulates immune responses.

The BNT162b2 mRNA vaccine developed by Pfizer and BioNTech is the first US Food and Drug Administration (FDA)-approved mRNA vaccine in history. The vaccine demonstrated 95% efficacy against symptomatic coronavirus disease 2019 (COVID-19) caused by severe acute respiratory syndrome coronavirus 2 (SARS-CoV-2) infection in a phase-III trial[1,2]. However, despite its widespread use, the mechanisms by which BNT162b2 stimulates protective immunity remain largely unknown. BNT162b2 comprises N^1-methyl-pseudouridine (m1Ψ) nucleoside-modified mRNA encapsulated in a lipid nanoparticle (LNP). Following administration in muscle, the mRNA is translated, resulting in the expression of the spike protein and spike-specific B and T cell responses[3]. Kariko et al. found that the m1Ψ-modification on RNA dampens the inflammatory response mediated by TLR3, TLR7 or RIG-I, and increases translational efficiency and biological stability[3,4]. mRNA vaccines encapsulated in LNPs were also found to induce a high magnitude of germinal center B (GC B) cell and follicular helper T cells (T_{FH}) responses after a single immunization[5–8].

Several studies have analyzed immune responses to the BNT162b2 vaccine in humans and revealed insights about the nature of the antibody and T cell responses to vaccination[1,2,9–13]. Despite our emerging understanding of immune responses to BNT162b2, there are major knowledge gaps on its mechanisms of action. For example, there is a paucity of understanding on the nature of the innate response to BNT162b2 and, in particular, how BNT162b2 is sensed by the host's innate immune system. Studies of mRNA vaccines against cancer demonstrate that they can trigger TLR4 (ref. [14]), TLR7 (ref. [15]) or STING[16] signaling pathways, but such knowledge is lacking in the context of BNT162b2. Arunachalam et al. used a systems vaccinology approach to analyze the innate and adaptive immune responses to vaccination with BNT162b2 in humans[9]. Our analysis demonstrated detectable neutralization antibody titers after primary immunization, which was enhanced considerably upon secondary immunization. Furthermore, there was only a modest innate immune response, at 1 or 7 d after primary immunization. Surprisingly however, secondary immunization with BNT162b2 induced a much higher magnitude of innate immune response than after primary vaccination[9]. This enhanced 'secondary innate response' was characterized by increased levels of IFN-γ in the plasma, enhanced transcriptional signatures of innate immunity and antiviral immunity in myeloid cells. However, the cellular sources of the rapidly produced IFN-γ and its role in the enhanced innate immune response after secondary vaccination remains unclear. Furthermore, although vaccination with BNT162b2 has been shown to induce substantial frequencies of antigen-specific CD8$^+$ T cell responses in the blood[9,17], there are currently no data on the nature of immune responses in tissues, as most studies have focused on analyzing immune responses in the blood. In addition, the in vivo distribution of the mRNA and the spike protein that it encodes, after intramuscular vaccination, remains poorly

[1]Institute for Immunity, Transplantation and Infection, Stanford University, Stanford, CA, USA. [2]Center for Biomedical Informatics, Department of Medicine, Stanford University School of Medicine, Stanford, CA, USA. [3]Department of Biochemistry & Stanford, ChEM-H, Stanford University, Stanford, CA, USA. [4]Sean N. Parker Center for Allergy & Asthma Research, Stanford, CA, USA. [5]Department of Psychiatry and Behavioral Sciences, Stanford University School of Medicine, Palo Alto, CA, USA. [6]Veterans Affairs Palo Alto Health Care System, Palo Alto, CA, USA. [7]Department of Microbiology and Immunology, Indiana University School of Medicine, Indianapolis, IN, USA. [8]Department of Physiological Chemistry, Genentech, South San Francisco, CA, USA. [9]Department of Pathology, Stanford University School of Medicine, Stanford, CA, USA. [10]Chan Zuckerberg Biohub, San Francisco, CA, USA. [11]Howard Hughes Medical Institute, Stanford University, Stanford, CA, USA. [12]Department of Medicine, Division of Pulmonary, Allergy and Critical Care Medicine, Stanford, CA, USA. [13]Department of Microbiology and Immunology, Stanford University School of Medicine, Stanford, CA, USA. ✉e-mail: bpulend@stanford.edu

understood. To address these knowledge gaps, we performed a detailed analysis of innate and adaptive immune responses to BNT162b2 vaccination in mice. In particular, we analyzed (1) the adaptive immune response induced by BNT162b2 after both primary and booster vaccines in organs including the lung and spleen; (2) the innate immune response in draining lymph nodes (dLNs), non-draining lymph nodes and other organs at the single-cell level, using systems immunology approaches; and (3) the innate sensing mechanisms that regulate antigen-specific antibody and T cell responses to BNT162b2 vaccination.

Results

BNT162b2 immunization stimulates robust germinal center responses. To evaluate immune responses to BNT162b2, we immunized C57BL/6 mice on days 0 and 21 with 5 µg BNT162b2 by intramuscular injection (Fig. 1a). Anti-spike binding IgG responses, comprising both IgG1 and IgG2c, increased significantly at 14 d after primary immunization and persisted until day 21, while the secondary immunization increased the response more than tenfold (Fig. 1b). Consistent with binding antibody responses, neutralizing antibody responses against the SARS-CoV-2 wild-type (WT) strain and variants of concern including B1.1.7 (alpha), B.1.351 (beta), P.1 (gamma), B.1.617.2 (delta) and B.1.429 (epsilon) were detected on day 21 and increased significantly following secondary immunization (Fig. 1c). While the neutralizing titers against the alpha and epsilon variants did not differ significantly from those of the WT strain, neutralizing antibody titers at day 42 against the beta, gamma and delta variants were lower by 4.2-fold, 2.5-fold and 3.9-fold, respectively relative to the titers against the WT strain (Fig. 1c), consistent with findings in humans[18]. In addition to serological responses, we examined the responses of GC B cells ($CD19^+CD38^-CD95^+$) and T_{FH} cells ($CD3^+CD4^+PD1^+CXCR5^+$) as well as plasma cells ($CD44^+CD138^+$). BNT162b2 immunization induced a strikingly high magnitude of GC B cells, T_{FH} cells and plasma cells in dLNs, which peaked on day 7 and decreased by day 21 (Fig. 1d–f). Collectively, these data demonstrate the potent stimulation of humoral immune responses by BNT162b2. In addition, we tested antibody responses in mice immunized with 0.2 µg of the vaccine, which is an equivalent dose to that used in humans based on body weight[19,20]. The antibody kinetics mirrored the response induced by the higher dose, but the magnitude was approximately tenfold lower (Extended Data Fig. 1a).

T cell response induced by BNT162b2 vaccination. Next, we measured antigen-specific T cell responses in spleen and lung on days 21 and 42 after vaccination following the prime-boost immunization strategy presented in Fig. 1a. While the primary immunization elicited detectable antigen-specific $CD4^+$ and $CD8^+$ T cell responses in both tissues consistent with previous reports[8,21], there was a striking increase in the frequency of antigen-specific $CD8^+$ T cells after secondary immunization, especially in the lung, where we observed a median of 10% MHC-I tetramer-positive $CD8^+$ T cells on day 42 (Fig. 2a). There was a robust induction of spike-specific $CD8^+$ T cells secreting IFN-γ, tumor necrosis factor (TNF) and interleukin (IL)-2 following in vitro stimulation with an overlapping peptide pool (Fig. 2b). The $CD4^+$ T cell responses were primarily of the T_H1 type with little induction of IL-4 response (Fig. 2c), consistent with previous reports[8,21]. As tissue-resident memory T cells (TRMs) play an essential role in preventing local infection[22,23], we measured TRM ($CD3^+CD8^+CD44^+CD69^+CD103^+$) levels in the lung at day 21 and day 42 after BNT162b2 immunization and found that BNT162b2 immunization did not induce TRMs in the lung (Fig. 2d), consistent with previous findings[24]. The low dose (0.2 µg) of immunization resulted in ~fivefold lower magnitude of T cell responses (Extended Data Fig. 1b–d).

BNT162b2 induces robust innate immune responses. To profile the innate immune response induced by BNT162b2, we first analyzed the dLNs by multiparametric flow cytometry (Extended Data Fig. 2a). Frequencies of monocytes ($CD11b^+Ly6C^{hi}$), plasmacytoid DCs (pDCs; $CD11c^{lo}PDCA1^+$) and $CD103^+$ migratory DCs (mDCs) increased significantly on day 1 and returned to baseline levels on day 7 (Extended Data Fig. 2b). In contrast, resident DCs (rDCs; both $CD8a^+$ and $CD11b^+$) decreased in frequency on day 1 but increased significantly on day 7 (Extended Data Fig. 2b). Further, multiple innate immune cells including monocytes, macrophages ($CD11b^+Ly6C^{lo}F4/80^+$), pDCs and DC subsets ($CD8a^+$ rDCs, $CD11b^+$ rDCs, $CD103^+$mDCs and $CD11b^+$mDCs) were highly activated, as indicated by the enhanced expression of the activation marker CD86 (Fig. 3a). The low dose (0.2 µg) of immunization induced lower levels of innate cell activation (Extended Data Fig. 1e). These innate cell types remained activated until day 3 after immunization (Fig. 3b). In comparison, the innate cells were moderately activated in the contralateral lymph nodes (non-dLNs), lung and spleen (Fig. 3c,d).

Next, we analyzed serum cytokine responses using a Luminex assay. BNT162b2 immunization induced the release of many cytokines, including MCP1, MIP1b, IL-6 and CXCL10, as well as IFN-γ, that peaked at 6 h after immunization (Fig. 3e) in contrast to the significantly elevated levels of only two cytokines/chemokines (IFN-γ and CXCL10) in human volunteers after receiving the same vaccine[9]. It should, however, be noted that in the study in humans, Arunachalam et al. only measured plasma cytokine levels at 1 and 7 d after vaccination, and not at the earlier time point of 6 h examined in the current mouse study[9]. All the cytokines, except IFN-γ, returned to normal levels at day 3 after immunization. Strikingly, there was a significant induction of IFN-α (IFN-α2 and IFN-α4) in mice at 6 h, which was not observed in humans at the 1-d time point we examined[9]. Of note, the lower dose (0.2 µg) of immunization did not induce IFN-α as seen in humans; however, there was also an absence of IFN-γ response (Extended Data Fig. 1f), suggesting that there was not a human equivalent dose of BNT162b2 in mice.

Single-cell transcriptomics of innate immunity to BNT162b2. To further understand the cellular and molecular mechanisms involved in the immunogenicity of BNT162b2, we performed single-cell transcriptional profiling of cells in the dLNs 1, 3 and 7 d after immunization (Fig. 4a). As a benchmark, we compared the responses to BNT162b2 with those of the live attenuated yellow fever vaccine YF-17D, one of the most effective vaccines ever developed in humans[25]. Our previous work showed that YF-17D activates multiple subsets of DCs via several different Toll-like receptors (TLRs) to stimulate potent adaptive immune responses[26,27]. We used an 'enrich-mix' strategy in which $CD11b^+$ myeloid cells, pDCs ($CD11b^-CD11c^{lo}PDCA\text{-}1^+$) and DCs ($CD11c^+MHC\text{-}II^+$) were enriched by cell sorting and then mixed with total cell suspension at a ratio of 1:1 (Fig. 4a). The resulting cell suspension was subjected to droplet-based single-cell gene expression profiling. After quality control, we obtained 52,788 high-quality transcriptomes (Fig. 4b). Using dimensionality reduction via uniform manifold approximation and projection (UMAP) and graph-based clustering, we identified 20 cell clusters containing all major innate and adaptive immune cell types (Fig. 4b and Extended Data Fig. 3a). First, we analyzed the number of differentially expressed genes (DEGs) within each cluster. The YF-17D vaccine stimulated a profound DEG response in multiple cell types, as seen in previous study[28], which peaked at day 1 and returned to baseline by day 7. Interestingly, the mRNA vaccine stimulated a larger number of DEGs, especially in monocyte/macrophage, DCs and natural killer (NK) cells on day 1 that persisted until day 7 (Fig. 4c). Gene-set enrichment analysis using blood transcriptional modules (BTMs) revealed activation of type I interferon and antiviral responses in multiple cell types, which

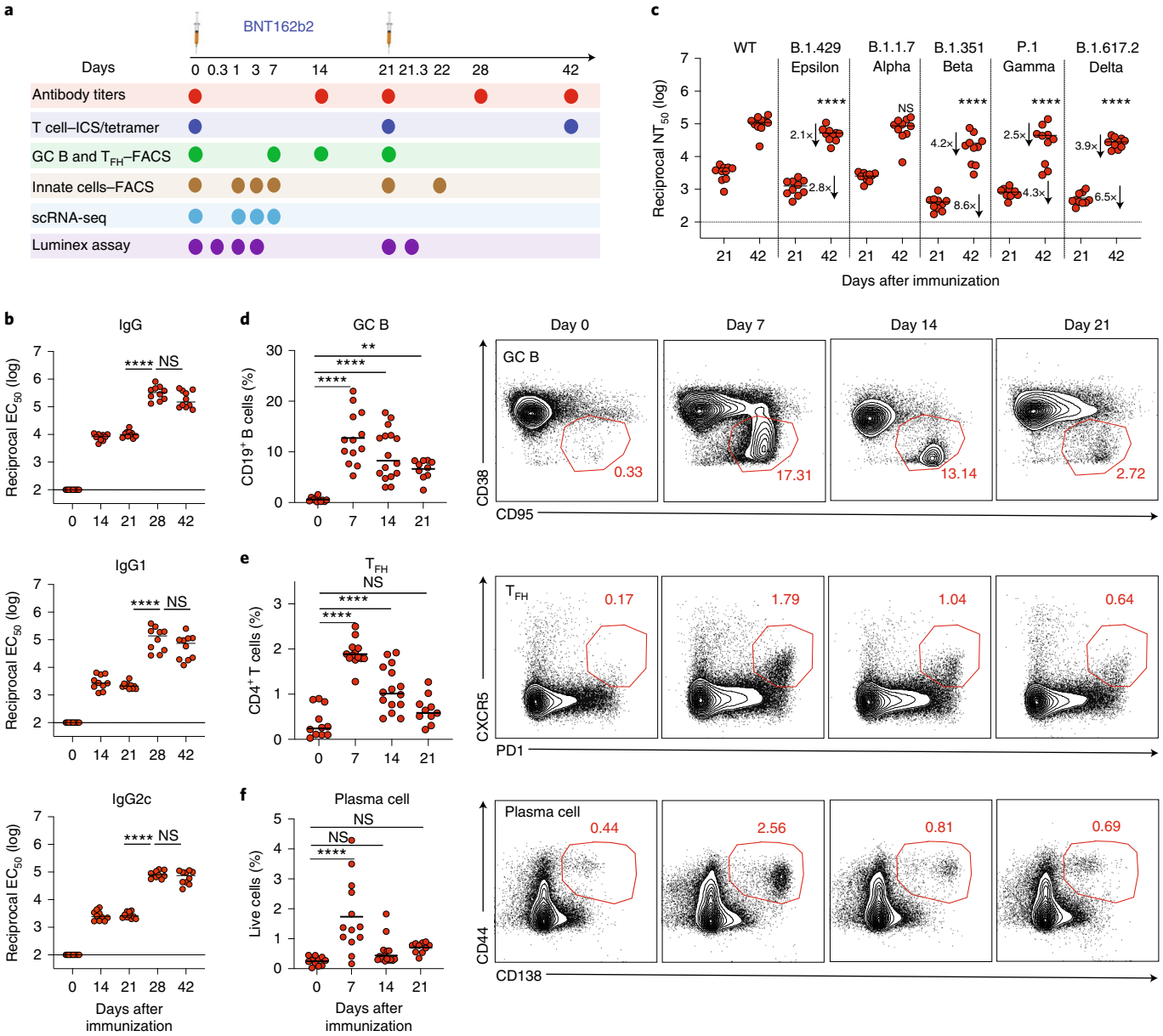


Fig. 1 | BNT162b2 vaccine induces robust germinal center B cell and T_{FH} cell response in mice. a, Experimental timeline and tests. FACS, fluorescence-activated cell sorting; ICS, intracellular cytokine staining. **b**, Serum anti-spike IgG, IgG1a and IgG2c binding titers (EC_{50}) detected by ELISA. **c**, Pseudotyped lentivirus neutralization antibody titers (NT_{50}) against SARS-CoV-2 WT and variants of concern (B.1.429, B.1.1.7, B.1.351, P.1 and B.1.617.2) measured at days 21 and 42. $n=10$ mice per time point in **b** and **c**. **d**–**f**, GC B cell (**d**), T_{FH} cell (**e**) and plasma cell (**f**) responses after BNT162b2 immunization. $n=11$, 13, 16 and 10 for days 0, 7, 14 and 21, respectively. Data were combined from two or more independent experiments. One-way analysis of variance (ANOVA) followed by Tukey's test was applied in **b**–**f**. $^{*}P<0.05$, $^{**}P<0.01$, $^{***}P<0.001$, $^{****}P<0.0001$. Differences between groups were considered significant for P values < 0.05. NS, not significant.

peaked at day 1 and returned to baseline levels by day 7 (Fig. 4d). In contrast, cell cycle-associated genes and transcription-associated genes increased at day 1 and persisted to day 7, especially in NK cells and T cells (Fig. 4d). The overall responses were comparable to those of the YF-17D immunization (Extended Data Fig. 3b,c).

Arunachalam et al. demonstrated that the BNT162b2 vaccination in humans results in an enhanced innate immune response following the secondary vaccination in comparison with the primary vaccination[9]. A crucial aspect of that study was the discovery of an innate cell cluster (C8) using single-cell transcriptional profiling that emerged 1 d after secondary vaccination, a ~100-fold increase in comparison to the first day after primary vaccination. We determined that these cells were a transcriptional counterpart of an epigenetically programmed monocyte population that Wimmers et al. described in humans vaccinated with the H5N1 avian influenza subunit vaccine adjuvated with AS03 (H5N1 + AS03) (ref. [29]). The core transcriptional signature of these cells was an increased expression of interferon-stimulated genes (ISGs; *ISG15*, *GBP1*, *IFITM3*, *IFIH1*, *ANKRD22*, *IFI35*, *MX1*, *IRF1*, *IRF7*, *IRF8* and *STAT1*) and decreased expression of AP-1 transcription factors encoded by *FOS* and *JUN*[9,29]. Therefore, we asked if a similar cell population would also emerge in response to mRNA vaccination in mice. We re-embedded C2_mono_macrophage (a cluster containing a mix of monocyte and macrophage populations) and C15_macrophage

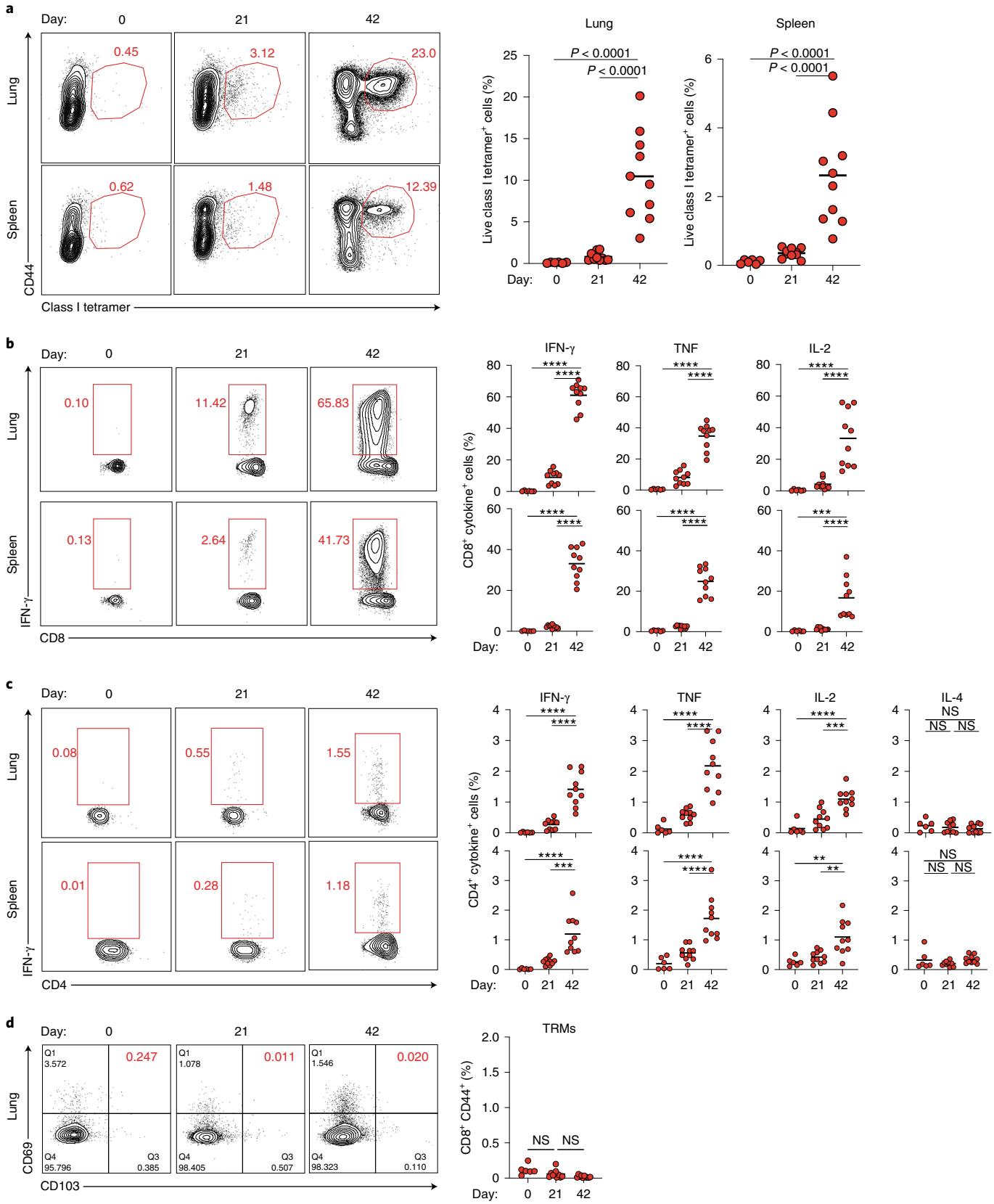


Fig. 2 | T cell response induced by BNT162b2 vaccination in mice. a, Class I tetramer-specific CD8+ T cell responses in lung and spleen at days 21 and 42 after BNT162b2 immunization. **b**,**c**, Antigen-specific CD8+ (**b**) and CD4+ (**c**) T cell responses in lung and spleen at days 21 and 42 as measured by ICS assay. **d**, TRMs in lung at days 21 and 42. Data were combined from two independent experiments. One-way ANOVA followed by Tukey's test was applied in **a**–**d**. $n = 6$ for day 0, and $n = 10$ for day 21 and day 42. $^{*}P < 0.05$, $^{**}P < 0.01$, $^{***}P < 0.001$, $^{****}P < 0.0001$.

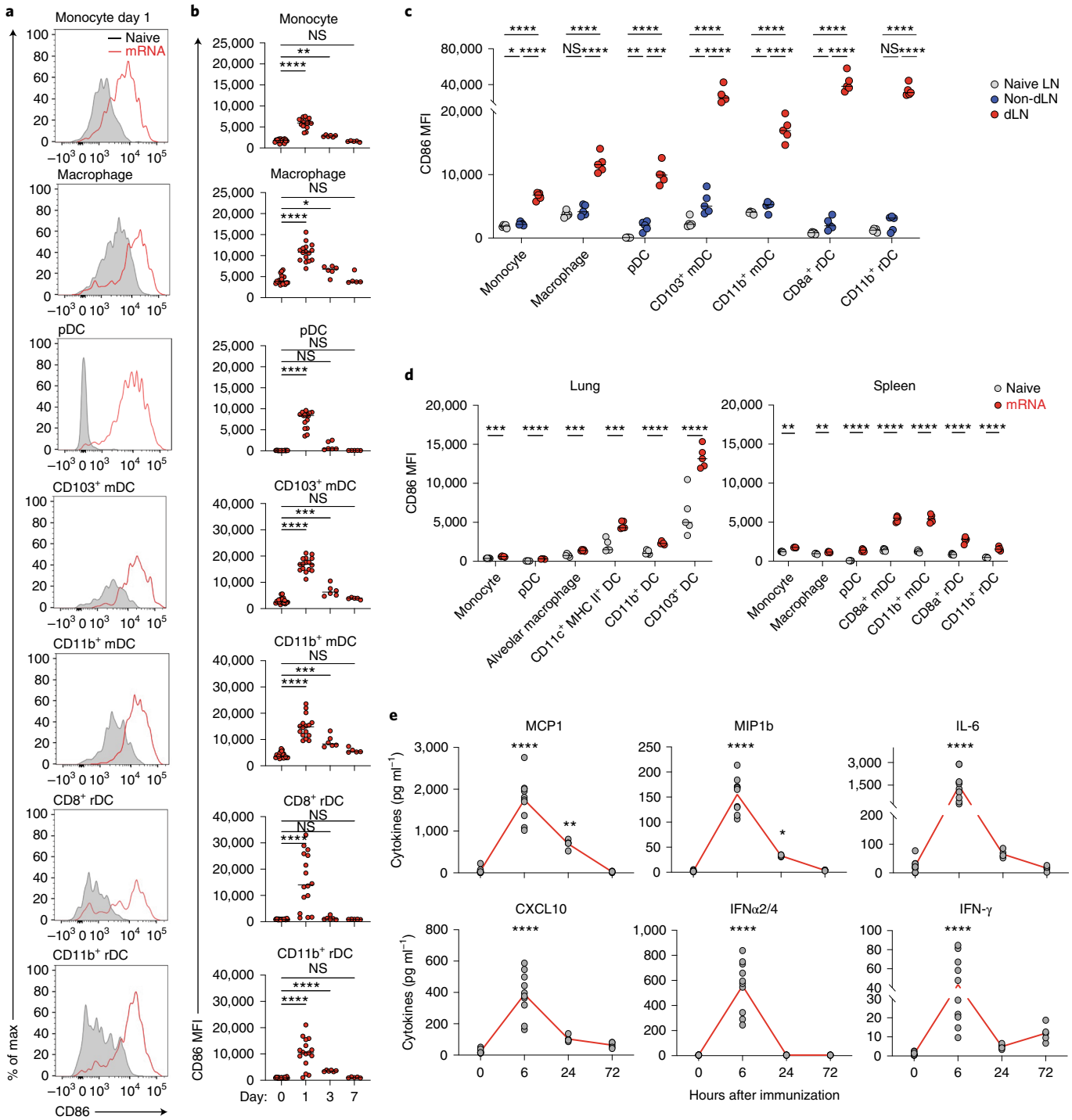


Fig. 3 | BNT162b2 induces robust innate immune response in draining lymph nodes. a, Activation of innate cells at day 1 after BNT162b2 immunization in dLNs indicated by activation marker CD86. **b**, Dynamics of innate cell activation at days 1, 3 and 7 after BNT162b2 immunization. $n = 20$, 16, 7 and 5 for days 0, 1, 3 and 7, respectively. **c**,**d**, Innate cell activation in contralateral lymph nodes (non-dLN) compared to that in dLNs (**c**), and in lung and spleen (**d**) at day 1 after prime. $n = 5$ for each group. **e**, Dynamics of cytokines in serum at 0, 6, 24 and 72 h after BNT162b2 immunization. $n = 10$ for 0 and 6 h; $n = 5$ for 24 h and 72 h. Data were combined from at least two independent experiments (**a**, **b** and **e**) or one representative of two independent experiments (**c** and **d**). One-way ANOVA followed by Tukey's test was applied in **b**–**e**. $^{*}P < 0.05$, $^{**}P < 0.01$, $^{***}P < 0.001$, $^{****}P < 0.0001$. MFI, mean fluorescence intensity.

clusters using genes that characterized the epigenetically remodeled monocyte population enriched in humans 21 d after vaccination with two doses of H5N1/AS03 (ref. [29]). Principal components were calculated from the 2,000 most variable genes within the cells originally part of macrophage clusters C2 and C15. Applying Louvain community detection to the nearest-neighbor graph structure derived from principal-component analysis embeddings with a resolution of 0.2, the monocytes/macrophages were segregated into 12 subclusters (Fig. 4e). Cluster membership differences between cells derived from mice treated with mRNA and YF-17D were mostly due to cells profiled on day 1 and day 3 (Fig. 4e). Strikingly, we found subclusters (3, 5, 7 and 8) that appeared within

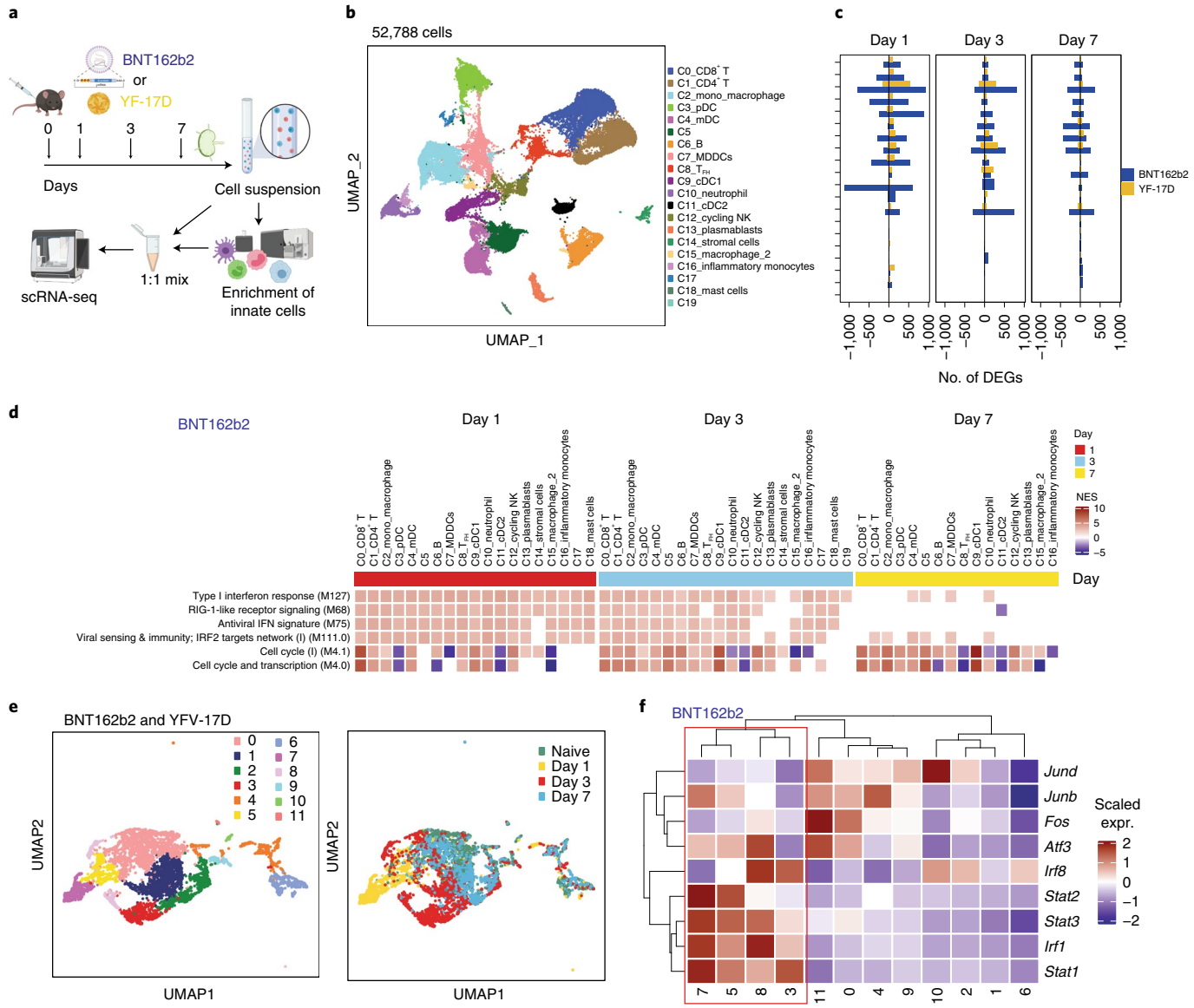


Fig. 4 | Single-cell transcriptional response induced by BNT162b2 and YF-17D immunization in dLNs. a, Experimental design and timeline. **b**, UMAP of cell types clustered by single-cell transcriptional analysis of 52,788 cells after quality control. MDDCs, monocyte-derived dendritic cells. **c**, DEGs induced by BNT162b2 and YF-17D immunization at days 1, 3 and 7. **d**, Significantly enriched interferon and cell cycle BTMs (false discovery rate < 0.05, absolute normalized enrichment score (NES) > 2) across all clusters from days 1 to 7 after BNT162b2 immunization. Only clusters with a significantly modulated pathway are shown. **e**, UMAP of subclusters in C2 (mono_macrophage) and C15 (macrophage) after BNT162b2 and YF-17D immunization, respectively. **f**, Heat map of key interferon response and AP-1 transcription factors after BNT162b2 immunization. Samples used for scRNA-seq were pooled from three independent experiments containing 8–10 mice.

1 and 3 d after immunization, with increased levels of *Irf8*, *Stat1*, *Stat2*, *Irf1* and *Stat3*, and decreased levels of *Atf3*, *Fos*, *Junb* and *Jund*, mirroring the innate immune cell populations described above (Fig. 4f and Extended Data Fig. 3d).

BNT162b2 stimulates enhanced secondary innate immune response. A hallmark of the immune response to BNT162b2 vaccination in humans is the striking increase in the innate immune response following secondary vaccination, relative to the response after primary vaccination[9]. To determine whether a similar effect was observed in mice, we measured serum cytokine/chemokine responses after the primary and secondary immunizations. Consistent with observations in humans[9], median IFN-γ response increased 8.6-fold, from 44.5 pg ml^{-1} at 6 h after immunization (day 0.3) to 383.1 pg ml^{-1} at 6 h after the secondary immunization (day 21.3; Fig. 5a). The data generated with the Luminex assay provided evidence that IFN-γ and other cytokines like IL-2, CCL2, CCL4 and CCL5 were enhanced at 6 h after the secondary immunization compared with those after the primary immunization, while there was no difference between prime and boost with a 0.2 µg dose (Extended Data Fig. 4a). Consistent with an increased IFN-γ level after secondary immunization, innate cells, including monocytes, macrophages and DCs, were more activated after secondary than after primary immunization, as judged by the level of CD86 expression (Fig. 5b).

In addition, we purified monocytes and quantified the expression of key ISGs and AP-1 transcription factors that distinguished cluster 8 from the other myeloid cells, defined in the human study

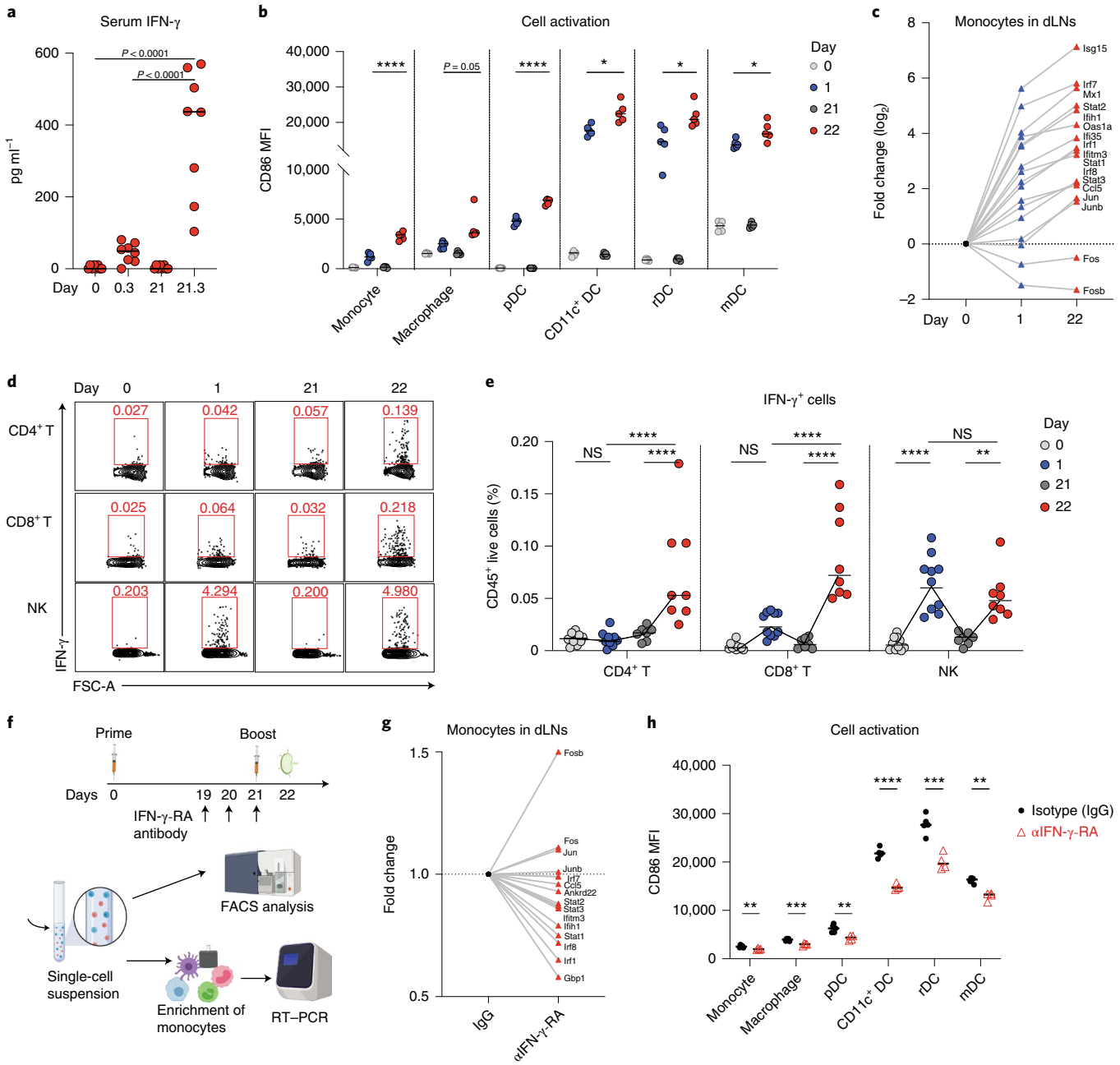


Fig. 5 | Enhanced innate immune response after boost is mediated by IFN-γ production. a, Serum IFN-γ measured by ELISA at days 0, 0.3 (6 h after prime), 21 and 21.3 (6 h after boost). $n = 8$ for each time point. **b**, Innate cell activation at days 0, 1, 21 and 22 after BNT162b2 immunization. $n = 5$. **c**, Fold change values of key interferon response genes and AP-1 transcription factors in monocytes at days 0, 1 and 22 after BNT162b2 immunization. **d**,**e**, Flow cytometry (**d**) and percentage (**e**) of cells producing IFN-γ in dLNs at the indicated times. $n = 10$ for days 0 and 1, and $n = 7$ and 8 for days 21 and 22, respectively. **f**, Experimental design and timeline. RT–PCR, PCR with reverse transcription. **g**, Fold change values of key interferon response genes and AP-1 transcription factors in IFN-γ-RA-neutralized group (αIFN-γ-RA) against isotype (IgG) control. **h**, Innate cell activation at day 22 after IFN-γ-RA neutralization. $n = 5$ for IgG group, $n = 4$ for αIFN-γ-RA-treated group. Data were combined from two independent experiments (**a** and **e**) or one representative of two independent experiments (**b**, **c**, **g** and **h**). One-way ANOVA followed by Tukey's test was applied in **a**. *P* values in **b** and **h** were determined using Student's *t*-tests (two-tailed). Two-way ANOVA followed by Tukey's test was applied in **e**. $^{*}P < 0.05$, $^{**}P < 0.01$, $^{***}P < 0.001$, $^{****}P < 0.0001$.

with BNT162b2 (ref. [9]). All the key ISGs (*Isg15*, *Mx1*, *Ifih1*, *Oas1a*, *Ifi35*, *Ifitm3*, *Ccl5*, *Irf1*, *Irf7*, *Irf8*, *Stat1*, *Stat2* and *Stat3*) were induced after the primary immunization, and importantly, the expression was increased further after the secondary immunization (Fig. 5c). Further, the AP-1 transcription factors encoded by *Fos* and *Fosb* were downregulated (Fig. 5c), as in previous studies[9,29]. Next, to identify the cellular origin of plasma IFN-γ, we performed ex vivo flow cytometry (Extended Data Fig. 4b). Notably, while the NK cells produced IFN-γ after both primary and secondary immunizations, CD4+ and CD8+ T cells contained the highest frequency of IFN-γ-expressing cells on day 22 (Fig. 5d,e). To determine whether the IFN-γ produced by T cells and NK cells within 1 d of secondary

immunization acted on myeloid cells to induce the expression of ISGs, we blocked the activity of IFN-γ in vivo with an IFN-γ receptor neutralizing antibody against the IFN-γ receptor, before secondary immunization on day 21 (Fig. 5f), and measured gene expression on day 22. We observed a significant reduction in the expression of all ISGs (*Gbp1*, *Ifih1*, *Ifitm3*, *Ankrd22*, *Ccl5*, *Irf1*, *Irf7*, *Irf8*, *Stat1*, *Stat2* and *Stat3*) in monocytes of anti-IFN-γ receptor antibody-treated mice versus mice treated with an isotype control (IgG), while the AP-1 transcription factors encoded by *Fos*, *Fosb*, *Jun* and *Junb* were upregulated (Fig. 5g). Furthermore, activation of monocytes, macrophages and DCs was significantly reduced in IFN-γ-receptor antibody-treated mice (Fig. 5h), suggesting that IFN-γ signaling plays an important role in the innate immune activation induced by BNT162b2. We also measured spike-specific T cell and antibody responses on day 42 after IFN-γ receptor blockade. We found that the antigen-specific CD4$^+$ and CD8$^+$ T cell responses did not differ significantly in the lung, nor was there a difference in antibody response (Extended Data Fig. 4c–e). However, there was a ~twofold reduction in the spike-specific CD8$^+$ T cells producing IFN-γ in the spleen (Extended Data Fig. 4c). To further delineate the relative importance of T cells versus NK cells in producing the burst of IFN-γ on day 22, we depleted NK or T cells (CD4$^+$ and CD8$^+$ T cells) before boost using NK1.1 or CD4/CD8-depletion antibodies. The T cell depletion, but not NK cell depletion, abrogated serum IFN-γ on day 22 (Extended Data Fig. 4f), 1 d after the boost demonstrating that the CD4$^+$ and CD8$^+$ T cells were the primary source of the circulating IFN-γ. Consistent with this, the activation of innate immune cells measured by mean fluorescence intensity of CD86 expression was more substantially reduced in T cell-depleted mice than in the control mice or mice depleted of NK cells (Extended Data Fig. 4g).

mRNA uptake by lymph node dendritic cells and macrophages. Many characteristics of LNP-mRNA vaccines, including size of the LNP, pK_a of the ionizable lipid, and lipid gradients, affect the tissue and cell specificity of the mRNA vaccine[15,30]. Using single-cell RNA-sequencing (scRNA-seq) data, we investigated the cells containing spike mRNA in the dLNs. We observed high levels of spike mRNA reads on day 1 that decreased sharply by day 3 (Fig. 6a). The reads were primarily restricted to clusters 2 and 4, which represent monocyte/macrophages and mDCs, respectively (Fig. 6a). Quantification of cells with at least one read per cell demonstrated that 40% of monocyte/macrophages and 20% of mDCs contained spike mRNA on day 1 (Fig. 6b). The frequency of these cells increased after vaccination (Fig. 6c). We also measured mRNA in various tissues using real-time PCR and found that the dLNs contained the highest concentration of mRNA (Fig. 6d). Interestingly, the spleen tissue also contained mRNA but at a much lower concentration (Fig. 6d). Consistent with the transcriptional data, serum concentration of spike protein increased on day 1 and decreased by day 7 (Fig. 6e). There was a small amount of mRNA in other tissues such as muscle, liver, lung and non-dLNs (Fig. 6e), consistent with previous reports[31]. Finally, we analyzed the gene expression profile associated with the spike mRNA signals in macrophages and mDCs (Fig. 6f). In both cell clusters, the spike mRNA signal was associated strongly with interferon-related and innate immune response-related BTMs including type I interferon response (M127), activated DCs (M64 and M67) in C2, chemokine cluster (II; M27.1), TLR and inflammatory signaling (M16) in C4, and RIG-I-like receptor signaling (M68) and antiviral IFN signature (M75) in both C2 and C4 (Fig. 6f), suggesting direct activation of innate immune signaling by the mRNA. Notably, *Ifih1*, the gene encoding MDA5, and downstream targets of MDA5 signaling were highly correlated with the spike mRNA signal in monocytes and macrophages (Fig. 6g). On the other hand, expression of TLRs and MyD88 was highly associated with the spike mRNA levels in the mDCs (Fig. 6g).

BNT162b2 stimulates CD8$^+$ T cell responses via MDA5–IFN-α axis. TLRs are the most studied sensors of pathogen-associated molecular patterns[32]. TLR3 and TLR7 recognize double-stranded and single-stranded RNA, respectively[33–35]. Therefore, we first examined whether deficiency of these receptors results in a diminished immune response to BNT162b2. However, immunization of *Tlr3*$^{-/-}$ or *Tlr7*$^{-/-}$ mice did not cause a reduction of antibody or T cell responses (Extended Data Fig. 5a–c), suggesting that they are not the primary sensors of BNT162b2 in vivo. Previous evidence indicates that the SARS-CoV-2 spike protein binds to and stimulates TLR2 and TLR4 signaling[36,37]. Further, we have shown that the immune responses to the seasonal flu and other unadjuvanted vaccines are controlled by microbiota via the TLR5 pathway[38]. Therefore, in addition to examining TLR3 and TLR7, we measured antibody and T cell responses in *Tlr2*$^{-/-}$, *Tlr4*$^{-/-}$ and *Tlr5*$^{-/-}$ mice. None of the mice demonstrated an impaired immune response to BNT162b2 vaccination (Extended Data Fig. 5d–i), providing evidence that these receptors are also not the primary sensors of BNT162b2.

Inflammasomes are critical regulators of innate immunity that regulate adaptive immunity to vaccines and adjuvants[39,40]. We examined the role of the inflammasome pathway using *Asc*$^{-/-}$ (also known as *Pycard*$^{-/-}$) and *Nlrp3*$^{-/-}$ mice and found no significant difference in antibody or T cell responses in comparison to WT mice (Extended Data Fig. 6a–c). Next, we examined the role of the cGAS–STING pathway, a cytoplasmic nucleic acid-sensing mechanism[41,42]. *Cgas*$^{-/-}$ and *Sting*$^{-/-}$ mice did not display a reduced response (Extended Data Fig. 7a–c), suggesting that these proteins do not play a role in immunogenicity of BTN162b2. Kim et al. reported that damage-associated molecular patterns, released during cell death pathways such as necroptosis, regulate immunity to adjuvants[43]. Like the adjuvant MF59 (ref. [43]), BNT162b2 induced damage-associated molecular pattern signals, including double-stranded DNA and HMGB1 peaking at 24 h after immunization, and uric acid peaking 2 d after immunization (Extended Data Fig. 8a–c). However, *Ripk3*$^{-/-}$ and *Gsdmd*$^{-/-}$ mice displayed no effect of BNT162b2-mediated T cell and antibody responses compared with littermate controls (Extended Data Fig. 8d–i).

The RIG-I-like receptor family of proteins sense cytosolic RNA and are a second family of putative sensors of BNT162b2[44,45]. To evaluate whether RIG-I-like receptors are involved in mRNA recognition, we immunized mice deficient in MDA5. There was no reduction in the antibody responses (Fig. 7a,b). Interestingly, *Mda5*$^{-/-}$ mice had a striking reduction in the frequency of antigen-specific CD8$^+$ T cells as evidenced by fewer class I tetramer-specific CD8$^+$ T cells and IFN-γ-producing CD8$^+$ T cells after primary (Extended Data Fig. 9) and secondary (Fig. 7c,d) immunizations, suggesting that the MDA5 sensing of BNT162b2 is responsible for the induction of spike-specific CD8$^+$ T cell responses. We also observed that the concentration of serum total IFN-α was below the detection limit in *Mda5*$^{-/-}$ mice, while the WT B6 mice produced as much as 2 ng ml^{-1} of IFN-α at 6 h, as measured by ELISA (Fig. 7e). Further, the activation of innate immune cells measured by CD86 expression was significantly downregulated in these mice (Fig. 7f). As type I interferons are known to directly stimulate clonal expansion of CD8$^+$ T cells[46,47], we examined whether mice deficient in IFNAR1 are likewise deficient in CD8$^+$ T cell responses. Consistent with our hypothesis, there was a striking reduction in spike-specific CD8$^+$ T cell frequencies enumerated by tetramer staining in the lung and spleen of *Ifnar1*$^{-/-}$ mice (Fig. 7g). In addition, there was also a significant but incomplete downregulation in the frequency of spike-specific T cells secreting IFN-γ (Fig. 7h); however, there was only a negligible effect on the antibody response (Fig. 7i). Moreover, the serum cytokine/chemokine responses (Fig. 7j,k) and the activation of innate immune cells measured by CD86 expression were also reduced (Fig. 7l). Collectively, these data show that MDA5 senses BNT162b2 to induce expression of IFN-α, which stimulates

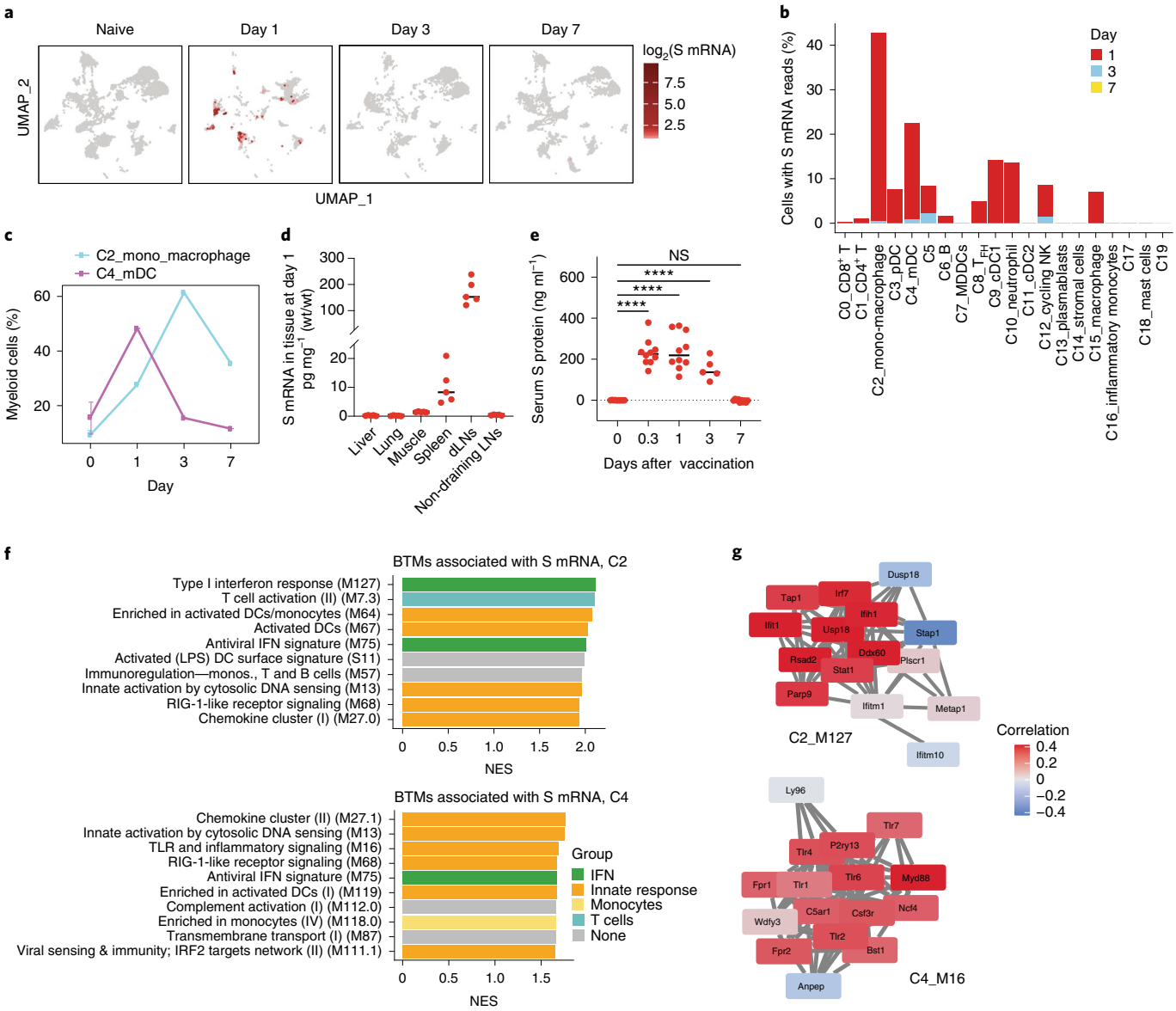


Fig. 6 | Uptake of BNT162b2 by dendritic cells and macrophages in draining lymph nodes. a, Distribution of spike mRNA at the single-cell level (read > 1 per cell) from days 1 to 7 after BNT162b2 immunization. Cell clusters of UMAP are as shown in Fig. 4b. **b**, The percentage of cells with spike mRNA reads in each cluster over time. **c**, The percentage of C2 and C4 in myeloid cells over time. **d**, Distribution of spike mRNA in tissues at day 1 after BNT162b2 immunization measured by TaqMan-based RT–PCR. $n = 5$ for each tissue. **e**, Spike protein in mouse serum detected by ELISA. $n = 5$ or 10. **f**, The BTMs associated with spike mRNA signal in C2_mono_macrophage and C4_mDCs. **g**, The correlation between spike mRNA signal and gene expression in BTM module M127 (type I interferon response) in C2_mono_macrophage and M16 (TLR and inflammatory signaling) in C4_mDCs, respectively. Samples used for scRNA-seq were pooled from three independent experiments containing 8–10 mice. Data were one representative of two independent experiments (**d**) or combined from two independent experiments (**e**). One-way ANOVA followed by Tukey's test was applied in **e**. $^{****}P < 0.0001$. LPS, lipopolysaccharide.

antigen-specific CD8$^+$ T cell expansion via IFNAR1, to promote a high magnitude of antigen-specific CD8$^+$ T cells. Thus, MDA5 deficiency leads to IFN-α deficiency, which in turn leads to reduced CD8$^+$ T cell response after primary vaccination, which then leads to reduced recall responses. Finally, we also detected a reduced frequency of CD8$^+$ T cells, and negligible reduction of IgG titers in *Batf3*$^{-/-}$ mice (Extended Data Fig. 10), which lack cross-presenting CD8α$^+$ DCs[48], suggesting the cross-presentation is important for BNT162b2-induced T cell responses.

Discussion

The current study, involving a detailed analysis of immune responses to vaccination of mice with the BNT162b2 vaccine, provided several new mechanistic insights (Fig. 8). As is the case in humans, after secondary immunization of mice, BNT162b2 induced a tenfold greater magnitude of antigen-specific binding and neutralizing antibodies, and potent GC B cell and T_{FH} responses. Surprisingly, there was a strikingly high magnitude of antigen-specific CD8$^+$ T cells in the lung and spleen, after the secondary immunization. The higher magnitude of T cell response in lung than in spleen is not unique to the mRNA vaccine, as we have observed this in mice immunized with YF-17D[49], and with AddaVax or MF59 plus Ova[43]. Experiments using a low dose (0.2 μg) of vaccine also resulted in similar B cell and T cell responses, but the magnitude was fivefold to tenfold lower than the high dose. Consistent with findings in humans[9], we observed in mice enhanced innate immune responses,

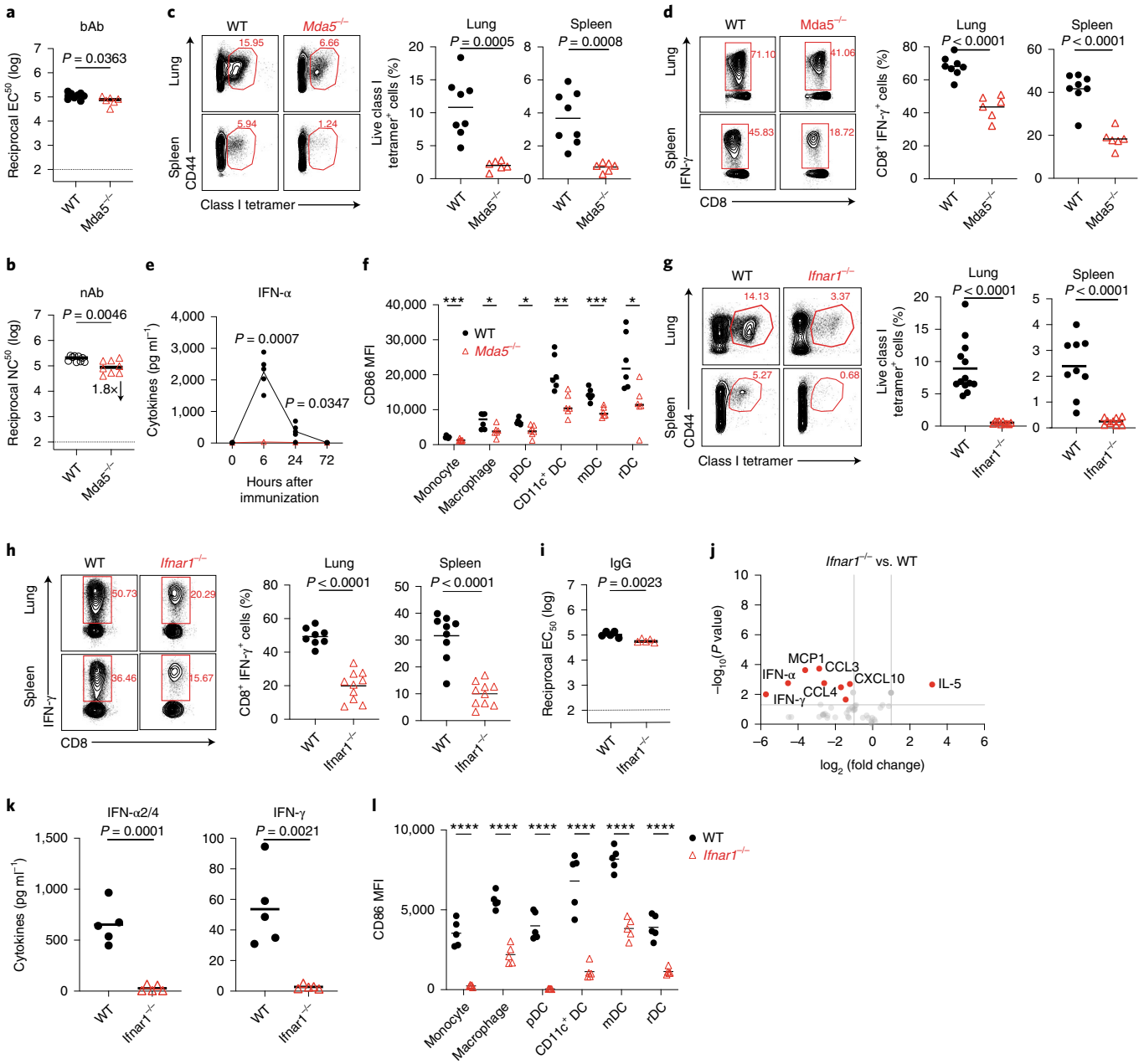


Fig. 7 | MDA5–IFNAR1 axis is important for BNT162b2-induced CD8⁺ T cell response. a,**b**, Binding antibody (bAb) (**a**) and neutralizing antibody (nAb) (**b**) titers of WT and *Mda5*$^{-/-}$ mice at day 42. In **a**, $n=8$ for WT, $n=6$ for *Mda5*$^{-/-}$. In **b**, $n=9$ for WT, $n=8$ for *Mda5*$^{-/-}$. **c**, Class I tetramer-specific CD8⁺ T cell response in the lung and spleen of WT and *Mda5*$^{-/-}$ mice measured at day 42 after BNT162b2 immunization as shown in Fig. 1a. **d**, Antigen-specific CD8⁺ T cell response in lung and spleen of WT and *Mda5*$^{-/-}$ mice detected at day 42 by ICS assay. In **c** and **d**, $n=8$ for WT, $n=6$ for *Mda5*$^{-/-}$. **e**, Serum total IFN-α levels in WT ($n=5$) and *Mda5*$^{-/-}$ ($n=4$) mice at 0, 6, 24 and 72 h measured by ELISA. **f**, Activation of innate cells in WT and *Mda5*$^{-/-}$ mice at day 1 after prime. $n=6$ for each group. **g**, Class I tetramer-specific CD8⁺ T cell response in lung and spleen tissue of WT and *Ifnar1*$^{-/-}$ mice measured at day 42. For lung, $n=13$ for WT, $n=10$ for *Ifnar1*$^{-/-}$; for spleen, $n=9$ for WT, $n=10$ for *Ifnar1*$^{-/-}$. **h**, Antigen-specific CD8⁺ T cell response in lung and spleen of WT and *Ifnar1*$^{-/-}$ mice detected at day 42 by ICS assay. For lung, $n=8$ for WT, $n=10$ for *Ifnar1*$^{-/-}$; for spleen, $n=9$ for WT, $n=10$ for *Ifnar1*$^{-/-}$. **i**, IgG titers of WT and *Ifnar1*$^{-/-}$ mice at day 42. $n=5$ for each group. **j**, Cytokines/chemokines in serum of WT and *Ifnar1*$^{-/-}$ mice at 6 h measured by Luminex. **k**, Serum IFN-α2/4 and IFN-γ levels in WT and *Ifnar1*$^{-/-}$ mice at 6 h. $n=5$ for each group. **l**, Activation of innate cells in WT and *Ifnar1*$^{-/-}$ mice at day 1 after prime. $n=5$ for each group. Data were combined from at least two independent experiments (**b**–**d** and **g** and **h**) or one representative experiment (**a**, **e**, **f** and **i**–**l**). *P* values were determined using Student's *t*-tests (two-tailed). $^{*}P<0.05$, $^{**}P<0.01$, $^{***}P<0.001$, $^{****}P<0.0001$.

including enhanced plasma IFN-γ concentrations, enhanced activation of DCs and myeloid cells in the dLNs, with a potent transcriptional signature of ISGs, and diminished expression of AP-1 transcription factor genes, after the secondary immunization with BNT162b2. We extended these findings to show that the CD4⁺ and CD8⁺ T cells were the primary source of serum IFN-γ 1 d after secondary immunization, which results in the enhanced myeloid cell activation after the secondary immunization. The heightened IFN-γ response following secondary immunization could conceivably enhance innate antiviral immunity during the first few days or weeks of vaccination, a period during which antigen-specific T cell and B cell responses are still nascent. In line with this notion,

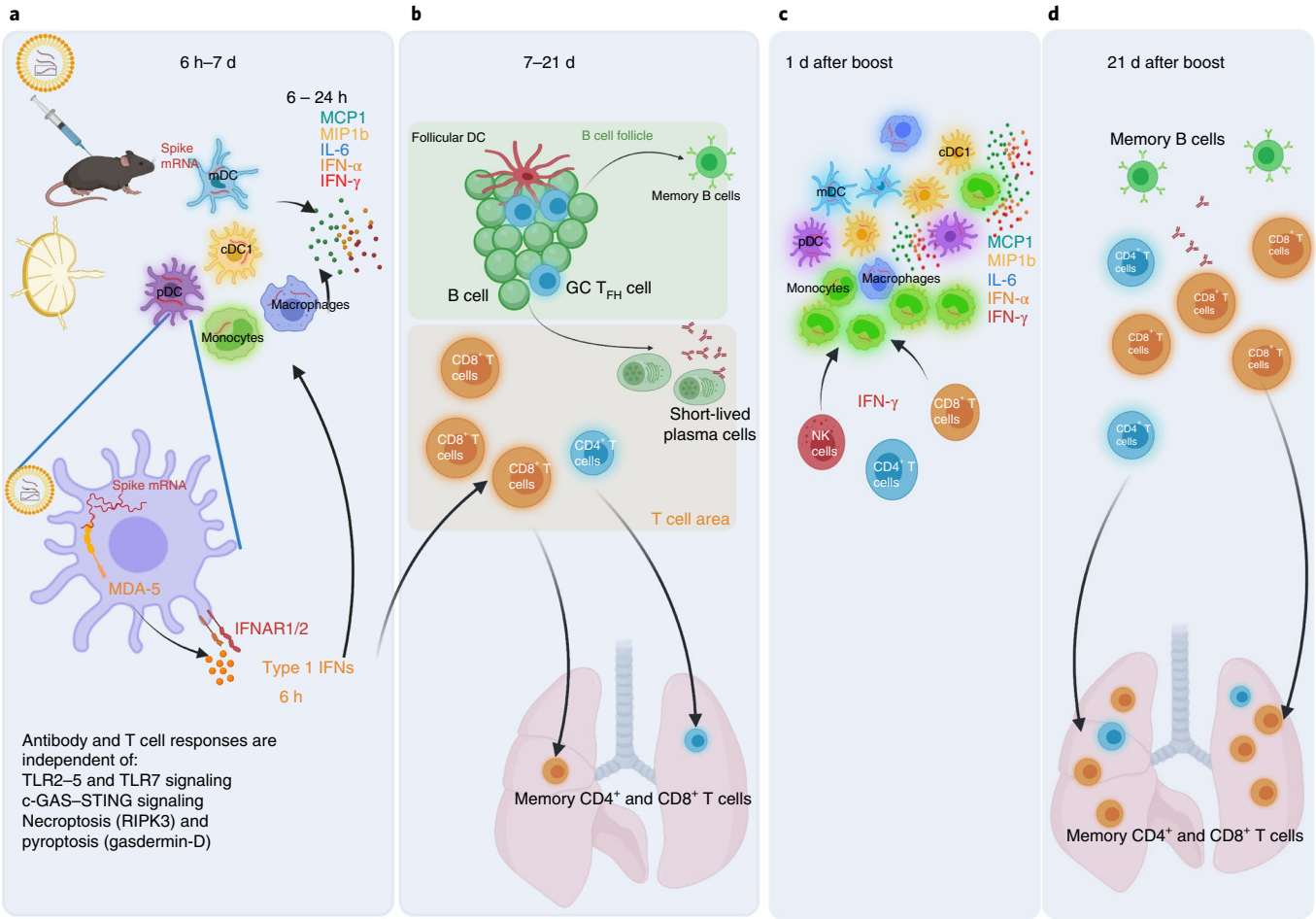


Fig. 8 | Depicting the mode of action of BNT162b2 in vivo. a. At 6 h to 7 d after BNT162b2 prime, DCs and macrophages in dLNs take up the vaccine and express spike proteins. These innate cells are highly activated and produce cytokines, including IL-6, IFN-α, IFN-γ, MCP1 and MIP1b. In this process, the MDA5–IFNAR1 signaling pathway is essential for IFN-α production and innate cell activation. **b**, At days 7 to 21, strong GC B and T_{FH} cell responses are induced in B cell follicles. The CD8$^+$ T cell response is increased mildly in both spleen and lung tissue. **c**, At days 1 to 3 after boost, much more IFN-γ is produced by NK, CD4$^+$ and CD8$^+$ T cells, contributing to the enhanced innate cell activation after boost. **d**, At 21 d after boost, the antibody response, CD4$^+$ and CD8$^+$ T cell responses increase significantly. The MDA5–IFNAR1 signaling pathway is essential for CD8$^+$ T cell responses in both spleen and lung tissue.

Wimmers et al. showed that vaccination with H5N1 + AS03 induces epigenetic changes in monocytes and myeloid DCs associated with enhanced IRF accessibility and heightened resistance to infection with unrelated blood-borne viruses, such as dengue virus and Zika virus[29]. Whether BNT162b2 can also cause the epigenetic changes on a genomic level to provide broader protection against other infectious diseases remains an open question in both humans and mice.

The distribution and dynamics of the BNT162b2 mRNA and the spike protein encoded by it, in tissues and cell types in vivo remains unclear. In this study, we found that BNT162b2 mRNA could be detected in mDCs and monocyte/macrophage subsets in the dLNs for at least 7 d following intramuscular immunization. Furthermore, mRNA could be detected in the spleen, and the spike protein itself was detectable in the serum, for up to 7 d after immunization.

Another insight to emerge from this study is how the innate immune system senses the BNT162b2 mRNA vaccine and modulates adaptive immunity. By analyzing responses in various strains of knockout mice, we found that induction of antigen-specific T cell and antibody responses was independent of TLR2–TLR5 and TLR7, or the STING–cGAS DNA-sensing pathway, and independent of NLRP3-dependent ASC inflammasome activation. Furthermore, mice deficient in RIP3 kinase and gasdermin D, the central mediators of necroptosis[50,51] and pyroptosis[52] respectively, mounted normal T and antibody responses to BNT162b2, arguing that these cell death pathways were not essential for the immunogenicity of this vaccine. However, we found that the MDA5–IFNAR1 signaling pathway is critical for the CD8$^+$ T cell response induced by BNT162b2. A previous study showed that MDA5 deficiency resulted in a modest impairment of antigen-specific CD8$^+$ T cell response following primary immunization with OVA+polyI:C, but a more pronounced impairment of secondary T cell responses[53]. MDA5 deficiency affects clonal expansion of CD8$^+$ T cells after primary as well as secondary immunization with BNT162b2 via impaired production of IFN-α, within the first few hours of primary vaccination. These data are consistent with studies showing a critical role for type I interferon responses in the clonal expansion of antigen-specific CD8$^+$ T cells[46]. mRNA is known to spontaneously form double-stranded RNA structures, and it is likely that MDA5 recognizes these double-stranded elements[54] in the target cells.

Whether these findings with BNT162b2 are applicable to other mRNA vaccines, such as mRNA-1273 from Moderna[55] and MRT5500 from Sanofi[56], remains to be determined. Although our data provide no evidence for a role for TLR2–TLR5 and TLR7, Alameh et al.

showed that GC B cell and T_{FH} cell responses induced by a different mRNA vaccine (a nucleoside-modified HA mRNA-LNP vaccine) is dependent on MyD88 but not MAVS[57]. Whether this difference is due to synergistic triggering through multiple TLRs, or differences between the BNT162b2 vaccine from Pfizer-BioNTech versus the vaccine used by Alameh et al. remains to be determined.

As will be appreciated, the aforementioned experiments in mice have revealed several new mechanistic insights about the innate and antigen-specific T and B cell responses induced by the BNT162b2 mRNA vaccine. A key question relates to the relevance of these various responses to protection against infection and disease caused by SARS-CoV-2. Israelow et al. found that mRNA-mediated protection from SARS-CoV-2 infection in mouse models is primarily mediated by humoral responses, while the cell-mediated immune responses are efficient in clearing infection[24]. The extent of the immunological defects observed in the mice deficient in MDA5 and IFNAR1, as well as the defects in secondary innate immunity caused by blockade of IFN-γ activity before secondary vaccination, remains to be determined. Finally, it should be remembered that, while the immune systems of mice and humans are broadly similar, nearly 80 million years of evolutionary divergence of these species have resulted in many differences in the details of how their immune systems work[58]. Therefore, the results obtained in mice should be interpreted in the context of similar studies in humans, in order to arrive at an integrated understanding of how our immune systems sense and respond to mRNA vaccines[58–60]. In summary, our study provides rich insights into the mechanism of BNT162b2's effects in vivo. These results not only help us better understand the mechanism of the BNT162b2 vaccine but also will help in the design of improved vaccines in the future.

Online content

Any methods, additional references, Nature Research reporting summaries, source data, extended data, supplementary information, acknowledgements, peer review information; details of author contributions and competing interests; and statements of data and code availability are available at https://doi.org/10.1038/s41590-022-01163-9.

Received: 20 October 2021; Accepted: 17 February 2022;
Published online: 14 March 2022

References

1. Polack, F. P. et al. Safety and efficacy of the BNT162b2 mRNA COVID-19 vaccine. *N. Engl. J. Med.* **383**, 2603–2615 (2020).
2. Walsh, E. E. et al. Safety and immunogenicity of two RNA-based COVID-19 vaccine candidates. *N. Engl. J. Med.* **383**, 2439–2450 (2020).
3. Kariko, K. et al. Incorporation of pseudouridine into mRNA yields superior nonimmunogenic vector with increased translational capacity and biological stability. *Mol. Ther.* **16**, 1833–1840 (2008).
4. Kariko, K., Buckstein, M., Ni, H. & Weissman, D. Suppression of RNA recognition by Toll-like receptors: the impact of nucleoside modification and the evolutionary origin of RNA. *Immunity* **23**, 165–175 (2005).
5. Turner, J. S. et al. SARS-CoV-2 mRNA vaccines induce persistent human germinal centre responses. *Nature* **596**, 109–113 (2021).
6. Lederer, K. et al. SARS-CoV-2 mRNA vaccines foster potent antigen-specific germinal center responses associated with neutralizing antibody generation. *Immunity* **53**, 1281–1295 e1285 (2020).
7. Pardi, N. et al. Nucleoside-modified mRNA vaccines induce potent T follicular helper and germinal center B cell responses. *J. Exp. Med.* **215**, 1571–1588 (2018).
8. Laczko, D. et al. A single immunization with nucleoside-modified mRNA vaccines elicits strong cellular and humoral immune responses against SARS-CoV-2 in mice. *Immunity* **53**, 724–732 (2020).
9. Arunachalam, P. S. et al. Systems vaccinology of the BNT162b2 mRNA vaccine in humans. *Nature* **596**, 410–416 (2021).
10. Tarke, A. et al. Impact of SARS-CoV-2 variants on the total $CD4^+$ and $CD8^+$ T cell reactivity in infected or vaccinated individuals. *Cell Rep. Med.* **2**, 100355 (2021).
11. Sahin, U. et al. BNT162b2 vaccine induces neutralizing antibodies and poly-specific T cells in humans. *Nature* **595**, 572–577 (2021).
12. Liu, J. et al. BNT162b2-elicited neutralization of B.1.617 and other SARS-CoV-2 variants. *Nature* **596**, 273–275 (2021).
13. Painter, M. M. et al. Rapid induction of antigen-specific $CD4^+$ T cells is associated with coordinated humoral and cellular immunity to SARS-CoV-2 mRNA vaccination. *Immunity* **54**, 2133–2142 (2021).
14. Zhang, H. et al. Delivery of mRNA vaccine with a lipid-like material potentiates antitumor efficacy through Toll-like receptor 4 signaling. *Proc. Natl Acad. Sci. USA* **118**, e2005191118 (2021).
15. Kranz, L. M. et al. Systemic RNA delivery to dendritic cells exploits antiviral defence for cancer immunotherapy. *Nature* **534**, 396–401 (2016).
16. Miao, L. et al. Delivery of mRNA vaccines with heterocyclic lipids increases anti-tumor efficacy by STING-mediated immune cell activation. *Nat. Biotechnol.* **37**, 1174–1185 (2019).
17. Sahin, U. et al. COVID-19 vaccine BNT162b1 elicits human antibody and T_H1 T cell responses. *Nature* **586**, 594–599 (2020).
18. Planas, D. et al. Reduced sensitivity of SARS-CoV-2 variant delta to antibody neutralization. *Nature* **596**, 276–280 (2021).
19. Nair, A. B. & Jacob, S. A simple practice guide for dose conversion between animals and human. *J. Basic Clin. Pharm.* **7**, 27–31 (2016).
20. Buschmann, M. D. et al. Nanomaterial delivery systems for mRNA vaccines. *Vaccines* **9**, 65 (2021).
21. Vogel, A. B. et al. BNT162b vaccines protect rhesus macaques from SARS-CoV-2. *Nature* **592**, 283–289 (2021).
22. Arunachalam, P. S. et al. T cell-inducing vaccine durably prevents mucosal SHIV infection even with lower neutralizing antibody titers. *Nat. Med.* **26**, 932–940 (2020).
23. Schenkel, J. M. et al. T cell memory. Resident memory $CD8^+$ T cells trigger protective innate and adaptive immune responses. *Science* **346**, 98–101 (2014).
24. Israelow, B. et al. Adaptive immune determinants of viral clearance and protection in mouse models of SARS-CoV-2. *Sci. Immunol.* **6**, eabl4509 (2021).
25. Pulendran, B. Learning immunology from the yellow fever vaccine: innate immunity to systems vaccinology. *Nat. Rev. Immunol.* **9**, 741–747 (2009).
26. Querec, T. et al. Yellow fever vaccine YF-17D activates multiple dendritic cell subsets via TLR2, 7, 8 and 9 to stimulate polyvalent immunity. *J. Exp. Med.* **203**, 413–424 (2006).
27. Querec, T. D. et al. Systems biology approach predicts immunogenicity of the yellow fever vaccine in humans. *Nat. Immunol.* **10**, 116–125 (2009).
28. Lee, A. et al. A molecular atlas of innate immunity to adjuvanted and live attenuated vaccines, in mice. *Nat. Commun.* **13**, 549 (2022).
29. Wimmers, F. et al. The single-cell epigenomic and transcriptional landscape of immunity to influenza vaccination. *Cell* **184**, 3915–3935 (2021).
30. Pardi, N., Hogan, M. J., Porter, F. W. & Weissman, D. mRNA vaccines—a new era in vaccinology. *Nat. Rev. Drug Discov.* **17**, 261–279 (2018).
31. Lindsay, K. E. et al. Visualization of early events in mRNA vaccine delivery in non-human primates via PET-CT and near-infrared imaging. *Nat. Biomed. Eng.* **3**, 371–380 (2019).
32. Iwasaki, A. & Medzhitov, R. Toll-like receptor control of the adaptive immune responses. *Nat. Immunol.* **5**, 987–995 (2004).
33. Alexopoulou, L., Holt, A. C., Medzhitov, R. & Flavell, R. A. Recognition of double-stranded RNA and activation of NF-κB by Toll-like receptor 3. *Nature* **413**, 732–738 (2001).
34. Diebold, S. S., Kaisho, T., Hemmi, H. & Akira, S. & Reis e Sousa, C. Innate antiviral responses by means of TLR7-mediated recognition of single-stranded RNA. *Science* **303**, 1529–1531 (2004).
35. Heil, F. et al. Species-specific recognition of single-stranded RNA via toll-like receptor 7 and 8. *Science* **303**, 1526–1529 (2004).
36. Zhao, Y. et al. SARS-CoV-2 spike protein interacts with and activates TLR4. *Cell Res.* **31**, 825 (2021).
37. Zheng, M. et al. TLR2 senses the SARS-CoV-2 envelope protein to produce inflammatory cytokines. *Nat. Immunol.* **22**, 829–838 (2021).
38. Oh, J. Z. et al. TLR5-mediated sensing of gut microbiota is necessary for antibody responses to seasonal influenza vaccination. *Immunity* **41**, 478–492 (2014).
39. Deets, K. A. & Vance, R. E. Inflammasomes and adaptive immune responses. *Nat. Immunol.* **22**, 412–422 (2021).
40. Pulendran, B., S Arunachalam, P. & O'Hagan, D. T. Emerging concepts in the science of vaccine adjuvants. *Nat. Rev. Drug Discov.* **20**, 454–475 (2021).
41. Sun, L., Wu, J., Du, F., Chen, X. & Chen, Z. J. Cyclic GMP-AMP synthase is a cytosolic DNA sensor that activates the type I interferon pathway. *Science* **339**, 786–791 (2013).
42. Ishikawa, H. & Barber, G. N. STING is an endoplasmic reticulum adaptor that facilitates innate immune signalling. *Nature* **455**, 674–678 (2008).
43. Kim, E. H. et al. Squalene emulsion-based vaccine adjuvants stimulate CD8 T cell, but not antibody responses, through a RIPK3-dependent pathway. *Elife* **9**, e52687 (2020).
44. Rehwinkel, J. & Gack, M. U. RIG-I-like receptors: their regulation and roles in RNA sensing. *Nat. Rev. Immunol.* **20**, 537–551 (2020).
45. Kato, H. et al. Differential roles of MDA5 and RIG-I helicases in the recognition of RNA viruses. *Nature* **441**, 101–105 (2006).

46. Kolumam, G. A., Thomas, S., Thompson, L. J., Sprent, J. & Murali-Krishna, K. Type I interferons act directly on CD8$^+$ T cells to allow clonal expansion and memory formation in response to viral infection. *J. Exp. Med.* **202**, 637–650 (2005).
47. Welsh, R. M., Bahl, K., Marshall, H. D. & Urban, S. L. Type 1 interferons and antiviral CD8$^+$ T cell responses. *PLoS Pathog.* **8**, e1002352 (2012).
48. Hildner, K. et al. Batf3 deficiency reveals a critical role for CD8α$^+$ dendritic cells in cytotoxic T cell immunity. *Science* **322**, 1097–1100 (2008).
49. Ravindran, R. et al. The amino acid sensor GCN2 controls gut inflammation by inhibiting inflammasome activation. *Nature* **531**, 523–527 (2016).
50. Zhang, D. W. et al. RIP3, an energy metabolism regulator that switches TNF-induced cell death from apoptosis to necrosis. *Science* **325**, 332–336 (2009).
51. Cho, Y. S. et al. Phosphorylation-driven assembly of the RIP1–RIP3 complex regulates programmed necrosis and virus-induced inflammation. *Cell* **137**, 1112–1123 (2009).
52. Shi, J. et al. Cleavage of GSDMD by inflammatory caspases determines pyroptotic cell death. *Nature* **526**, 660–665 (2015).
53. Wang, Y., Cella, M., Gilfillan, S. & Colonna, M. Cutting edge: polyinosinic:polycytidylic acid boosts the generation of memory CD8$^+$ T cells through melanoma differentiation-associated protein 5 expressed in stromal cells. *J. Immunol.* **184**, 2751–2755 (2010).
54. Wu, B. et al. Structural basis for dsRNA recognition, filament formation, and antiviral signal activation by MDA5. *Cell* **152**, 276–289 (2013).
55. Corbett, K. S. et al. SARS-CoV-2 mRNA vaccine design enabled by prototype pathogen preparedness. *Nature* **586**, 567–571 (2020).
56. Kalnin, K. V. et al. Immunogenicity and efficacy of mRNA COVID-19 vaccine MRT5500 in preclinical animal models. *NPJ Vaccines* **6**, 61 (2021).
57. Alameh, M. G. et al. Lipid nanoparticles enhance the efficacy of mRNA and protein subunit vaccines by inducing robust T follicular helper cell and humoral responses. *Immunity* **54**, 2877–2892 (2021).
58. Pulendran, B. & Davis, M. M. The science and medicine of human immunology. *Science* **369**, eaay4014 (2020).
59. Davis, M. M. A prescription for human immunology. *Immunity* **29**, 835–838 (2008).
60. Mestas, J. & Hughes, C. C. Of mice and not men: differences between mouse and human immunology. *J. Immunol.* **172**, 2731–2738 (2004).

Publisher's note Springer Nature remains neutral with regard to jurisdictional claims in published maps and institutional affiliations.

© The Author(s), under exclusive licence to Springer Nature America, Inc. 2022

Methods

Mice and immunization. C57BL/6, B6129SF2/J, *Tlr2*$^{-/-}$, *Tlr3*$^{-/-}$, *Tlr4*$^{-/-}$, *Tlr5*$^{-/-}$ and *Tlr7*$^{-/-}$ mice were purchased from Jackson Laboratories. *Ripk3*$^{-/-}$ and *Gsdmd*$^{-/-}$ mice and littermates were gifts from Genentech (A. Gitlin). *Ifnar1*$^{-/-}$, *Mda5*$^{-/-}$, *Sting*$^{-/-}$, *cGas*$^{-/-}$ and *Batf3*$^{-/-}$ mice were bred in our animal facility at Stanford University. *Asc*$^{-/-}$ and *Nlrp3*$^{-/-}$ mice were initially obtained from Genentech (V. Dixit) and maintained in our private colony at Jackson Laboratories. *Tlr3*$^{-/-}$ mice are on the B6129SF2/J background, while other strains are on C57BL/6 background. Mice were matched for sex and aged between 8 and 14 weeks.

Discarded remnant material (Pfizer/BioNTech) was used within manufacturer's guidelines for stability at 50 µl of BNT162b2 mRNA vaccine (5 or 0.2 µg per mouse), as described in previous study[61]. In addition, because this was not available for purchase and as only remnant (otherwise to be discarded) material could be used at the time (as the product was approved for emergency use authorization only), we obtained approval from the Dean of Research at Stanford, Office for General Counsel at Stanford, and the FDA-Center for Biologics Evaluation and Research vaccines division). For immunization, mice were injected intramuscularly with 50 µl of BNT162b2 mRNA vaccine (5 or 0.2 µg per mouse) or subcutaneously at the base of the tail with 100 µl of 10^6 plaque-forming units of YF-17D. All mice in this study were maintained under specific pathogen-free conditions, a 12-h light/12-h dark cycle and temperatures of ~18–23 °C with 40–60% humidity, and were handled according to the protocol approved by the Institutional Animal Care and Use Committee of Stanford University.

Flow cytometry analysis of innate cells. Draining iliac lymph nodes from BNT162b2-immunized mice and draining inguinal lymph nodes from YF-17D-immunized mice, along with whole lung or spleen, were collected and digested with 1 mg ml^{-1} collagenase type IV (Worthington) for 20 min at 37 °C, followed by smashing with a 100-µm strainer to make a single-cell suspension. Red blood cells from the lung and spleen were lysed before staining. Single-cell samples were then stained with Zombie UV (1:300 dilution; BUV496; BioLegend, 423107), anti-Ly6C (1:500 dilution; BV780; BioLegend, 128041), anti-Ly6G (1:400 dilution; APC-Cy7; BioLegend, 127624), anti-CD19 (1:100 dilution; BB700; BD, 566411), anti-CD3 (1:100 dilution; BB700; BD, 742175), anti-MHCII (1:400 dilution; AF700; eBioscience, 56-5321-82), anti-CD11b (1:100 dilution; BV650; BioLegend, 101239), anti-CD11c (1:400 dilution; BV421; BioLegend, 117330), anti-CD86 (1:300 dilution; A647; BioLegend, 105020), anti-Siglec-F (1:400, PE-CF594; BD, 562757), anti-CD45 (1:200 dilution; BV610; BioLegend, 103140), anti-CD169 (1:200 dilution; PE-Cy7; BioLegend, 142412), anti-PDCA-1 (1:200 dilution; BUV563; BD, 749275), anti-CD8a (1:200 dilution; BUV805; BD, 612898), anti-CD103 (1:100 dilution; PE; eBioscience, 12-1031-82), anti-NK1.1 (1:200 dilution; BV510; BioLegend, 108738) and anti-F4/80 (1:100 dilution; BUV737; BD, 749283). Data were collected on a BD FACSymphony analyzer with BD FACSDiva (v8.0.1).

Flow cytometry analysis of GC B, T_{FH} and plasma cells in lymph nodes. dLNs were collected and smashed with a 100-µm strainer to make a single-cell suspension followed by staining for viability with Ghost Dye Violet 510 (Tonbo Biosciences) for 5 min on ice in 1× PBS-2 mM EDTA. After washing out viability dye, cells were blocked with Fc receptor antibody α-CD16/32 (clone 2.4G2, BD) for 5 min on ice before staining with fluorochrome-conjugated antibodies in FACS staining buffer (1× PBS, 3% FBS, 1 mM EDTA, 0.02% sodium azide): CD3 (1:50 dilution; clone 17A2, BioLegend), CD4 (1:200 dilution; clone GK1.5, BioLegend), CXCR5 (1:50 dilution; clone L138D7, BioLegend), PD1 (1:200 dilution; clone 29F.1A12, BioLegend), CD19 (1:200 dilution; clone 6D5/CD19, BioLegend), CD95 (1:200 dilution; clone Jo2, BD Biosciences), CD38 (1:200 dilution; clone 90, BioLegend), CD44 (1:300 dilution; clone IM7, BioLegend) and CD138 (1:200 dilution; clone 281-2; BD Biosciences). Surface staining was carried out for 30 min on ice followed by fixation for 10 min in room temperature. Data were acquired in LSR-II and analyzed using FlowJo analysis software v10.

Intracellular cytokine staining assay. Whole spleen and lung samples were collected 42 d after prime (21 d after boost). Briefly, mononuclear populations from the lung were isolated from the interphase of a 70–40% Percoll gradient of single suspension prepared by enzymatic digestion with 1 mg ml^{-1} type IV collagenase and DNase I. Single-cell suspensions from the spleen were prepared without digestion. Cells were plated at ~2×10^6 cells per well in 96-well U-shaped plates and restimulated with S-specific overlapping peptide pools (1 µg ml^{-1} of each peptide) in complete RPMI 1640 medium for overnight incubation at 37 °C in the presence of brefeldin-A (10 µg ml^{-1}). At day 2, cells were stained with Ghost Dye Violet 510 (Tonbo Biosciences) for 10 min on ice in 1× PBS-2 mM EDTA. After washing out viability dye, cells were blocked with Fc receptor antibody α-CD16/32 (clone 2.4G2, BD) for 5 min on ice before staining with fluorochrome-conjugated antibodies in FACS staining buffer (1× PBS, 2% FBS): CD3 (1:50 dilution; clone 145-2C11, BioLegend), CD8α (1:200 dilution; clone 53-6.7, BioLegend), CD4 (1:200 dilution; clone RM4-5, BioLegend), CD44 (1:400 dilution; clone IM7, BioLegend), CD69 (1:200 dilution; clone H1.2F3; BioLegend) and CD45 (1:200 dilution; clone 30-F11, BioLegend). Cells were incubated for 30 min on ice for surface staining followed by fixation and permeabilization in BD Fix/Perm buffer and then stained intracellularly with fluorochrome-conjugated antibodies in Fix/Perm buffer: IFN-γ (1:100 dilution; clone XMG1.2, BioLegend), TNF (1:100 dilution; clone MP6-XT22, BioLegend), IL-2 (1:100 dilution; clone JES6-5H4, BioLegend) and IL-4 (1:100 dilution; clone 11B11, BioLegend) per the manufacturer's recommendation. Data were acquired in LSR-II and analyzed using FlowJo v10.

Antigen-specific tetramer and tissue-resident memory T cell staining. After staining cells with viability dye, cells were surface stained with anti-CD3 (1:50 dilution; clone 145-2C11, BioLegend), CD8α (1:200 dilution; clone 53-6.7, BioLegend), CD4 (1:200 dilution; clone RM4-5, BioLegend), CD44 (1:400 dilution; clone IM7, BioLegend), CD45 (1:200 dilution; clone 30-F11, BioLegend), CD69 (1:200 dilution; clone H1.2F3, BioLegend), CD103 (1:200 dilution; clone 2E7, BioLegend) and Spike S-specific Tetramer (1:200 dilution; residues 539–546, VNFNFNGL, H-2K(B)), followed by fixation. Data were acquired in LSR-II and analyzed with FlowJo v10.

Flow cytometry analysis of IFN-γ-producing cells in lymph nodes. After staining cells with viability dye, cells were surface stained with anti-CD3 (clone 145-2C11, BioLegend), CD8α (clone 53-6.7, BioLegend), CD4 (clone RM4-5, BioLegend), CD44 (clone IM7, BioLegend), CD45 (clone 30-F11, BioLegend), NK1.1 (clone PK136, BioLegend) and TCR delta (1:100 dilution; clone Gl3, BioLegend), fixed and permeabilized in BD Fix/Perm buffer, and stained intracellularly with anti-IFN-γ (XMG1.2, BioLegend) according to the manufacturer's recommendation. Data were acquired in LSR-II and analyzed with FlowJo v10. To block IFN-γ receptor, 1 mg per mouse of IFN-γ receptor neutralizing antibody (clone 2E2, BioXCell, BE0287) or isotype control (IgG, BioXCell, BE0091) was given intraperitoneally on days 19, 20 and 21 after prime. Then, mice were boosted at day 21 after prime, and lymph nodes were collected at day 1 after boost. To delete T cells or NK cells, 0.3 mg per mouse of anti-mouse CD8 (clone YTS 169.4, BioXCell, BE0117), anti-mouse CD4 (clone GK1.5, BioXCell, BE0003-1) or anti-mouse NK1.1 (clone PK136, BioXCell, BE0036) or isotype control (clone LTF-2, BioXCell, BE0090 for anti-CD4/CD8; or clone C1.18.4, BioXCell, BE0085 for anti-NK1.1) was given intraperitoneally on day 20 after priming. Mice were boosted at day 21. Serum IFN-γ levels and innate cell activation in spleen were checked at day 22.

Luminex assay. The assay was performed by the Human Immune Monitoring Center at Stanford University. Mouse 48-plex Procarta kits (EPX480-20834-901) were purchased from Thermo Fisher and used according to the manufacturer's recommendations with modifications as described below. Beads were added to a 96-well plate and washed in a BioTek ELx405 washer. Samples were added to the plate containing the mixed antibody-linked beads and incubated overnight at 4 °C with shaking. Cold (4 °C) and room temperature incubation steps were performed on an orbital shaker at 500–600 r.p.m. Following the overnight incubation, plates were washed in a BioTek ELx405 washer and biotinylated detection antibody was added for 60 min at room temperature with shaking. Plates were washed as described above and streptavidin-PE was added. After incubation for 30 min at room temperature, a wash was performed as above and reading buffer was added to the wells. Each sample was measured in singlets. Plates were read on a FM3D FlexMap instrument with a lower bound of 50 beads per sample per cytokine/chemokine. Custom Assay Chex control beads were purchased from Radix BioSolutions, and were added to all wells.

Anti-spike binding ELISA. SARS-CoV-2 spike protein was purchased from Sino Biologicals (40589-V08B1). High-binding 96-well plates were coated with 100 ng of spike protein diluted at a concentration of 2 mg ml^{-1} in PBS. The plates were washed once and blocked with 3% non-fat milk for 1 h at room temperature. Sera samples serially diluted in 1% non-fat milk containing PBS were added to the plates and incubated at 37 °C for 1 h. The plates were washed 3× with PBS-T, and horseradish peroxidase-conjugated goat anti-mouse IgG, IgG1 or IgG2c (SouthernBiotech, 1:6,000 dilution) in PBS-T containing 1% non-fat milk was added and incubated for 1 h at room temperature. Wells were washed three times with PBS-T before addition of 3,3′,5,5′-tetramethylbenzidine substrate solution (Thermo Pierce). The reaction was stopped after 3 min by addition of 0.16 M sulfuric acid. The optical density at 450 nm was measured with a Bio-Rad microplate reader.

Pseudotyped lentivirus virus production. Viral transfections were done in HEK293T cells using Bio T transfection reagent. Five million cells were seeded in D10 medium (DMEM + 10% FBS, L-glutamate, penicillin, streptomycin and 10 mM HEPES) in 10-cm plates 1 d before transfection. A five-plasmid system[62] was used for viral production. The spike vector contained the 21 amino acid truncated form of the SARS-CoV-2 spike sequence from the Wuhan-Hu-1 strain of SARS-CoV-2. Plasmids were added to D10 medium in the following ratios: 10 µg pHAGE-Luc2-IRS-ZsGreen, 3.4 µg FL spike, 2.2 µg HDM-Hgpm2, 2.2 µg HDM-Tat1b and 2.2 µg pRC-CMV-Rev1b in a final volume of 1 ml; 30 µl of Bio T was then added. Transfection reactions were incubated for 10 min at room temperature, and then added up to 10 ml with D10 medium. This mixture was added slowly to plated cells. Culture medium was removed 24 h after transfection

and replaced with fresh D10 medium. Viral supernatants were collected 72 h after transfection by spinning at 300*g* for 5 min followed by filtering through a 0.45-µm filter. Viral stocks were aliquoted and stored at −80 °C until ready for use.

Neutralization assay. The target cells used for infection in viral neutralization assays were from a HeLa cell line stably overexpressing the SARS-CoV-2 receptor, ACE2, as well as the protease known to process SARS-CoV-2, TMPRSS2 (ref. [63]). ACE2/TMPRSS2/HeLa cells were plated 1 d before infection at 5,000 cells per well or 2 d before infection at 2,500 cells per well. White-walled, clear-bottom, 96-well plates were used for the assay (Thermo Fisher Scientific). On the day of the assay, dilutions of serum were made into sterile D10 medium to a final volume of 30 µl. Samples were run in technical duplicate in each experiment. All other wells contained only D10 medium. A virus mixture was made containing the virus of interest (for example, SARS-CoV-2 with a 21 amino acid deletion on the C terminus), D10 medium (DMEM + 10% FBS, L-glutamine, 100 U ml^{-1} penicillin, 100 U ml^{-1} streptomycin and 10 mM HEPES) and polybrene. Virus dilutions into medium were selected such that a suitable signal would be obtained in the virus-only wells. A suitable signal was selected such that the virus-only wells would achieve a luminescence of at least >10,000 relative light units. Sixty microliters of this virus mixture was added to each of the serum dilutions to make a final volume of 120 µl in each well. Virus-only wells were made containing 60 µl D10 medium and 60 µl virus mixture. Cell-only wells were made containing 120 µl of D10 medium. The diluted serum/virus mixture was left to incubate for 1 h at 37 °C. Following incubation, the medium was removed from the cells on the plates made 1 or 2 d before, replaced with 100 µl of diluted serum/virus dilutions, and incubated at 37 °C for approximately 48 h. Infectivity readout was performed by measuring luciferase with a microplate reader (BioTek). Normalized values were fit with a three-parameter nonlinear regression inhibitor curve in GraphPad Prism (v9.2.0) to obtain NT_{50} (half neutralizing antibody titer) values.

Spike protein detection in serum. SARS-CoV-2 (2019-nCoV) Spike Detection ELISA Kit (Sino Biological, KIT40591) was used to measure spike protein in mouse serum according to the manufacturer's protocol. First, plates were washed three times followed by the addition of standard and diluted samples (2 µl mouse serum was added into 98 µl dilution buffer). Plates were then incubated for 2 h. After incubation, plates were washed three times and incubated with detection antibody for 1 h. Again, the plates were washed three times and 200 µl of substrate solution were added for 20 min. Finally, 50 µl stop solution were added and the optical density at 450 nm was measured with a microplate reader (Bio-Rad). All incubations were conducted at room temperature.

Spike mRNA vaccine detection by RT–PCR. Tissues were taken at day 1 after immunization. Tissues were weighted and homogenized with a bead miller (Fisher). Total RNA was purified with a PureLink RNA mini kit (Invitrogen). RNA purified from BNT162b2 mRNA vaccine was diluted serially and served as the standard. A Luna universal probe one-step RT–PCR kit (NEB) was used to measure the cycle threshold (Ct) of purified RNA with mRNA vaccine-specific primers (mVac-F: 5′-TACCAAGCTGAACGACCTGT, mVac-R: 5′-TTGCTGTTC CAGGCAATCAC, mVac-Probe: 5′-FAM-TGCCCGACGACTTCACCGGC-IBFQ).

IFN-γ, IFN-α and damage-associated molecular pattern signal detection. Serum IFN-γ and IFN-α levels were determined in serum samples by ELISA. Serum IFN-γ was detected with the Quantikine ELISA kit (R&D Systems, MIF00). IFN-α in serum was measured using ELISA sets (PBL, 421201). HMGB1 was detected with the Chemiluminescence ELISA kit (Novus Biologicals, NBP262782). ELISAs were performed according to the manufacturers' instructions. Serum double-stranded DNA concentrations were determined with a Quant-iT PicoGreen dsDNA Kit (Invitrogen, P11496). Uric acid in serum was measured with a Uric Acid Assay Kit (Abcam, ab65344).

scRNA-seq samples and preparation. Draining iliac lymph nodes from BNT162b2-immunized mice and draining inguinal lymph nodes from YF-17D-immunized mice were collected and digested into single-cell suspensions. One million total cells were set aside on ice. The rest of the cells were incubated with biotinylated CD3, CD19 and NK1.1 antibodies on ice for 20 min. Streptavidin-labeled magnetic beads (BD IMag Streptavidin Particles Plus-DM) were added and incubated on ice for 30 min. Unbonded cells were collected and $CD11b^+$ myeloid cells, pDCs ($CD11c^{lo}CD11b^-$PDCA-1+) and DCs ($CD11c^+$MHC-II^+) were sorted with flow cytometry. Sorted cells were combined with total lymphocytes at a 1:1 ratio and resuspended in cold PBS supplemented with 1% BSA (Miltenyi) and 0.5 U $µl^{-1}$ RNase Inhibitor (Sigma Aldrich). Cells were partitioned into gel beads-in emulsion (GEMs) using the 10x Chromium 3′ V3 chemistry system (10x Genomics). The released RNA was reverse transcribed in the C1000 touch PCR instrument (Bio-Rad), in accordance with the manufacturer's recommendations. Barcoded cDNA was extracted from the GEMs by post-GEM RT-Cleanup and amplified for 12 cycles. Amplified cDNA was subjected to 0.6x SPRI beads cleanup (Beckman, B23318). Twenty five percent of the amplified cDNA was subjected to enzymatic fragmentation, end repair, A-tailing, adaptor ligation and 10X specific sample indexing per the manufacturer's protocol. Sequencing libraries were generated and the quality was assessed through Bioanalyzer (Agilent) analysis. Libraries were pooled and sequenced on the HiSeq 4000 instrument (Illumina) with a targeted read depth of 40,000 read pairs per cell.

scRNA-seq data analysis. Cell Ranger v3.1.0 (10x Genomics) was used to quantify transcript levels against the 10x Genomics GRCh38 reference (v3.0.0). Raw count data were filtered to remove cells with a mitochondrial RNA fraction of >20% of total RNA counts per cell, cells with <100 unique features or cells with <200 total reads. The filtered count matrix was used to create a Seurat[64] (v3.1.4) object. Filtered read counts were scaled by a factor of 10,000 and log transformed. Doublets were identified with scds[65] (v1.2.0); cells with a doublet score in the top decile were removed. The remaining 52,788 cells were processed with the default Seurat pipeline. Specifically, the most variable 2,000 RNA features were used to perform principal-component analysis on the log-transformed counts. The first 25 components were used for further downstream analyses, including clustering and UMAP projections. Clusters were identified with Seurat SNN graph construction followed by Louvain community detection on the resultant graph with a resolution of 0.2, yielding 20 clusters. Differential expression for each time point compared to the baseline was calculated with a Wilcoxon rank-sum test. Gene-set enrichment analysis was run using all genes ranked by Wald statistic.

Macrophage clusters C2 and C15 were re-embedded using genes that characterized an epigenetically remodeled monocyte population enriched in humans 21 d after vaccination with two doses of H5N1/AS03 (ref. [29]). Principal components were calculated from the most variable genes within this set; Louvain community detection was again used with a resolution of 0.2 to determine cluster identity. Complex Heatmap (v2.2.0) was used for all heat maps. All analysis was performed in R (v3.6.3).

Quantification and statistical analysis. scRNA-seq statistical analysis was completed as described above. All other statistical analysis was performed with Prism (GraphPad Software v9.2.0). For comparing two groups, *P* values were determined using Student's *t*-tests (two-tailed). For comparing more than two groups, one-way ANOVAs followed by Tukey's test were applied. Differences between groups were considered significant for P values < 0.05. No statistical methods were used to predetermine sample sizes, but our sample sizes are similar to those reported in previous publications[38,43]. Mice were assigned to the various experimental groups randomly. Data collection and analysis were not performed blind to the conditions of the experiments. Data distribution was assumed to be normal, but this was not formally tested. No data points were excluded from the analyses.

Reporting Summary. Further information on research design is available in the Nature Research Reporting Summary linked to this article.

Data availability

Single-cell RNA-seq data are publicly accessible in the Gene Expression Omnibus under accession code GSE179131. All analyses and visualizations were performed in R (v3.6.3). Source data are provided with this paper.

Code availability

Computer code is available upon reasonable request.

References

61. Warren, C. M. et al. Assessment of allergic and anaphylactic reactions to mRNA COVID-19 vaccines with confirmatory testing in a US regional health system. *JAMA Netw. Open* **4**, e2125524 (2021).
62. Crawford, K. H. D. et al. Protocol and reagents for pseudotyping lentiviral particles with SARS-CoV-2 spike protein for neutralization assays. *Viruses* **12**, 513 (2020).
63. Rogers, T. F. et al. Isolation of potent SARS-CoV-2 neutralizing antibodies and protection from disease in a small animal model. *Science* **369**, 956–963 (2020).
64. Stuart, T. et al. Comprehensive integration of single-cell data. *Cell* **177**, 1888–1902 (2019).
65. Bais, A. S. & Kostka, D. scds: computational annotation of doublets in single-cell RNA-sequencing data. *Bioinformatics* **36**, 1150–1158 (2020).

Acknowledgements

We thank Ed Mockarski and Pratyusha Mandal for their advice and help during the early stages of this work. We thank the technical support from the Stanford Shared FACS Facility. Sorting was performed on an instrument in the Shared FACS Facility purchased by Parker Institute for Cancer Immunotherapy (PICI). We thank D. Wagh from Stanford Functional Genomics for preparing the single-cell library construction. We thank L. Witt, B. Betts and T. Chang from Stanford Health care system for providing remnant vaccines. We thank the National Institutes of Health tetramer core facility for providing the spike-specific tetramer for $CD8^+$ T cell detection. We thank B. Franco from Stanford Veterinary Service Center (VSC) for technical support. The study was supported by NIH grants (R37 DK057665, R37 AI048638, U19 AI090023 and U19 AI057266 to R. Ahmed;

U19 AI159840 to S. Foung), the Bill and Melinda Gates Foundation, and the Soffer Fund endowment and Open Philanthropy to B.P.

Author contributions

C.L., P.S.A. and B.P. designed research, interpreted data and wrote the manuscript. C.L. organized and led the research and analyzed the data. A.L. helped with innate cells staining. L.G., M.T., J.Z.A., R.V., N.R. and Y.F. helped with T cell analysis. M.K.S. performed the scRNA-seq data analysis. F.W. and A.L. helped to prepare samples for scRNA-seq. M.S. and P.A.W. conducted neutralization assays. E.V., Y.W. and M.T. took care of mice. D.D., R.H. and H.P. helped to provide remnant vaccine vials. W.L., P.K., A.D.G., P.K. and K.C.N. provided the analysis tools and key resources.

Competing interests

B.P. has served or is serving on the External Immunology Network of GSK, and on the scientific advisory boards of Sanofi, Medicago, CircBio and Boehringer-Ingelheim. A.D.G. is a visiting scientist at Genentech. The other authors declare no competing interests.

Additional information

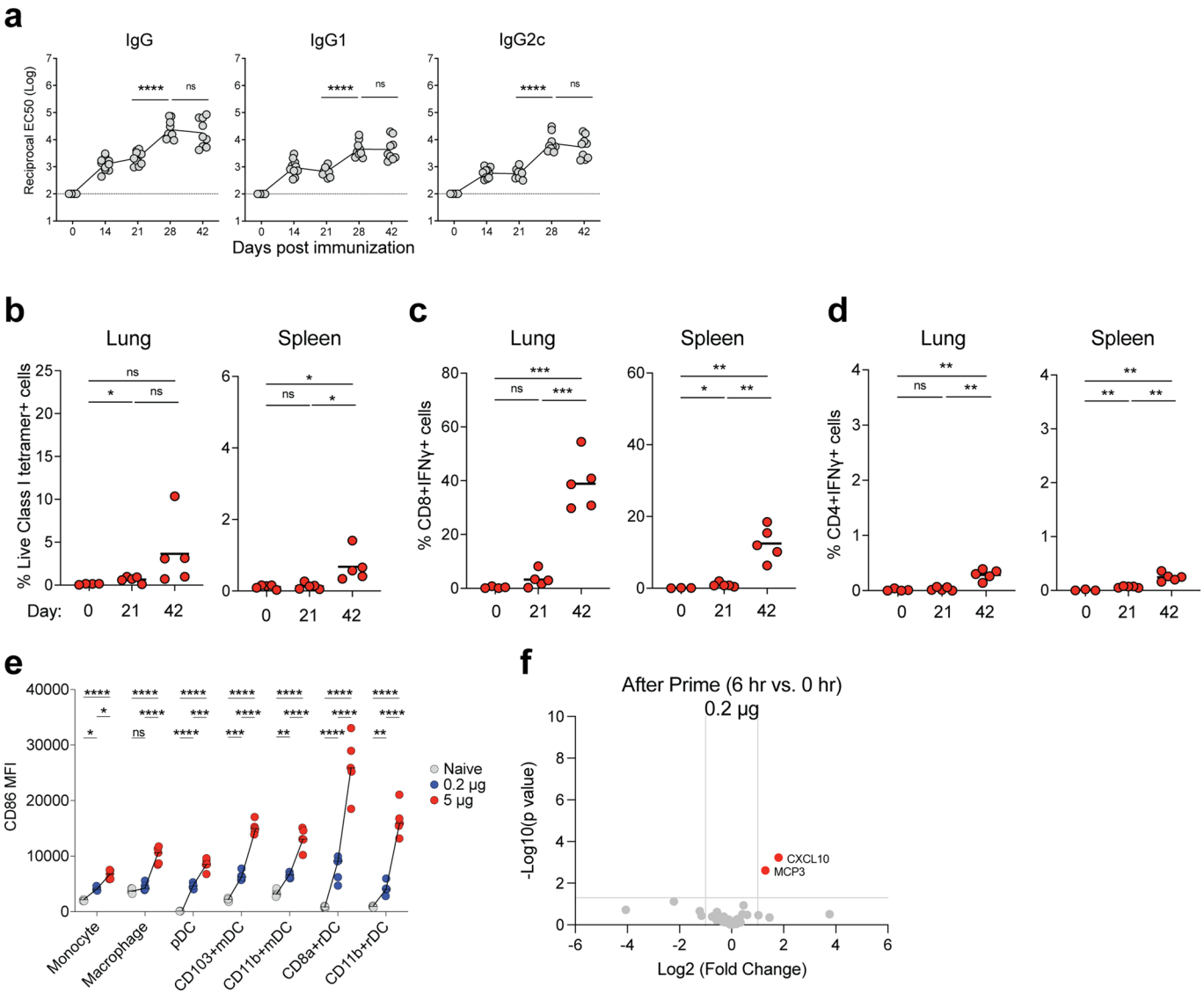
Extended data is available for this paper at https://doi.org/10.1038/s41590-022-01163-9.

Supplementary information The online version contains supplementary material available at https://doi.org/10.1038/s41590-022-01163-9.

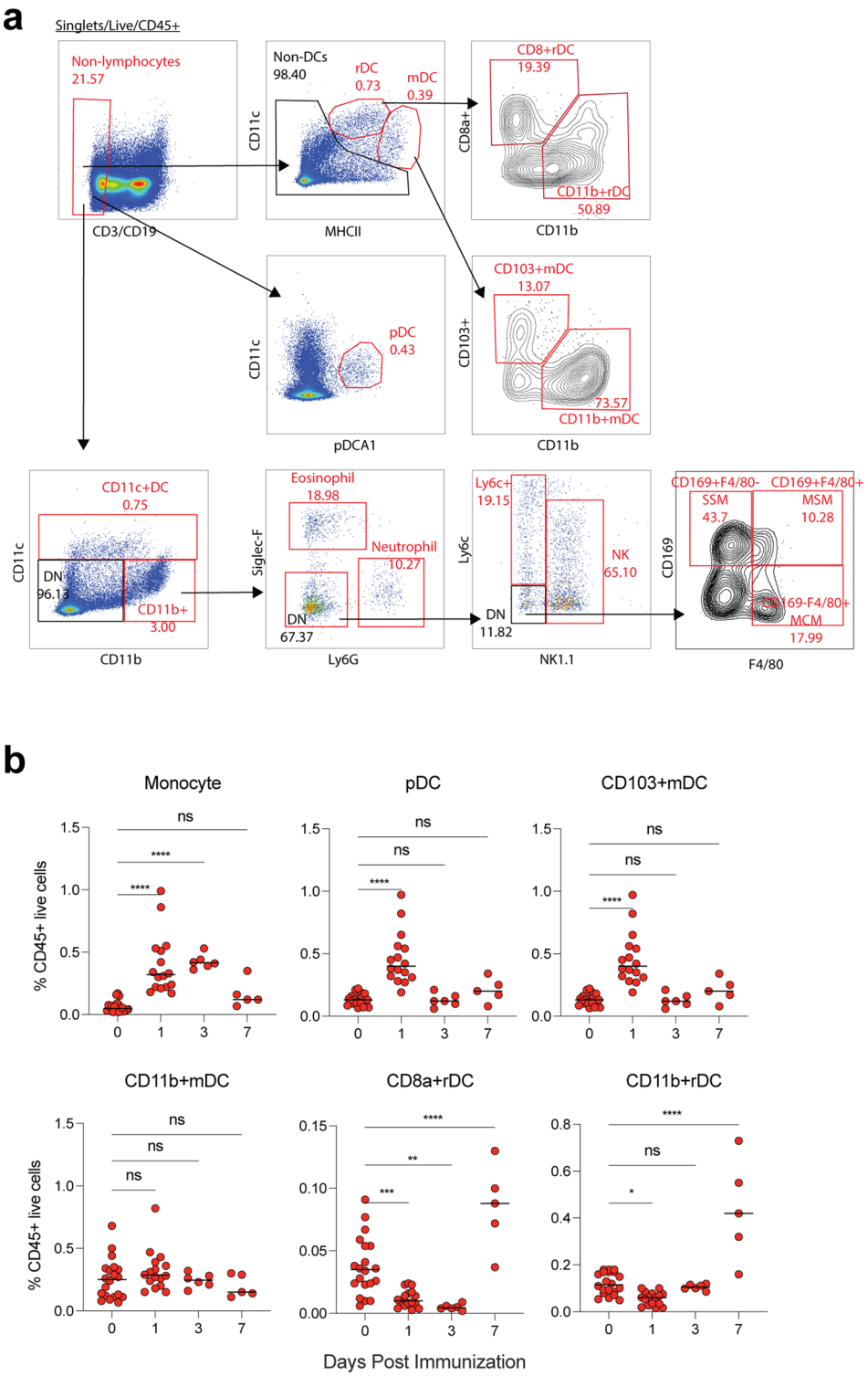
Correspondence and requests for materials should be addressed to Bali Pulendran.

Peer review information *Nature Immunology* thanks Olivier Schwartz and the other, anonymous, reviewer(s) for their contribution to the peer review of this work. Primary Handling Editor: N. Bernard, in collaboration with the *Nature Immunology* team. Peer reviewer reports are available.

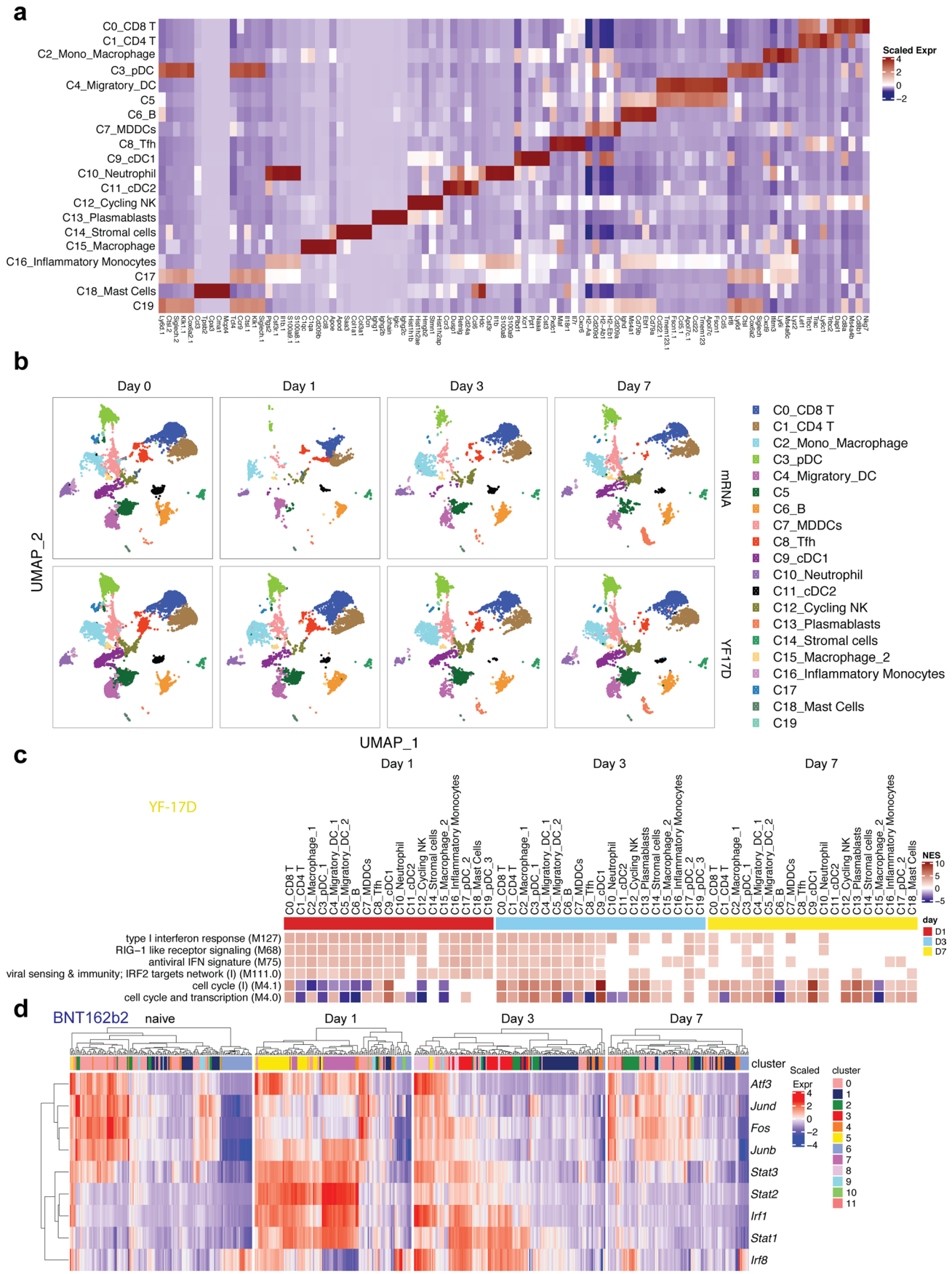
Reprints and permissions information is available at www.nature.com/reprints.



Extended Data Fig. 1 | Immune response induced by low immunization dose in mice. a, S binding titers induced by low dose (0.2 µg/mouse) of BNT162b2 immunization measured by ELISA. **b**, Class I tetramer specific CD8 T cell response in lung and spleen of mice measured at days 21 and 42 after BNT162b2 immunization (0.2 µg/mouse). **c-d**, Antigen specific CD8 **(c)** and CD4 **(d)** T cell response in lung and spleen of mice detected at days 21 and 42 by intracellular cytokine staining (ICS) assay. **e**, Comparison between the activation of innate cells in dLNs induced by low (0.2 µg/mouse) and high immunization doses (5 µg/mouse). **f**, Cytokines/chemokines produced at 6 h post prime with low (0.2 µg/mouse) dose detected by Luminex assay. Data were combined from two independent experiments **(a)** or one representative experiment **(b-f)**. One-Way ANOVA followed by Tukey's test was applied (a-e). P-values were determined using Student's t-tests (two-tailed) (f). *P < 0.05, **P < 0.01, ***P < 0.001, ****P < 0.0001.

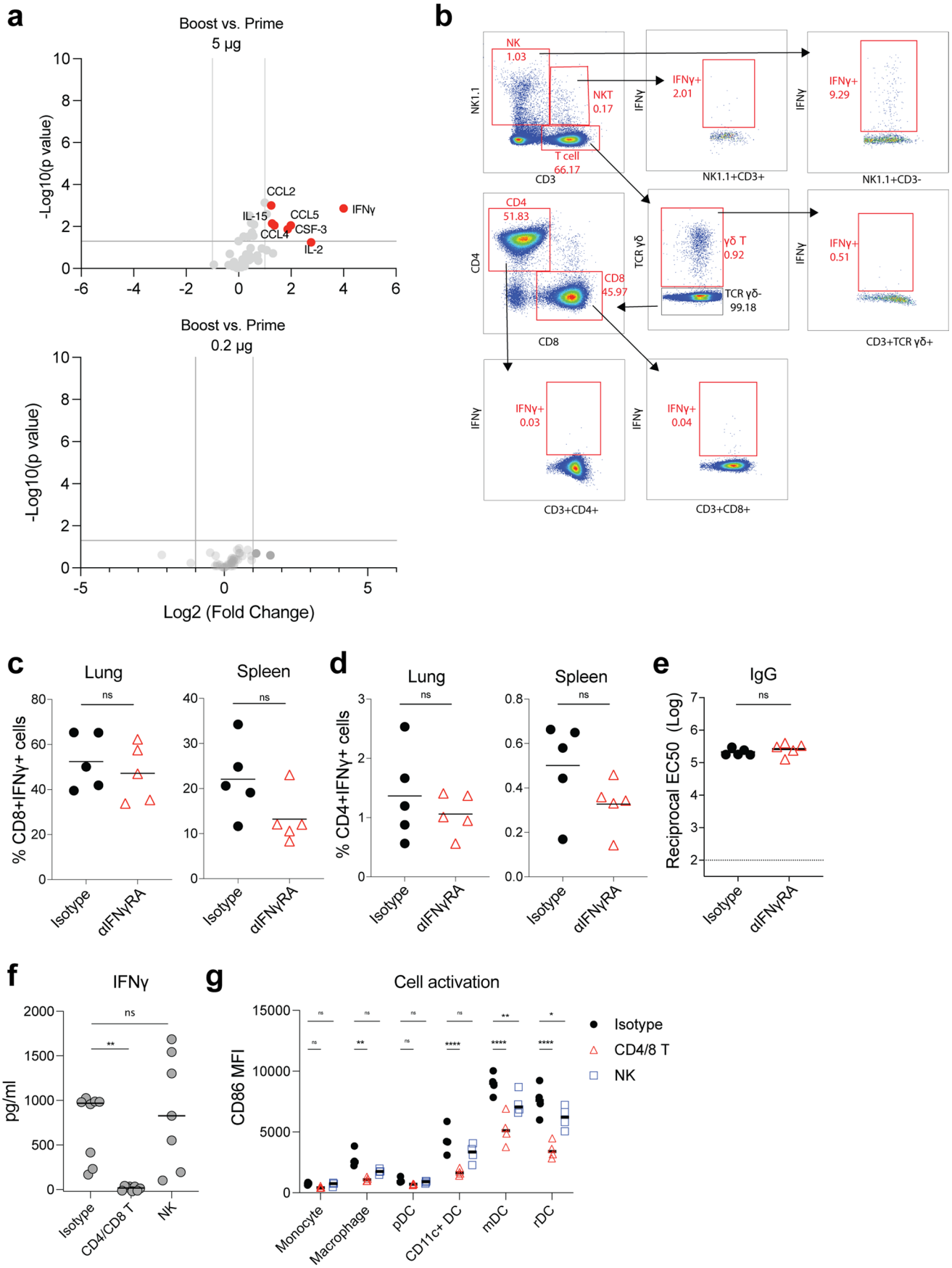


Extended Data Fig. 2 | Innate cells activated by BNT162b2. a, Gating strategy. **b**, Frequency of innate cells in live CD45 + cells after BNT162b2 immunization in dLNs. Data were combined from at least two independent experiments. One-Way ANOVA followed by Tukey's test was applied in (**b**). *P < 0.05, **P < 0.01, ***P < 0.001, ****P < 0.0001.



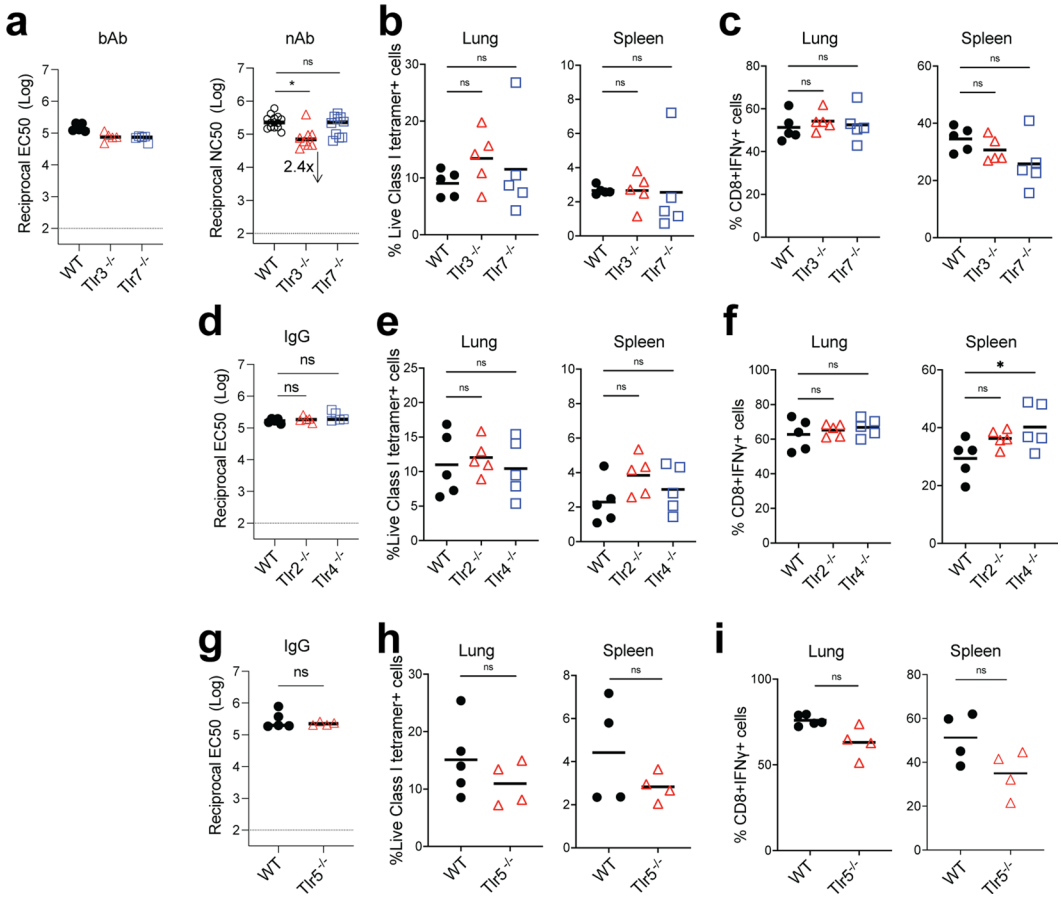
Extended Data Fig. 3 | See next page for caption.

Extended Data Fig. 3 | scRNAseq analysis of immune response induced by BNT162b2 and YF-17D. a, Clusters and their associated cluster-specific genes. **b**, UMAP of cell types clustered by single-cell transcriptional analysis at indicated time. **c**, Significantly enriched interferon BTMs (false discovery rate [FDR] < 0.05, absolute normalized enrichment score [NES] > 2) across all clusters from days 1 to 7 after YF-17D immunization. Only clusters with a significantly modulated pathway are shown. **d**, Heatmap of key interferon response and AP-1 transcription factors after BNT162b2 immunization over time. Samples used for scRNAseq were pooled from three independent experiments containing 8-10 mice.

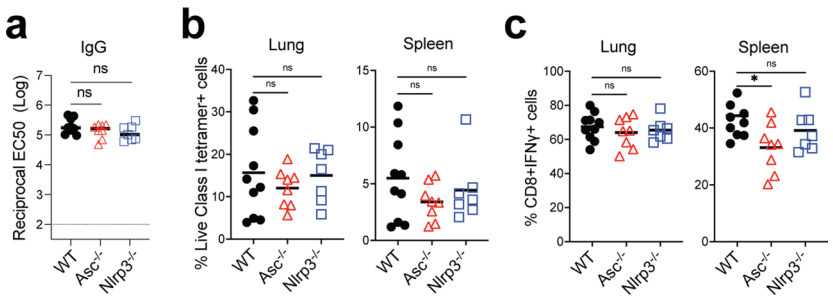


Extended Data Fig. 4 | See next page for caption.

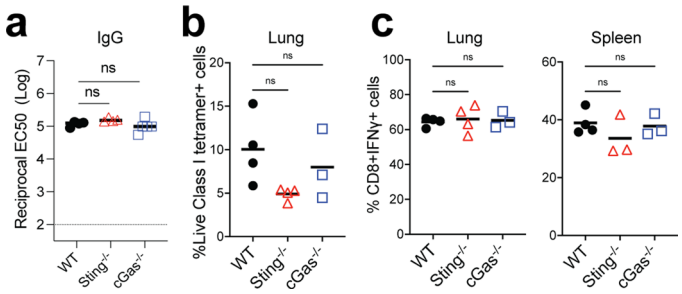
Extended Data Fig. 4 | IFNγ production after prime and boost. a, Luminex assay of serum cytokines/chemokines at 6 h post-prime and boost with 5 μg/mouse and 0.2 μg/mouse, respectively. Data were combined from five mice for each group. **b**, Gating strategy to analyze IFNγ producing cells in dLNs. **c-e**, CD8 + and CD4 + T cell responses, and IgG titer at day 42 after blocking of IFNγ receptor. Mice were treated with IFNγ receptor neutralizing antibody or isotype control before boost at day 21. **f**, Serum IFNγ level at day 22 (1 day after boost) after T cells (CD4 and CD8 T cells) or NK cells depletion at day 21. **g**, Innate cell activation in spleen at 1 day post boost after T or NK cell depletion. P-values were determined using Student's t-tests (two-tailed) (**a, c-e**), One-Way ANOVA (**f**), or Two-way ANOVA (**g**). *$P < 0.05$, **$P < 0.01$, ***$P < 0.001$, ****$P < 0.0001$.



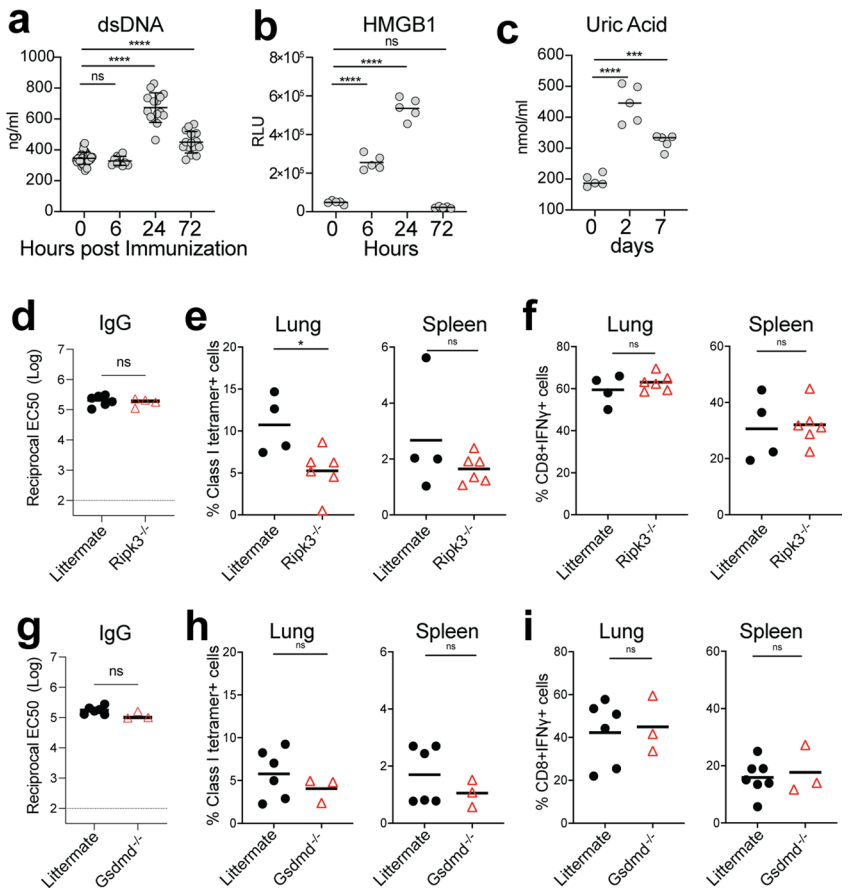
Extended Data Fig. 5 | Roles of TLRs for BNT162b2-induced antibody and T cell response. bAb and nAb titers of WT and *Tlr3*$^{-/-}$, *Tlr7*$^{-/-}$ **(a)**, bAb (IgG) titers of WT and *Tlr2*$^{-/-}$, *Tlr4*$^{-/-}$ **(d)**, *Tlr5*$^{-/-}$ **(g)** mice at day 42. CD8 + T cell response in WT and *Tlr3*$^{-/-}$, *Tlr7*$^{-/-}$ **(b-c)**, *Tlr2*$^{-/-}$, Tlr4$^{-/-}$ **(e-f)**, and *Tlr5*$^{-/-}$ **(h-i)** mice. Data were combined from two independent experiments. One-Way ANOVA followed by Tukey's test was applied in (**a-f**). P-values in (**g-i**) were determined using Student's t-tests (two-tailed). *P < 0.05, **P < 0.01.



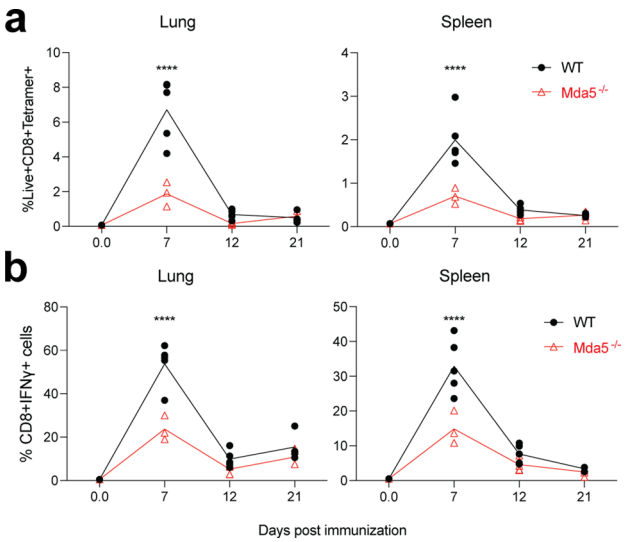
Extended Data Fig. 6 | Roles of inflammasome for BNT162b2-induced antibody and T cell response. a, IgG titers of WT, *Asc*$^{-/-}$, and *Nlrp3*$^{-/-}$ mice at day 42. **(b-c)**, CD8 + T cell response in WT, *Asc*$^{-/-}$, and *Nlrp3*$^{-/-}$ mice. Data were combined from two independent experiments. One-Way ANOVA followed by Tukey's test was applied. *P < 0.05.



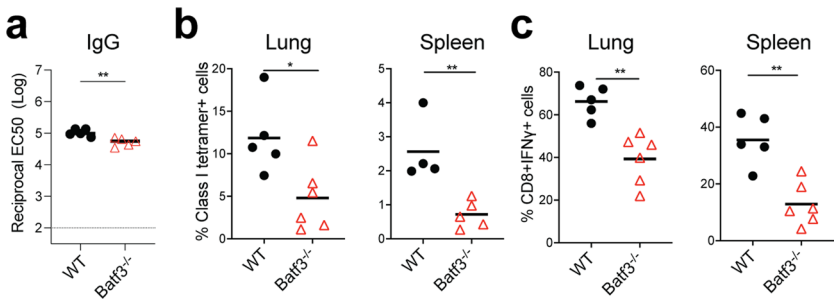
Extended Data Fig. 7 | Role of cGAS and STING for BNT162b2-induced antibody and T cell response. a, IgG titers of WT, *cGas*$^{-/-}$, and *Sting*$^{-/-}$ mice at day 42. **(b-c)**, CD8 + T cell response in WT, *cGas*$^{-/-}$, and *Sting*$^{-/-}$ mice. Data are one representative of two independent experiments. One-Way ANOVA followed by Tukey's test was applied.



Extended Data Fig. 8 | Role of cell death in BNT162b2-induced antibody and T cell response. a-c, DAMP signals including dsDNA **(a)**, HMGB1 **(b)**, and uric acid **(c)** induced by BNT162b2 immunization at the indicated time. **d**, IgG titers of littermate and *Ripk3*$^{-/-}$ mice at day 42. **e-f**, CD8 + T cell response in littermate and *Ripk3*$^{-/-}$ mice. **g**, IgG titers of littermate and *Gsdmd*$^{-/-}$ mice at day 42. **h-i**, CD8 + T cell response in littermate and *Gsdmd*$^{-/-}$ mice. Data were one representative of at least two independent experiments **(a)**, or one representative experiment **(b-i)**. One-Way ANOVA followed by Tukey's test was applied in (**a-c**). P-values in (**d-i**) were determined using Student's t-tests (two-tailed). *$P < 0.05$, ***$P < 0.001$, ****$P < 0.0001$.



Extended Data Fig. 9 | Role of MDA5 in BNT162b2-induced T cell response after prime. a-b, CD8 + T cell response in WT and *Mda5*$^{-/-}$ mice at indicated time post prime. P-values were determined using two-way ANOVA. ****P < 0.0001.



Extended Data Fig. 10 | Role of Batf3 in BNT162b2-induced antibody and T cell response. a, IgG titers of WT and *Batf3*$^{-/-}$ mice at day 42. **b**, CD8 + T cell response in WT and *Batf3*$^{-/-}$ mice. Data were one representative of three independent experiments. P-values were determined using Student's t-tests (two-tailed). *P < 0.05, **P < 0.01.

nature portfolio

Corresponding author(s): Bali Pulendran

Last updated by author(s): Jan 29, 2022

Reporting Summary

Nature Portfolio wishes to improve the reproducibility of the work that we publish. This form provides structure for consistency and transparency in reporting. For further information on Nature Portfolio policies, see our Editorial Policies and the Editorial Policy Checklist.

Statistics

For all statistical analyses, confirm that the following items are present in the figure legend, table legend, main text, or Methods section.

n/a	Confirmed
☐	☒ The exact sample size (*n*) for each experimental group/condition, given as a discrete number and unit of measurement
☐	☒ A statement on whether measurements were taken from distinct samples or whether the same sample was measured repeatedly
☐	☒ The statistical test(s) used AND whether they are one- or two-sided *Only common tests should be described solely by name; describe more complex techniques in the Methods section.*
☒	☐ A description of all covariates tested
☐	☒ A description of any assumptions or corrections, such as tests of normality and adjustment for multiple comparisons
☐	☒ A full description of the statistical parameters including central tendency (e.g. means) or other basic estimates (e.g. regression coefficient) AND variation (e.g. standard deviation) or associated estimates of uncertainty (e.g. confidence intervals)
☐	☒ For null hypothesis testing, the test statistic (e.g. *F*, *t*, *r*) with confidence intervals, effect sizes, degrees of freedom and *P* value noted *Give P values as exact values whenever suitable.*
☒	☐ For Bayesian analysis, information on the choice of priors and Markov chain Monte Carlo settings
☒	☐ For hierarchical and complex designs, identification of the appropriate level for tests and full reporting of outcomes
☒	☐ Estimates of effect sizes (e.g. Cohen's *d*, Pearson's *r*), indicating how they were calculated

Our web collection on statistics for biologists contains articles on many of the points above.

Software and code

Policy information about availability of computer code

Data collection	BD FACSDiva software version 8.0.1 was used for collecting the flow cytometry data on the LSRII.2 and BD FACSymphony machine.
Data analysis	FlowJo software v.10.0 (Treestar Inc); GraphPad Prism version 9.0.1; Adobe Illustrator 25.0. All statistical analysis are two-sided. All analyses and visualizations of sc-RNAseq data were performed in R (V3.6.3). Computer code is available upon reasonable request.

For manuscripts utilizing custom algorithms or software that are central to the research but not yet described in published literature, software must be made available to editors and reviewers. We strongly encourage code deposition in a community repository (e.g. GitHub). See the Nature Portfolio guidelines for submitting code & software for further information.

Data

Policy information about availability of data

All manuscripts must include a data availability statement. This statement should provide the following information, where applicable:

- Accession codes, unique identifiers, or web links for publicly available datasets
- A description of any restrictions on data availability
- For clinical datasets or third party data, please ensure that the statement adheres to our policy

Single-Cell RNAseq data are publicly accessible in the GEO under accession numbers GSE179131.

Field-specific reporting

Please select the one below that is the best fit for your research. If you are not sure, read the appropriate sections before making your selection.

☒ Life sciences ☐ Behavioural & social sciences ☐ Ecological, evolutionary & environmental sciences

For a reference copy of the document with all sections, see nature.com/documents/nr-reporting-summary-flat.pdf

Life sciences study design

All studies must disclose on these points even when the disclosure is negative.

Sample size	No statistical test was used to determine the number of samples. Sample sizes were determined as appropriate to evaluate detection of large vaccine effects based on several studies done by us and others.
Data exclusions	No data were excluded from any of the analysis.
Replication	All the assays were repeated with biological replicates in each experiment, and all the repeats are successful.
Randomization	The study involved the same batch of mice (C57BL/6) that were obtained from Jackson laboratories. Mice were allocated to cages with 3-5 mice per cage, and each cage was assigned to an immunization group.
Blinding	All the experiments were conducted in an unblinded way since the investigators were involved in overall conduct of the study.

Reporting for specific materials, systems and methods

We require information from authors about some types of materials, experimental systems and methods used in many studies. Here, indicate whether each material, system or method listed is relevant to your study. If you are not sure if a list item applies to your research, read the appropriate section before selecting a response.

Materials & experimental systems

n/a	Involved in the study
☐	☒ Antibodies
☒	☐ Eukaryotic cell lines
☒	☐ Palaeontology and archaeology
☐	☒ Animals and other organisms
☒	☐ Human research participants
☒	☐ Clinical data
☒	☐ Dual use research of concern

Methods

n/a	Involved in the study
☒	☐ ChIP-seq
☐	☒ Flow cytometry
☒	☐ MRI-based neuroimaging

Antibodies

Antibodies used

Antibody, Fluorophore, Vendor, Cat #, Clone, Lot #

anti-Ly6C, BV780, Biolegend, # 128041, HK1.4, B311364
anti-Ly6G, APC-Cy7, Biolegend, # 127624, 1A8, B294666
anti-CD19, BB700, BD, # 566411, 1D3, 0079006
anti-CD3, BB700, BD, #742175, 17A2, 0202623
anti-MHCII, AF700, eBioscience, #56-5321-82, M5/114.15.2, 2210930
anti-CD11b, BV650, Biolegend, #101239, M1/70, B335585
anti-CD11c, BV421, Biolegend, #117330, N418, B294539
anti-CD86, A647, Biolegend, #105020, GL-1, B245405
anti-Siglec-F, PE-CF594, BD, #562757, E50-2440, 0064626
anti-CD24, BUV395, BD, #744471, M1/69, 1102765
anti-CD45, BV605, Biolegend, #103140, 30-F11, B313899
anti-CD169, PE-Cy7, Biolegend, #142412, 3D6.112, B264616
anti-PDCA-1, BUV563, BD, #749275, 927, 1271522
anti-CD8a, BUV805, BD, #612898, 53-6.7, 0328533
anti-CD103, PE, eBioscience, #12-1031-82, 2E7, 2054351
anti-NK1.1, BV510, Biolegend, #108738, PK136, B326849
anti-F4/80, BUV737, BD, #749283, T45-2342, 1168211
anti CD3, BV785, Biolegend, #100355, 145-2C11, B303965
anti-CD4, BV650, Biolegend, #100555, RM4-5, B250896
anti-CD8, BV711, BD, #563046, 53-6.7, 0239184
anti-CD69, PECy7, Biolegend, # 104511, H1.2F3, B291440

anti-CD103, PerCP-Cy5.5, BioLegend, #121416, 2E7, B314149
anti-CD44, BV421, Biolegend, #103040, IM7, B306124
anti-CD45, BV605, Biolegend, #103139, 30-F11, B301866
anti-IFNγ, APC, Biolegend, #505810, XMG1.2, B290393a
anti-TNFa, FITC, Biolegend, #506304, MP6-XT22, B271488
anti-IL2, AF700, Biolegend, #503818, JES6-5H4, B335226
anti-IL4, PerCPCy5.5, Biolegend, #504124, 11B11, B301560
anti-CD95, PECy7, BD Biosciences, #557653, Jo2, 0321061
anti-CD19, PerCP-Cy5.5, BioLegend, #115534, 6D5,B288784
anti-CD38, BUV395, BD Biosciences, #740245, 90,1242465
anti-CD44 , APC-Cy7, BioLegend, #103062, IM7, B290267
anti-CD138, BV605, BD Biosciences, #563147, 281-2, 1097493
anti-CD3, A700, BioLegend, #100216, 17A2, B323639
anti-CD4, BV650, BioLegend, #100469,GK1.5, B311210
anti-CXCR5, BV711, BioLegend, #145529, L138D7,B315903
anti-PD1, PECF594, BioLegend, #135228, 29F.1A12, B320108
anti-γδ TCR, A488, BioLegend, #144611, GL3, B343654

Validation

All antibodies used were evaluated by the manufacturers as provided in their websites.
Biolegend:https://www.biolegend.com/en-us/quality/product-development
BD:https://www.biocompare.com/Antibody-Manufacturing/355107-Antibody-Manufacturing-Perspectives-BD-Bioscience/
Thermofisher: https://www.thermofisher.com/us/en/home/life-science/antibodies/invitrogen-antibody-validation.html

Animals and other organisms

Policy information about studies involving animals; ARRIVE guidelines recommended for reporting animal research

Laboratory animals

C57BL/6, B6129SF2/J, Tlr2-/-, Tlr3-/-, Tlr4-/-, and Tlr5-/- mice were purchased from Jackson Laboratories. Ripk3-/-, Gsdmd-/-, and littermates were gifts from Genentech Inc (Alex Gitlin). Ifnar1-/-, Mda5-/-, Sting-/-, cGas-/-, and Batf3-/- mice were bred in our animal facility at Stanford University. Asc-/- and Nlrp3-/- mice were originally from Vishva M Dixit lab in Genetech, Tlr7-/- mice were originally from S.Akira lab (Osaka University). Asc-/-, Nlrp3-/- and Tlr7-/- mice were then maintained and provided by Jackson Laboratories. Mice were sex-matched and aged between 8 and 14 weeks.

Wild animals

No wild animals were used in this study.

Field-collected samples

No field-collected samples were used in this study.

Ethics oversight

All mice in this study were maintained under specific pathogen-free conditions, 12 light/12 dark cycle, temperatures of ~18-23°C with 40-60% humidity, and handled according to the protocol approved by the Institutional Animal Care and Use Committee (IACUC) of Stanford University.

Note that full information on the approval of the study protocol must also be provided in the manuscript.

Flow Cytometry

Plots

Confirm that:

☒ The axis labels state the marker and fluorochrome used (e.g. CD4-FITC).

☒ The axis scales are clearly visible. Include numbers along axes only for bottom left plot of group (a 'group' is an analysis of identical markers).

☒ All plots are contour plots with outliers or pseudocolor plots.

☒ A numerical value for number of cells or percentage (with statistics) is provided.

Methodology

Sample preparation

1, Flow cytometry analysis of innate cells: Draining iliac lymph nodes from BNT162b2 immunized mice, draining inguinal lymph nodes from YF-17D immunized mice, along with whole lung or spleen, were harvested and digested with 1 mg/mL collagenase type IV (Worthington) for 20 min at 37 °C, followed by smashing with a 100 µm strainer to make a single-cell suspension. Red blood cells from the lung and spleen were lysed before staining.
2, Flow cytometry of GC B, TFH, and plasma cells in lymph nodes: dLNs were harvested and smashed with a 100 µm strainer to make a single-cell suspension followed by staining for viability with Ghost Dye Violet 510 (Tonbo Biosciences) for 5 min on ice in 1x PBS-2mM EDTA.
3, Intracellular cytokine staining assay: Whole Spleen and lung were harvested at 42 days post-prime (21 days post-boost). Briefly, mononuclear populations from the lung were isolated from the interphase of a 70-40% Percoll gradient of single suspension prepared by enzymatic digestion with 1 mg/mL type IV collagenase and DNase I. Single-cell suspensions from the spleen were prepared without digestion. Cells were plated at ~2 x 10^6 cells/well in 96-well U-shaped plates and re-stimulated with S-specific overlapping peptide pools (1 µg/mL of each peptide) in complete RPMI1640 medium for overnight

incubation at 37 °C in the presence of brefeldin-A (10 µg/mL). At day 2, cells were stained with Ghost Dye Violet 510 (Tonbo Biosciences) for 10 min on ice in 1x PBS-2mM EDTA.
4, scRNAseq samples and preparation: Draining iliac lymph nodes from BNT162b2 immunized mice and draining inguinal lymph nodes from YF-17D immunized mice were harvested and digested into single-cell suspensions. One million total cells were set aside on ice. The rest of the cells were incubated with biotinylated CD3, CD19, and NK1.1 Ab on ice for 20 min. Streptavidin-labeled magnetic beads (BD IMag™ Streptavidin Particles Plus-DM) were added and incubated on ice for 30 min. Unbonded cells were collected and CD11b+ myeloid cells, pDCs (CD11clo, CD11b-PDCA-1+), and DCs (CD11c+MHC-II+) were sorted with flow cytometry. Sorted cells were combined with total lymphocytes at a 1:1 ratio and resuspended in cold PBS supplemented with 1% BSA (Miltenyi) and 0.5 U/µL RNase Inhibitor (Sigma Aldrich). Cells were partitioned into Gel Beads-in emulsion (GEMs) using the 10x Chromium 3' V3 chemistry system (10x Genomics).

Instrument

Cells were analyzed with an LSRII.2 or BD FACSymphony analyzer at the Stanford Shared FACS Facility.

Software

BD FACSDiva software version 8.0.1 was used for collecting the flow cytometry data on the LSRII.2 machine.
FlowJo software v.10.0 (Treestar Inc) was used to analyze the flow cytometry data.

Cell population abundance

For scRNAseq samples and preparation: CD11b+ myeloid cells, pDCs (CD11clo, CD11b-PDCA-1+), and DCs (CD11c+MHC-II+) were sorted with flow cytometry after remove CD3, CD19, and NK1.1 with Streptavidin-labeled magnetic beads (BD IMag™ Streptavidin Particles Plus-DM). Sorted cells were combined with total lymphocytes at a 1:1 ratio and resuspended in cold PBS supplemented with 1% BSA (Miltenyi) and 0.5 U/µL RNase Inhibitor (Sigma Aldrich) for scRNAseq analysis.

Gating strategy

Cells were selected based on FSC-A vs. SSC-A, singlets were selected using FSC-A vs. FSC-H. Live CD45+CD3+ T cells were used for analysis of antigen-specific T cells. CD4 and CD8 T cells were selected as CD3+CD8-CD4+ or CD3+ CD8+. Live CD45+CD3 +CD19-CD4+PD1+CXCR5+ T cells were gated as TFH cells, Live CD45+CD3-CD19+CD38-CD95+ cells were gated as GC B cells, Live CD44+CD138+ cells were gated as plasma cells. Gating strategies for innate immune cells, NKT, and γδ T cells are provided in the manuscript.

☒ Tick this box to confirm that a figure exemplifying the gating strategy is provided in the Supplementary Information.

nature portfolio

https://doi.org/10.1038/s41590-022-01163-9

Supplementary information

Mechanisms of innate and adaptive immunity to the Pfizer-BioNTech BNT162b2 vaccine

In the format provided by the authors and unedited

Mechanisms of innate and adaptive immunity to the Pfizer-BioNTech BNT162b2 vaccine

Chunfeng Li[1], Audrey Lee[1], Lilit Grigoryan[1], Prabhu S. Arunachalam[1], Madeleine K. D. Scott[1,2], Meera Trisal[1], Florian Wimmers[1], Mrinmoy Sanyal[3], Payton A. Weidenbacher[3], Yupeng Feng[1], Julia Adamska[1], Erika Valore[1], Yanli Wang[1], Rohit Verma[1], Noah Reis[1], Diane Dunham[4], Ruth O'Hara[5], Helen Park[6], Wei Luo[7], Alexander Gitlin[8,9], Peter Kim[3,10], Purvesh Khatri[1,2], Kari C. Nadeau[4,11,12], Bali Pulendran[1,9,13,*]

[1]Institute for Immunity, Transplantation and Infection, Stanford University, Stanford, CA, USA.

[2]Center for Biomedical Informatics, Department of Medicine, Stanford University School of Medicine, Stanford, CA 94305, USA.

[3]Department of Biochemistry & Stanford, ChEM-H, Stanford University, Stanford, CA 94305, USA.

[4]Sean N. Parker Center for Allergy & Asthma Research, Stanford, CA, USA.

[5]Department of Psychiatry and Behavioral Sciences, Stanford University School of Medicine, Palo Alto, CA, USA

[6]Veterans Affairs Palo Alto Health Care System, Palo Alto, CA, USA.

[7]Department of Microbiology and Immunology, Indiana University School of Medicine, Indianapolis, IN, USA

[8]Department of Physiological Chemistry, Genentech, South San Francisco, CA, USA.

[9]Department of Pathology, Stanford University School of Medicine, Stanford University, Stanford, CA, USA.

[10]Chan Zuckerberg Biohub, San Francisco, CA 94158, USA

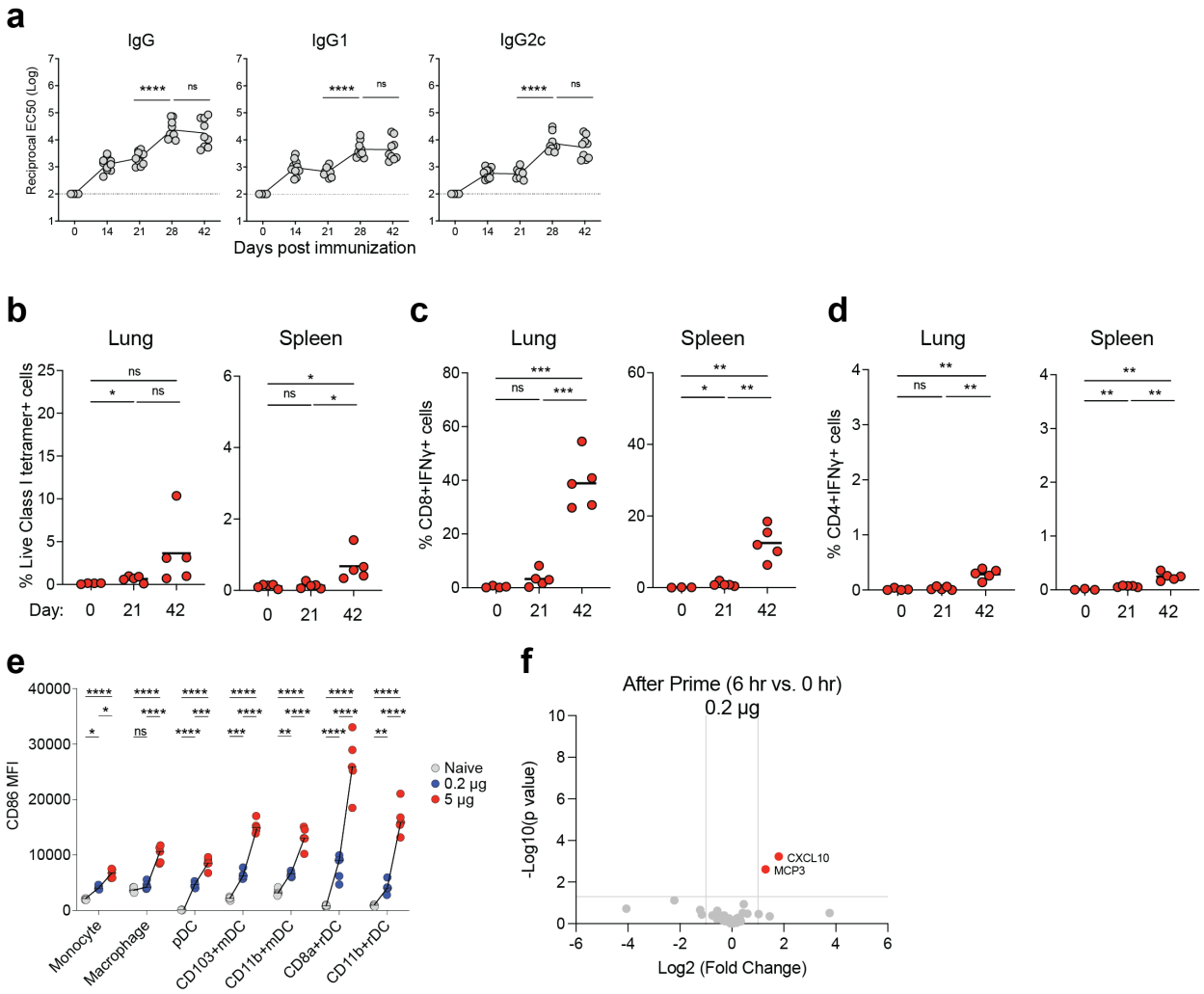
[11]Howard Hughes Medical Institute, Stanford University, Stanford, CA, USA.

[12]Department of Medicine, Division of Pulmonary, Allergy and Critical Care Medicine, Stanford, CA, USA.

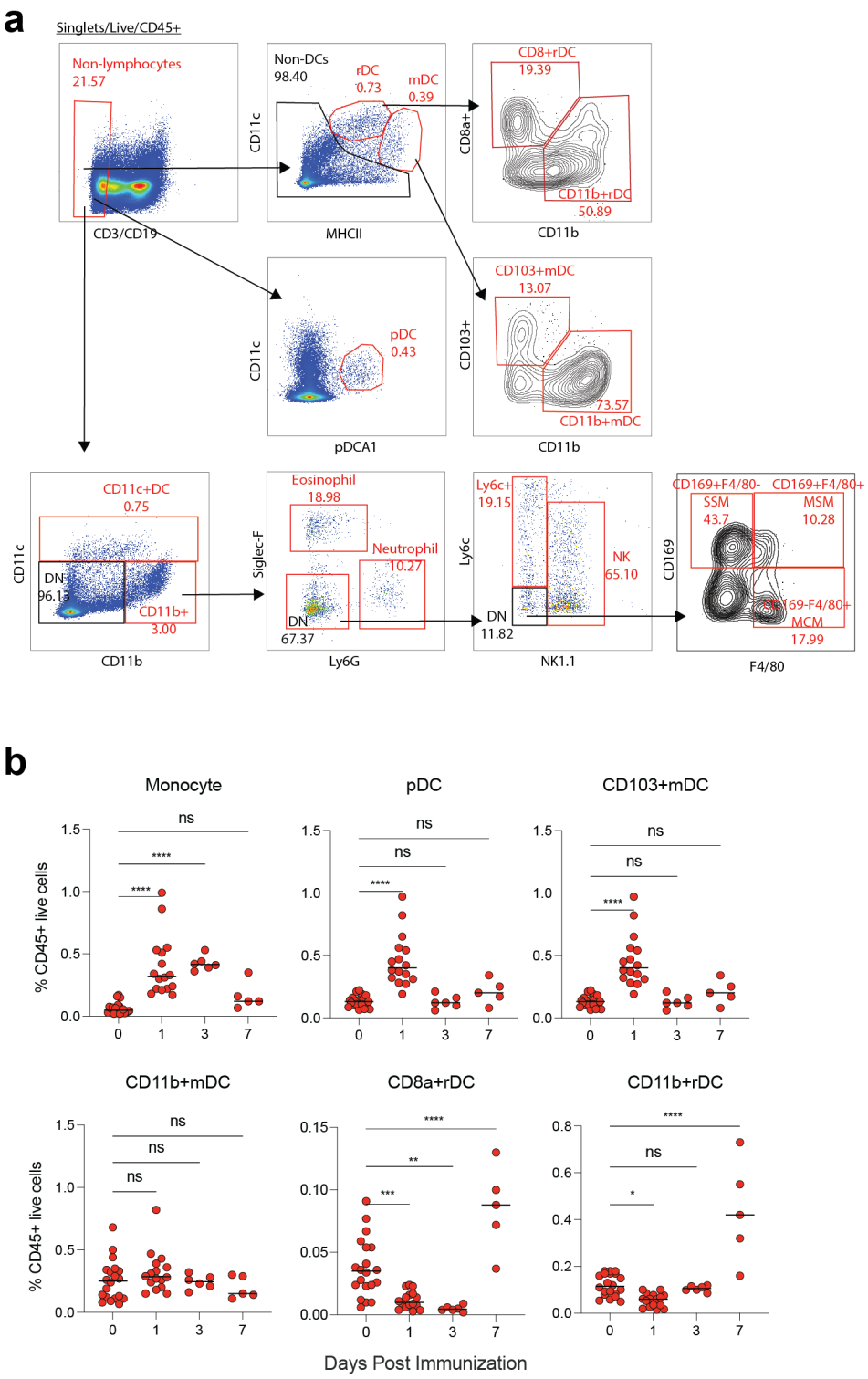
[13]Department of Microbiology and Immunology, Stanford University School of Medicine, Stanford University, Stanford, CA, USA.

*Correspondence to Bali Pulendran: bpulend@stanford.edu

Extended data Figure Legends

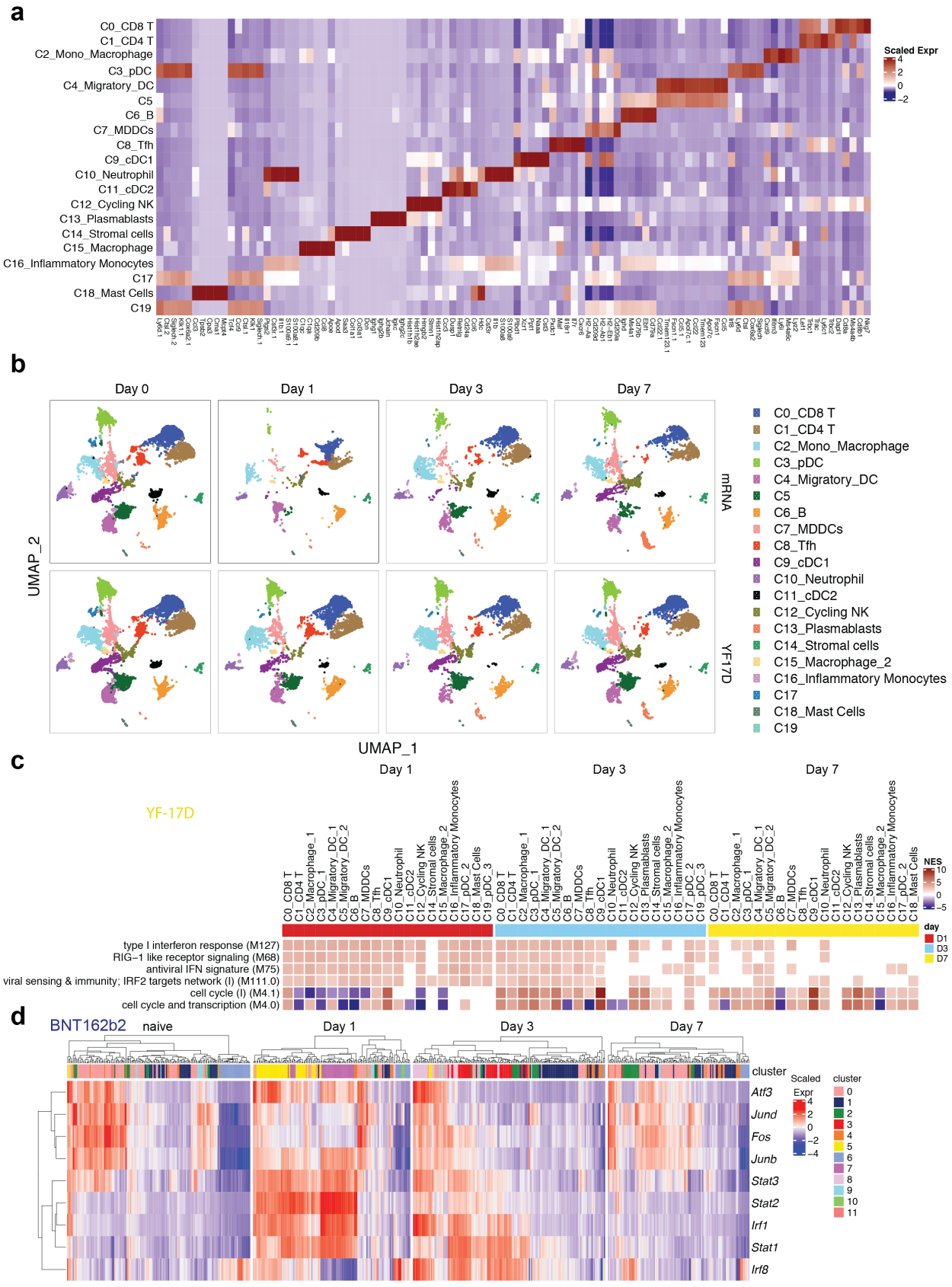


Extended Data Fig. 1 Immune response induced by low immunization dose in mice. a, S binding titers induced by low dose (0.2 µg/mouse) of BNT162b2 immunization measured by ELISA. **b,** Class I tetramer specific CD8 T cell response in lung and spleen tissue of mice measured at days 21 and 42 after BNT162b2 immunization (0.2 µg/mouse). **c-d,** Antigen specific CD8 **(c)** and CD4 **(d)** T cell response in lung and spleen tissue of mice detected at days 21 and 42 by intracellular cytokine staining (ICS) assay. **e,** Comparison between the activation of innate cells in dLNs induced by low (0.2 µg/mouse) and high immunization doses (5 µg/mouse). **f,** Cytokines/chemokines produced at 6 h post prime with low (0.2 µg/mouse) dose detected by Luminex assay. Data were combined from two independent experiments **(a)** or one representative experiment **(b-f).** One-Way ANOVA followed by Tukey's test was applied (a-e). P-values were determined using Student's t-tests (two-tailed) (f). *P<0.05, **P<0.01, ***P<0.001, ****P<0.0001.

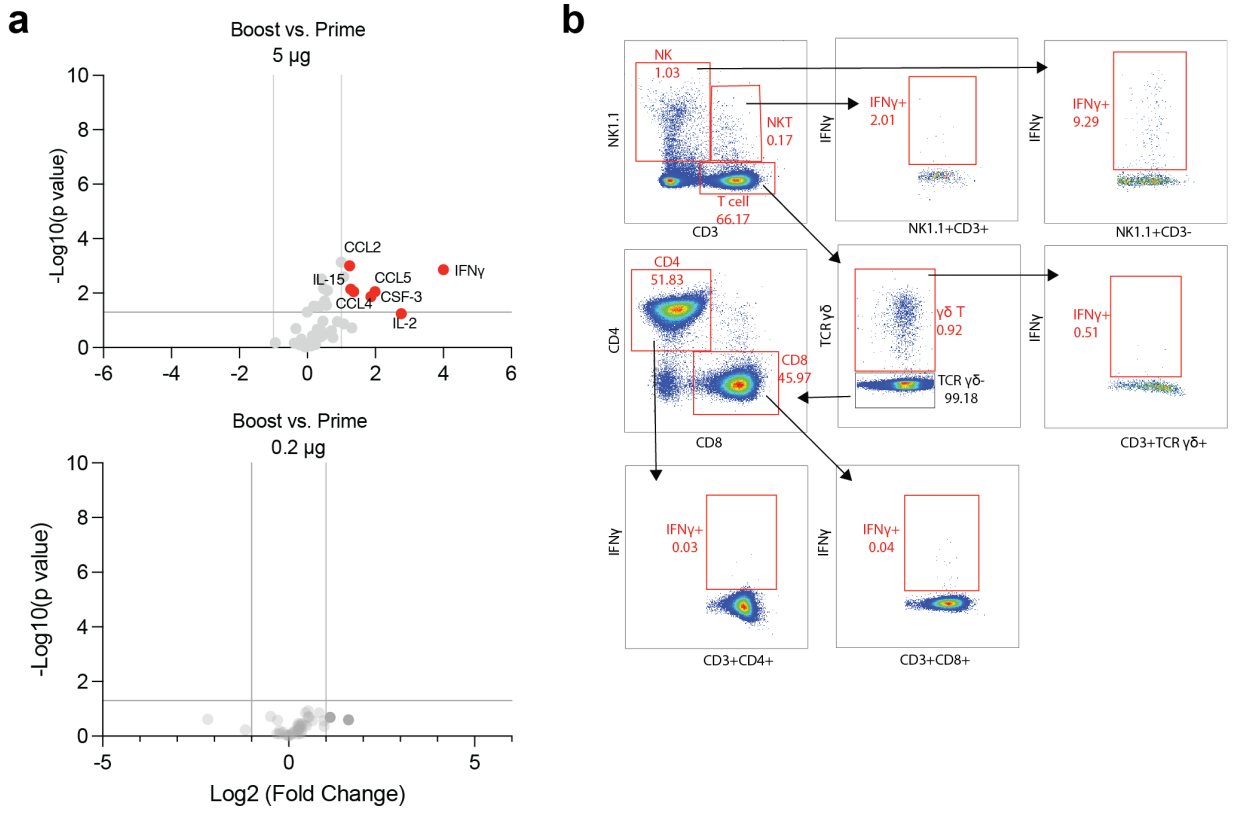


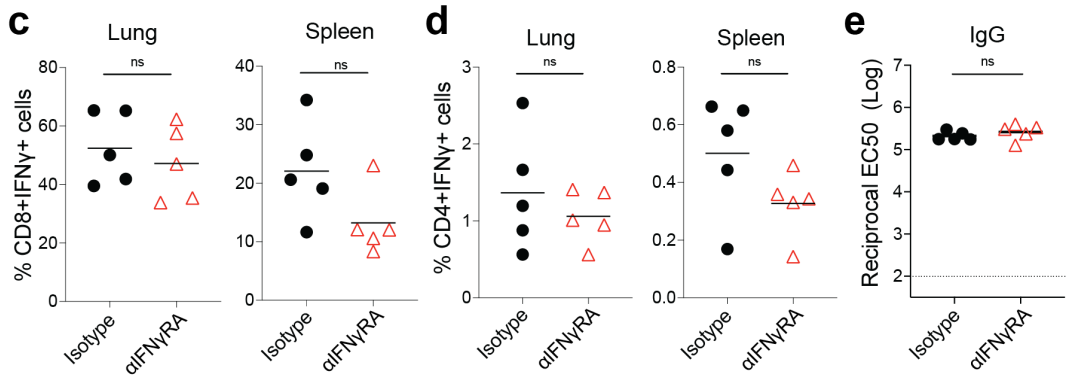
Extended Data Fig. 2 Innate cells activated by BNT162b2. a, Gating strategy. **b,** Frequency of innate cells in live CD45+ cells after BNT162b2 immunization in dLNs. Data were combined from at least two

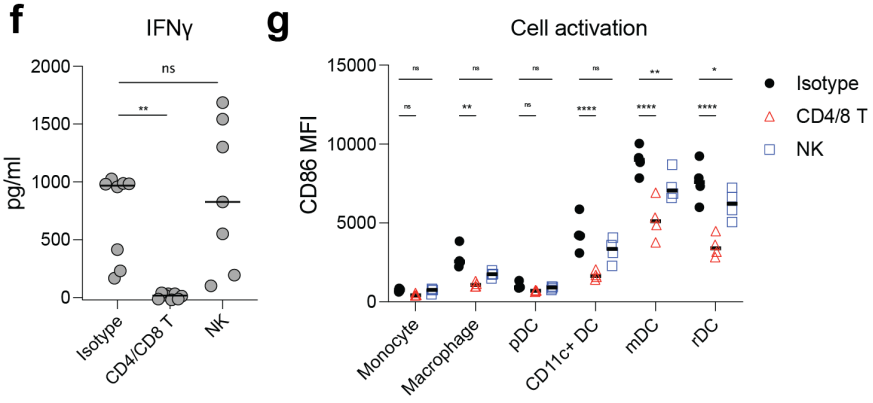
independent experiments. One-Way ANOVA followed by Tukey's test was applied in (**b**). *P<0.05, **P<0.01, ***P<0.001, ****P<0.0001.


a
C0_CD8 T
C1_CD4 T
C2_Mono_Macrophage
C3_pDC
C4_Migratory_DC
C5
C6_B
C7_MDDCs
C8_Tfh
C9_cDC1
C10_Neutrophil
C11_cDC2
C12_Cycling NK
C13_Plasmablasts
C14_Stromal cells
C15_Macrophage
C16_Inflammatory Monocytes
C17
C18_Mast Cells
C19
Scaled Expr
4
2
0
−2
b
Day 0
Day 1
Day 3
Day 7
UMAP_2
UMAP_1
mRNA
YF17D
C0_CD8 T
C1_CD4 T
C2_Mono_Macrophage
C3_pDC
C4_Migratory_DC
C5
C6_B
C7_MDDCs
C8_Tfh
C9_cDC1
C10_Neutrophil
C11_cDC2
C12_Cycling NK
C13_Plasmablasts
C14_Stromal cells
C15_Macrophage_2
C16_Inflammatory Monocytes
C17
C18_Mast Cells
C19
c
YF-17D
Day 1
Day 3
Day 7
C0_CD8 T
C1_CD4 T
C2_Macrophage_1
C3_pDC_1
C4_Migratory_DC_1
C5_Migratory_DC_2
C6_B
C7_MDDCs
C8_Tfh
C9_cDC1
C10_Neutrophil
C11_cDC2
C12_Cycling NK
C13_Plasmablasts
C14_Stromal cells
C15_Macrophage_2
C16_Inflammatory Monocytes
C17_pDC_2
C18_Mast Cells
C19_pDC_3
NES
10
5
0
−5
day
D1
D3
D7
type I interferon response (M127)
RIG−1 like receptor signaling (M68)
antiviral IFN signature (M75)
viral sensing & immunity; IRF2 targets network (I) (M111.0)
cell cycle (I) (M4.1)
cell cycle and transcription (M4.0)
d
BNT162b2
naive
Day 1
Day 3
Day 7
cluster
Scaled Expr
4
2
0
−2
−4
cluster
0
1
2
3
4
5
6
7
8
9
10
11
Atf3
Jund
Fos
Junb
Stat3
Stat2
Irf1
Stat1
Irf8

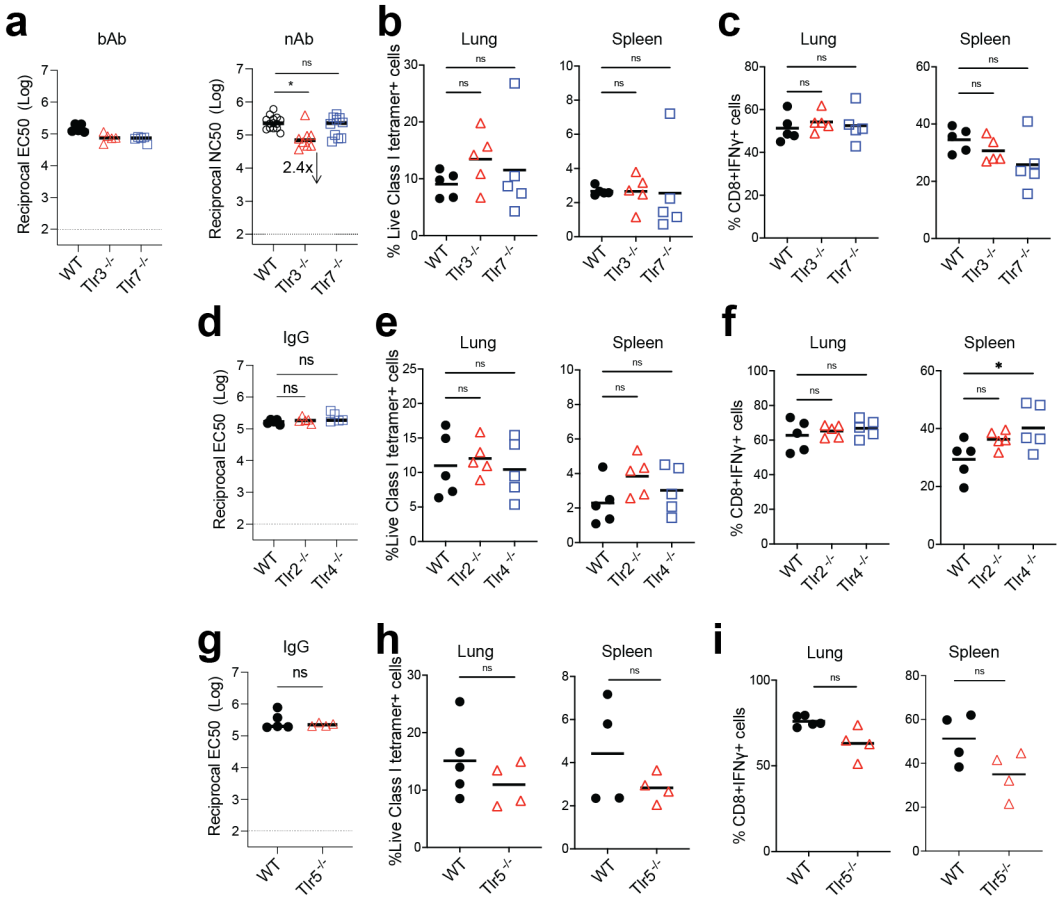
Extended Data Fig. 3 scRNAseq analysis of immune response induced by BNT162b2 and YF-17D. a, Clusters and their associated cluster-specific genes. **b,** UMAP of cell types clustered by single-cell transcriptional analysis at indicated time. **c,** Significantly enriched interferon BTMs (false discovery rate [FDR]< 0.05, absolute normalized enrichment score [NES]> 2) across all clusters from days 1 to 7 after YF-17D immunization. Only clusters with a significantly modulated pathway are shown. **d,** Heatmap of key interferon response and AP-1 transcription factors after BNT162b2 immunization over time. Samples used for scRNAseq were pooled from three independent experiments containing 8-10 mice.


a
Boost vs. Prime
5 µg
-Log10(p value)
CCL2
IFNγ
IL-15
CCL5
CSF-3
CCL4
IL-2
Boost vs. Prime
0.2 µg
-Log10(p value)
Log2 (Fold Change)
b
NK
1.03
NKT
0.17
T cell
66.17
NK1.1
CD3
IFNγ+
2.01
IFNγ
NK1.1+CD3+
IFNγ+
9.29
NK1.1+CD3-
CD4
51.83
CD8
45.97
CD4
CD8
TCR γδ
γδ T
0.92
TCR γδ-
99.18
IFNγ+
0.51
CD3+TCR γδ+
IFNγ+
0.03
CD3+CD4+
IFNγ+
0.04
CD3+CD8+

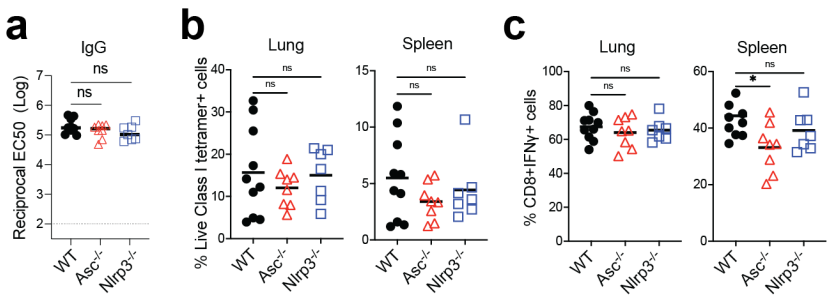

c
Lung
Spleen
% CD8+IFNγ+ cells
ns
Isotype
αIFNγRA
d
Lung
Spleen
% CD4+IFNγ+ cells
ns
Isotype
αIFNγRA
e
IgG
Reciprocal EC50 (Log)
ns
Isotype
αIFNγRA


f
IFNγ
pg/ml
ns
**
Isotype
CD4/CD8 T
NK
g
Cell activation
CD86 MFI
Isotype
CD4/8 T
NK
Monocyte
Macrophage
pDC
CD11c+ DC
mDC
rDC

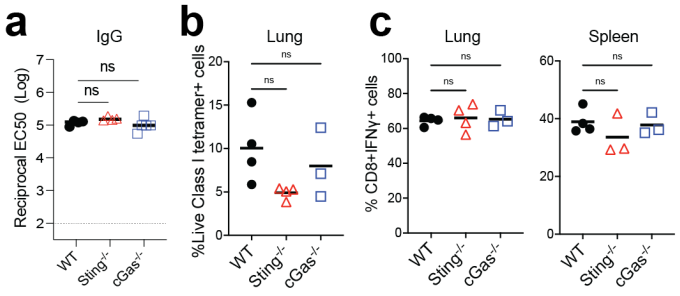
Extended Data Fig. 4 IFNγ production after prime and boost. a, Luminex assay of serum cytokines/chemokines at 6 h post-prime and boost with 5 μg/mouse and 0.2 μg/mouse, respectively. Data were combined from five mice for each group. **b,** Gating strategy to analyze IFNγ producing cells in dLNs. **c-e,** CD8+ and CD4+ T cell responses, and IgG titer at day 42 after blocking of IFNγ receptor. Mice were treated with IFNγ receptor neutralizing antibody or isotype control before boost at day 21. **f**, Serum IFNγ level at day 22 (1 day after boost) after T cells (CD4 and CD8 T cells) or NK cells depletion at day 21. **g**, Innate cell activation in spleen at 1 day post boost after T or NK cell depletion. Data were combined from two independent experiments (**f**), or from one experiment (**a, c-e**). P-values were determined using Student's t-tests (two-tailed) (**a, c-e**), One-Way ANOVA (**f**), or Two-way ANOVA (**g**). *P<0.05, **P<0.01, ***P<0.001, ****P<0.0001.



Extended Data Fig. 5 Roles of TLRs for BNT162b2-induced antibody and T cell response. bAb and nAb titers of WT and *Tlr3*$^{-/-}$, *Tlr7*$^{-/-}$ **(a),** bAb (IgG) titers of WT and *Tlr2*$^{-/-}$, *Tlr4*$^{-/-}$ **(d),** *Tlr5*$^{-/-}$ **(g)** mice at day 42. CD8+ T cell response in WT and *Tlr3*$^{-/-}$, *Tlr7*$^{-/-}$ **(b-c),** *Tlr2*$^{-/-}$, Tlr4$^{-/-}$ **(e-f),** and *Tlr5*$^{-/-}$ **(h-i)** mice. Data were combined from two independent experiments. One-Way ANOVA followed by Tukey's test was applied in (**a-f**). P-values in (**g-i**) were determined using Student's t-tests (two-tailed). *P<0.05, **P<0.01.

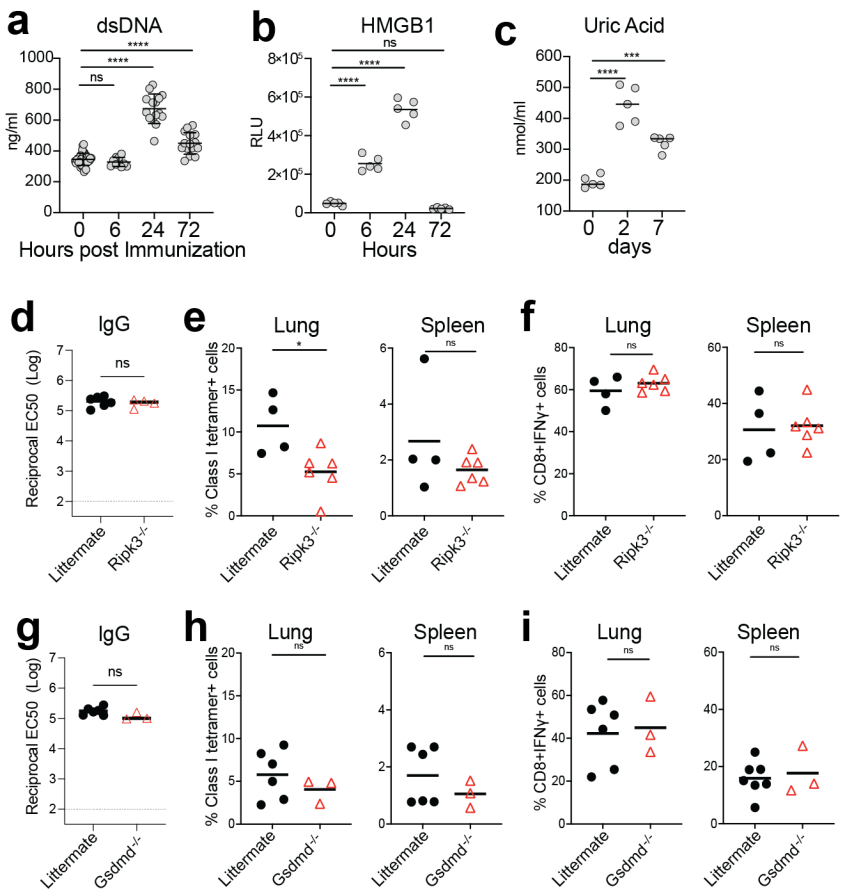


Extended Data Fig. 6 Roles of the inflammasome for BNT162b2-induced antibody and T cell response. **a,** IgG titers of WT, *Asc*$^{-/-}$, and *Nlrp3*$^{-/-}$ mice at day 42. **(b-c),** CD8+ T cell response in WT, *Asc*$^{-/-}$, and *Nlrp3*$^{-/-}$ mice. Data were combined from two independent experiments. One-Way ANOVA followed by Tukey's test was applied. *P<0.05.

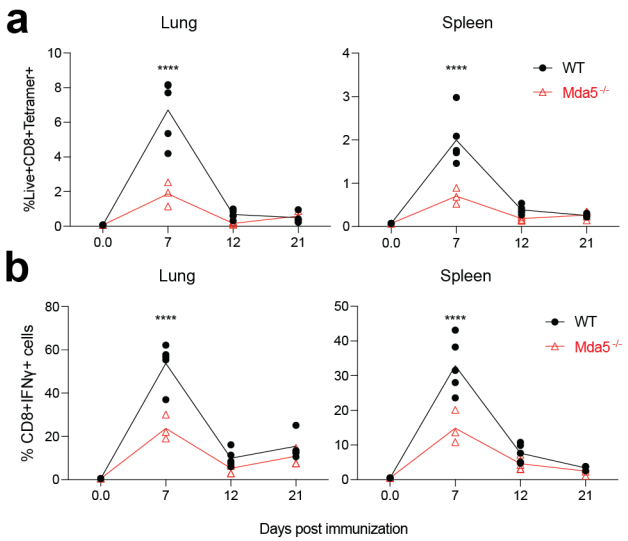


Extended Data Fig. 7 Role of cGAS and STING for BNT162b2-induced antibody and T cell response.

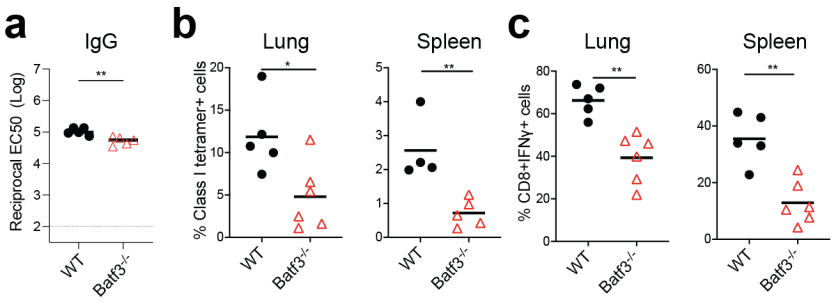
a, IgG titers of WT, *cGas*$^{-/-}$, and *Sting*$^{-/-}$ mice at day 42. **(b-c),** CD8+ T cell response in WT, *cGas*$^{-/-}$, and *Sting*$^{-/-}$ mice. Data are one representative of two independent experiments. One-Way ANOVA followed by Tukey's test was applied.



Extended Data Fig. 8 Role of cell death in BNT162b2-induced antibody and T cell response. a-c, DAMP signals including dsDNA **(a),** HMGB1 **(b),** and uric acid **(c)** induced by BNT162b2 immunization at the indicated time. **d,** IgG titers of littermate and *Ripk3*$^{-/-}$ mice at day 42. **e-f,** CD8+ T cell response in littermate and *Ripk3*$^{-/-}$ mice. **g,** IgG titers of littermate and *Gsdmd*$^{-/-}$ mice at day 42. **h-i,** CD8+ T cell response in littermate and *Gsdmd*$^{-/-}$ mice. Data were one representative of at least two independent experiments **(a),** or one representative experiment **(b-i).** One-Way ANOVA followed by Tukey's test was applied in (**a-c**). P-values in (**d-i**) were determined using Student's t-tests (two-tailed). *P<0.05, ***P<0.001, ****P<0.0001.



Extended Data Fig. 9 Role of MDA5 in BNT162b2-induced T cell response after prime. a-b, CD8+ T cell response in WT and *Mda5*$^{-/-}$ mice at indicated time post prime. P-values were determined using two-way ANOVA. ****P<0.0001.



Extended Data Fig. 10 Role of Batf3 in BNT162b2-induced antibody and T cell response. a, IgG titers of WT and *Batf3*$^{-/-}$ mice at day 42. **b,** CD8+ T cell response in WT and *Batf3*$^{-/-}$ mice. Data were one representative of three independent experiments. P-values were determined using Student's t-tests (two-tailed). *P<0.05, **P<0.01.

nature portfolio

Corresponding author(s): Bali Pulendran

Last updated by author(s): Jan 29, 2022

Reporting Summary

Nature Portfolio wishes to improve the reproducibility of the work that we publish. This form provides structure for consistency and transparency in reporting. For further information on Nature Portfolio policies, see our Editorial Policies and the Editorial Policy Checklist.

Statistics

For all statistical analyses, confirm that the following items are present in the figure legend, table legend, main text, or Methods section.

n/a	Confirmed
☐	☒ The exact sample size (*n*) for each experimental group/condition, given as a discrete number and unit of measurement
☐	☒ A statement on whether measurements were taken from distinct samples or whether the same sample was measured repeatedly
☐	☒ The statistical test(s) used AND whether they are one- or two-sided *Only common tests should be described solely by name; describe more complex techniques in the Methods section.*
☒	☐ A description of all covariates tested
☐	☒ A description of any assumptions or corrections, such as tests of normality and adjustment for multiple comparisons
☐	☒ A full description of the statistical parameters including central tendency (e.g. means) or other basic estimates (e.g. regression coefficient) AND variation (e.g. standard deviation) or associated estimates of uncertainty (e.g. confidence intervals)
☐	☒ For null hypothesis testing, the test statistic (e.g. *F*, *t*, *r*) with confidence intervals, effect sizes, degrees of freedom and *P* value noted *Give P values as exact values whenever suitable.*
☒	☐ For Bayesian analysis, information on the choice of priors and Markov chain Monte Carlo settings
☒	☐ For hierarchical and complex designs, identification of the appropriate level for tests and full reporting of outcomes
☒	☐ Estimates of effect sizes (e.g. Cohen's *d*, Pearson's *r*), indicating how they were calculated

Our web collection on statistics for biologists contains articles on many of the points above.

Software and code

Policy information about availability of computer code

Data collection	BD FACSDiva software version 8.0.1 was used for collecting the flow cytometry data on the LSRII.2 and BD FACSymphony machine.
Data analysis	FlowJo software v.10.0 (Treestar Inc); GraphPad Prism version 9.0.1; Adobe Illustrator 25.0. All statistical analysis are two-sided. All analyses and visualizations of sc-RNAseq data were performed in R (V3.6.3). Computer code is available upon reasonable request.

For manuscripts utilizing custom algorithms or software that are central to the research but not yet described in published literature, software must be made available to editors and reviewers. We strongly encourage code deposition in a community repository (e.g. GitHub). See the Nature Portfolio guidelines for submitting code & software for further information.

Data

Policy information about availability of data

All manuscripts must include a data availability statement. This statement should provide the following information, where applicable:

- Accession codes, unique identifiers, or web links for publicly available datasets
- A description of any restrictions on data availability
- For clinical datasets or third party data, please ensure that the statement adheres to our policy

Single-Cell RNAseq data are publicly accessible in the GEO under accession numbers GSE179131.

Field-specific reporting

Please select the one below that is the best fit for your research. If you are not sure, read the appropriate sections before making your selection.

☒ Life sciences ☐ Behavioural & social sciences ☐ Ecological, evolutionary & environmental sciences

For a reference copy of the document with all sections, see nature.com/documents/nr-reporting-summary-flat.pdf

Life sciences study design

All studies must disclose on these points even when the disclosure is negative.

Sample size	No statistical test was used to determine the number of samples. Sample sizes were determined as appropriate to evaluate detection of large vaccine effects based on several studies done by us and others.
Data exclusions	No data were excluded from any of the analysis.
Replication	All the assays were repeated with biological replicates in each experiment, and all the repeats are successful.
Randomization	The study involved the same batch of mice (C57BL/6) that were obtained from Jackson laboratories. Mice were allocated to cages with 3-5 mice per cage, and each cage was assigned to an immunization group.
Blinding	All the experiments were conducted in an unblinded way since the investigators were involved in overall conduct of the study.

Reporting for specific materials, systems and methods

We require information from authors about some types of materials, experimental systems and methods used in many studies. Here, indicate whether each material, system or method listed is relevant to your study. If you are not sure if a list item applies to your research, read the appropriate section before selecting a response.

Materials & experimental systems

n/a	Involved in the study
☐	☒ Antibodies
☒	☐ Eukaryotic cell lines
☒	☐ Palaeontology and archaeology
☐	☒ Animals and other organisms
☒	☐ Human research participants
☒	☐ Clinical data
☒	☐ Dual use research of concern

Methods

n/a	Involved in the study
☒	☐ ChIP-seq
☐	☒ Flow cytometry
☒	☐ MRI-based neuroimaging

Antibodies

Antibodies used

Antibody, Fluorophore, Vendor, Cat #, Clone, Lot #

anti-Ly6C, BV780, Biolegend, # 128041, HK1.4, B311364
anti-Ly6G, APC-Cy7, Biolegend, # 127624, 1A8, B294666
anti-CD19, BB700, BD, # 566411, 1D3, 0079006
anti-CD3, BB700, BD, #742175, 17A2, 0202623
anti-MHCII, AF700, eBioscience, #56-5321-82, M5/114.15.2, 2210930
anti-CD11b, BV650, Biolegend, #101239, M1/70, B335585
anti-CD11c, BV421, Biolegend, #117330, N418, B294539
anti-CD86, A647, Biolegend, #105020, GL-1, B245405
anti-Siglec-F, PE-CF594, BD, #562757, E50-2440, 0064626
anti-CD24, BUV395, BD, #744471, M1/69, 1102765
anti-CD45, BV605, Biolegend, #103140, 30-F11, B313899
anti-CD169, PE-Cy7, Biolegend, #142412, 3D6.112, B264616
anti-PDCA-1, BUV563, BD, #749275, 927, 1271522
anti-CD8a, BUV805, BD, #612898, 53-6.7, 0328533
anti-CD103, PE, eBioscience, #12-1031-82, 2E7, 2054351
anti-NK1.1, BV510, Biolegend, #108738, PK136, B326849
anti-F4/80, BUV737, BD, #749283, T45-2342, 1168211
anti CD3, BV785, Biolegend, #100355, 145-2C11, B303965
anti-CD4, BV650, Biolegend, #100555, RM4-5, B250896
anti-CD8, BV711, BD, #563046, 53-6.7, 0239184
anti-CD69, PECy7, Biolegend, # 104511, H1.2F3, B291440

anti-CD103, PerCP-Cy5.5, BioLegend, #121416, 2E7, B314149
anti-CD44, BV421, Biolegend, #103040, IM7, B306124
anti-CD45, BV605, Biolegend, #103139, 30-F11, B301866
anti-IFNγ, APC, Biolegend, #505810, XMG1.2, B290393a
anti-TNFa, FITC, Biolegend, #506304, MP6-XT22, B271488
anti-IL2, AF700, Biolegend, #503818, JES6-5H4, B335226
anti-IL4, PerCPCy5.5, Biolegend, #504124, 11B11, B301560
anti-CD95, PECy7, BD Biosciences, #557653, Jo2, 0321061
anti-CD19, PerCP-Cy5.5, BioLegend, #115534, 6D5,B288784
anti-CD38, BUV395, BD Biosciences, #740245, 90,1242465
anti-CD44 , APC-Cy7, BioLegend, #103062, IM7, B290267
anti-CD138, BV605, BD Biosciences, #563147, 281-2, 1097493
anti-CD3, A700, BioLegend, #100216, 17A2, B323639
anti-CD4, BV650, BioLegend, #100469,GK1.5, B311210
anti-CXCR5, BV711, BioLegend, #145529, L138D7,B315903
anti-PD1, PECF594, BioLegend, #135228, 29F.1A12, B320108
anti-γδ TCR, A488, BioLegend, #144611, GL3, B343654

Validation

All antibodies used were evaluated by the manufacturers as provided in their websites.
Biolegend:https://www.biolegend.com/en-us/quality/product-development
BD:https://www.biocompare.com/Antibody-Manufacturing/355107-Antibody-Manufacturing-Perspectives-BD-Bioscience/
Thermofisher: https://www.thermofisher.com/us/en/home/life-science/antibodies/invitrogen-antibody-validation.html

Animals and other organisms

Policy information about studies involving animals; ARRIVE guidelines recommended for reporting animal research

Laboratory animals

C57BL/6, B6129SF2/J, Tlr2-/-, Tlr3-/-, Tlr4-/-, and Tlr5-/- mice were purchased from Jackson Laboratories. Ripk3-/-, Gsdmd-/-, and littermates were gifts from Genentech Inc (Alex Gitlin). Ifnar1-/-, Mda5-/-, Sting-/-, cGas-/-, and Batf3-/- mice were bred in our animal facility at Stanford University. Asc-/- and Nlrp3-/- mice were originally from Vishva M Dixit lab in Genetech, Tlr7-/- mice were originally from S.Akira lab (Osaka University). Asc-/-, Nlrp3-/- and Tlr7-/- mice were then maintained and provided by Jackson Laboratories. Mice were sex-matched and aged between 8 and 14 weeks.

Wild animals

No wild animals were used in this study.

Field-collected samples

No field-collected samples were used in this study.

Ethics oversight

All mice in this study were maintained under specific pathogen-free conditions, 12 light/12 dark cycle, temperatures of ~18-23°C with 40-60% humidity, and handled according to the protocol approved by the Institutional Animal Care and Use Committee (IACUC) of Stanford University.

Note that full information on the approval of the study protocol must also be provided in the manuscript.

Flow Cytometry

Plots

Confirm that:

☒ The axis labels state the marker and fluorochrome used (e.g. CD4-FITC).

☒ The axis scales are clearly visible. Include numbers along axes only for bottom left plot of group (a 'group' is an analysis of identical markers).

☒ All plots are contour plots with outliers or pseudocolor plots.

☒ A numerical value for number of cells or percentage (with statistics) is provided.

Methodology

Sample preparation

1, Flow cytometry analysis of innate cells: Draining iliac lymph nodes from BNT162b2 immunized mice, draining inguinal lymph nodes from YF-17D immunized mice, along with whole lung or spleen, were harvested and digested with 1 mg/mL collagenase type IV (Worthington) for 20 min at 37 °C, followed by smashing with a 100 µm strainer to make a single-cell suspension. Red blood cells from the lung and spleen were lysed before staining.
2, Flow cytometry of GC B, TFH, and plasma cells in lymph nodes: dLNs were harvested and smashed with a 100 µm strainer to make a single-cell suspension followed by staining for viability with Ghost Dye Violet 510 (Tonbo Biosciences) for 5 min on ice in 1x PBS-2mM EDTA.
3, Intracellular cytokine staining assay: Whole Spleen and lung were harvested at 42 days post-prime (21 days post-boost). Briefly, mononuclear populations from the lung were isolated from the interphase of a 70-40% Percoll gradient of single suspension prepared by enzymatic digestion with 1 mg/mL type IV collagenase and DNase I. Single-cell suspensions from the spleen were prepared without digestion. Cells were plated at ~2 x 10^6 cells/well in 96-well U-shaped plates and re-stimulated with S-specific overlapping peptide pools (1 µg/mL of each peptide) in complete RPMI1640 medium for overnight

incubation at 37 °C in the presence of brefeldin-A (10 µg/mL). At day 2, cells were stained with Ghost Dye Violet 510 (Tonbo Biosciences) for 10 min on ice in 1x PBS-2mM EDTA.
4, scRNAseq samples and preparation: Draining iliac lymph nodes from BNT162b2 immunized mice and draining inguinal lymph nodes from YF-17D immunized mice were harvested and digested into single-cell suspensions. One million total cells were set aside on ice. The rest of the cells were incubated with biotinylated CD3, CD19, and NK1.1 Ab on ice for 20 min. Streptavidin-labeled magnetic beads (BD IMag™ Streptavidin Particles Plus-DM) were added and incubated on ice for 30 min. Unbonded cells were collected and CD11b+ myeloid cells, pDCs (CD11clo, CD11b-PDCA-1+), and DCs (CD11c+MHC-II+) were sorted with flow cytometry. Sorted cells were combined with total lymphocytes at a 1:1 ratio and resuspended in cold PBS supplemented with 1% BSA (Miltenyi) and 0.5 U/µL RNase Inhibitor (Sigma Aldrich). Cells were partitioned into Gel Beads-in emulsion (GEMs) using the 10x Chromium 3' V3 chemistry system (10x Genomics).

Instrument

Cells were analyzed with an LSRII.2 or BD FACSymphony analyzer at the Stanford Shared FACS Facility.

Software

BD FACSDiva software version 8.0.1 was used for collecting the flow cytometry data on the LSRII.2 machine.
FlowJo software v.10.0 (Treestar Inc) was used to analyze the flow cytometry data.

Cell population abundance

For scRNAseq samples and preparation: CD11b+ myeloid cells, pDCs (CD11clo, CD11b-PDCA-1+), and DCs (CD11c+MHC-II+) were sorted with flow cytometry after remove CD3, CD19, and NK1.1 with Streptavidin-labeled magnetic beads (BD IMag™ Streptavidin Particles Plus-DM). Sorted cells were combined with total lymphocytes at a 1:1 ratio and resuspended in cold PBS supplemented with 1% BSA (Miltenyi) and 0.5 U/µL RNase Inhibitor (Sigma Aldrich) for scRNAseq analysis.

Gating strategy

Cells were selected based on FSC-A vs. SSC-A, singlets were selected using FSC-A vs. FSC-H. Live CD45+CD3+ T cells were used for analysis of antigen-specific T cells. CD4 and CD8 T cells were selected as CD3+CD8-CD4+ or CD3+ CD8+. Live CD45+CD3 +CD19-CD4+PD1+CXCR5+ T cells were gated as TFH cells, Live CD45+CD3-CD19+CD38-CD95+ cells were gated as GC B cells, Live CD44+CD138+ cells were gated as plasma cells. Gating strategies for innate immune cells, NKT, and γδ T cells are provided in the manuscript.

☒ Tick this box to confirm that a figure exemplifying the gating strategy is provided in the Supplementary Information.

nature research

Peer Review Information

Journal: Nature Immunology
Manuscript Title: Mechanisms of innate and adaptive immunity to the Pfizer-BioNTech BNT162b2 vaccine
Corresponding author name(s): Bali Pulendran

Reviewer Comments & Decisions:

Decision Letter, initial version:

Subject: Decision on Nature Immunology submission NI-A33009

Message: 10th Nov 2021

Dear Dr. Pulendran,

Your Article, "Mechanisms of innate and adaptive immunity to the Pfizer-BioNTech BNT162b2 vaccine" has now been seen by 2 referees. You will see from their comments below that while they find your work of interest, some important points are raised. We are very interested in the possibility of publishing your study in Nature Immunology, but would like to consider your response to these concerns in the form of a revised manuscript before we make a final decision on publication.

We also took a look at your author response and can confirm that that suggested revisions you have outlined are suitable for further consideration; however, we would like to note that anything that takes you more than ~6 weeks can be omitted - we certainly do not want you to do experiments that would take 4 months.

We therefore invite you to revise your manuscript taking into account all reviewer and editor comments. Please highlight all changes in the manuscript text file in Microsoft Word format.

We are committed to providing a fair and constructive peer-review process. Do not hesitate to contact us if there are specific requests from the reviewers that you believe are technically impossible or unlikely to yield a meaningful outcome.

When revising your manuscript:

* Include a "Response to referees" document detailing, point-by-point, how you addressed each referee comment. If no action was taken to address a point, you must provide a compelling argument. This response will be sent back to the referees along with the revised manuscript.

* If you have not done so already please begin to revise your manuscript so that it conforms to our Article format instructions at http://www.nature.com/ni/authors/index.html. Refer also to any guidelines provided in this letter.

* Please include a revised version of any required reporting checklist. It will be available to referees to aid in their evaluation of the manuscript goes back for peer review. They are available here:

Reporting summary:
https://www.nature.com/documents/nr-reporting-summary.pdf

When submitting the revised version of your manuscript, please pay close attention to our href="https://www.nature.com/nature-research/editorial-policies/image-integrity">Digital Image Integrity Guidelines. and to the following points below:

-- that unprocessed scans are clearly labelled and match the gels and western blots presented in figures.
-- that control panels for gels and western blots are appropriately described as loading on sample processing controls
-- all images in the paper are checked for duplication of panels and for splicing of gel lanes.

Finally, please ensure that you retain unprocessed data and metadata files after publication, ideally archiving data in perpetuity, as these may be requested during the peer review and production process or after publication if any issues arise.

Please use the link below to submit your revised manuscript and related files:
[REDACTED]

Note: This URL links to your confidential home page and associated information about manuscripts you may have submitted, or that you are reviewing for us. If you wish to forward this email to co-authors, please delete the link to your homepage.

We hope to receive your revised manuscript within two weeks. If you cannot send it within this time, please let us know. We will be happy to consider your revision so long as nothing similar has been accepted for publication at Nature Immunology or published elsewhere.

Please do not hesitate to contact me if you have any questions or would like to discuss these revisions further.

Nature Immunology is committed to improving transparency in authorship. As part of our efforts in this direction, we are now requesting that all authors identified as 'corresponding author' on published papers create and link their Open Researcher and Contributor Identifier (ORCID) with their account on the Manuscript Tracking System (MTS), prior to acceptance. ORCID helps the scientific community achieve unambiguous attribution of all

scholarly contributions. You can create and link your ORCID from the home page of the MTS by clicking on 'Modify my Springer Nature account'. For more information please visit please visit www.springernature.com/orcid.

We look forward to seeing the revised manuscript and thank you for the opportunity to review your work.

Sincerely,

Nick Bernard, PhD
Senior Editor
Nature Immunology

Reviewers' Comments:

Reviewer #1:
Remarks to the Author:
Chunfeng Li and colleagues performed an extensive analysis of the mechanisms of innate and adaptive immunity to the Pfizer-biontech BNT162b2 vaccine. They combined various techniques including flow cytometry, measurement of chemokines and cytokines, viral neutralization tests, single cell transcriptomic analysis, use of KO mice lacking various immune sensors, to provide a large overview of the impact of the Pfizer vaccine on the activation and role of the main immune cell subsets. It is shown that induction of antibody and T cell responses to BNT162b2 was not dependent on signaling via TLRs 2, 3 ,4 ,5, inflammasome activation, necroptosis or pyroptosis. CD8 T cell responses are shown to be dependent on type I IFN-dependent MDA5 signaling. This is an excellent work with important information regarding the function of mRNA-based vaccines.

Main concerns

1. Vaccine dose. The authors used a dose of 5 µg per mouse. In humans, the vaccine dose is 30 µg. A mouse weights approximatively 20 g and a human weights 60 kg. The authors thus injected in their mice about 500 times more mRNA/kg than the vaccine dose in humans. This high concentration may generate innate and inflammatory responses that are not relevant to humans. Did the authors try lower doses of vaccine? This should be tested or at least discussed as a limitation of the study.

2. No viral challenge was performed in the different KO mice. This should be discussed as another limitation of the study. Some SARs-CoV-2 variants (beta and gamma variants for instance) have been shown to naturally infect mice, without the need of expressing the human ACE2 receptor, which may facilitate the use of various KO mice in future studies. Other teams have performed similar but less extensive studies in mice which included viral challenge. For instance, Iwasaki's team recently studied the adaptive immune determinants of viral clearance and protection in mouse models of SARS-CoV-2 (Science immunology). It is interesting to see that in this recent article, the vaccine dose was only 1 µg. The recent literature should be discussed.

Reviewer #2:
Remarks to the Author:
Review of Li et al

This paper from the Pulendran laboratory follows their elegant systems-based studies over the past several years evaluating the immunological correlates of responses against influenza, SARS-CoV-2, and yellow fever vaccines or viral infections. Their recent study of human responses to BNT162b2 published in Nature showed that booster vaccination stimulated an enhanced innate immune response as compared to primary vaccination, with a greater frequency of CD14+CD16+ inflammatory monocytes, a higher concentration of plasma IFNγ, and a transcriptional signature of innate antiviral immunity. In the current study, they performed analogous immunization studies in mice with the same (remnant) vaccine to determine the mechanistic basis for these observations as well as to evaluate immune responses in key tissues (e.g., draining lymph node [dLN], spleen, and lung). In addition to showing robust B and T cell responses (which has been seen by others), they report several potentially interesting observations: (a) high levels of antigen-specific CD8+ T cells in the lung after intramuscular boosting that appear dependent on MDA5 and type I IFN signaling; (b) rapid activation of specific myeloid cell subsets, some which contain vaccine mRNA in the dLN at early time points; (c) enhanced early serum cytokine/chemokine responses including IFNγ, which was important for innate immune cell activation; and (d) the unanticipated dispensability of many pathogen sensors (TLRs, NLR, etc.) for vaccine-mediated induction of B and T cell responses. The authors conclude that their study provides new insights into how BNT162b2 stimulates immune responses in vivo.

There are many strengths to this paper including the important question it addresses, the generally high-quality data, the clarity in writing, the rigor of design, the concordance of some of the findings (IFNγ induction and transcriptional patterns of activation of myeloid cell subsets) with published human studies, the analysis of multiple tissues, and the remarkable attempt to identify a key sensor that sets of the inflammatory process. Notwithstanding this, and despite a large body of careful work, there are some weaknesses (detailed below) that must be addressed to provide greater mechanistic clarity. For example, despite finding elevated levels of IFNγ in mice and humans, and showing it modulates myeloid cell activation, the impact of this cytokine on primary or secondary B and T cell responses was never tested. Moreover, the potential impact of MDA5 and type I IFN signaling on survival of memory CD8+ T cells has been largely passed over, which could affect their conclusion regarding the innate impact of these molecules/pathway on anamnestic CD8+ T cell responses after BNT162b2 boosting. The mouse studies were performed to provide new mechanistic insight as to why BNT162b2 induces such robust adaptive immunity. Beyond showing that the vaccine rapidly activates innate immune myeloid cells, which they already demonstrated in humans (Arunachalam et al., 2021), the main novel mechanistic take-aways require further delineation.

Major Comments

1. IFNγ and lack of direct linkage to B and T cell phenotypes. (a) In their recent analysis of mRNA vaccine responses in humans, the same authors showed that BNT162b2 induced a much greater innate immune response after boosting than after primary vaccination, and this was associated with increased plasma levels of IFNγ, enhanced transcriptional signatures of innate immunity, and antiviral immunity in myeloid cells (Arunachalam et

al., 2021). In the current mouse paper, the authors demonstrate a similar augmented IFNγ response occurs soon after boosting (Fig 5a), determine which cells produce it (NK/T), and link this to activation (CD86 expression) of myeloid cells. However, a key advantage of performing studies in mice is the ability to test the significance of the IFNγ response for adaptive B and T cell responses. The authors should use their neutralizing anti-IFNγ antibody to test the functional impact of IFNγ on the primary or secondary B and T cell responses induced by BNT162b2. If there were no major impact, what is the significance of the IFNγ induction beyond myeloid cell activation? (b) While they show in Fig 5e clearly that both NK and T cells are sources of IFNγ, it is not clear which is more important for the increased innate immune response seen after boosting – given that NK produced IFNγ is present in both primary and secondary responses, it would seem that T cell-derived IFNγ mediates this – could immune cell depletion studies confirm this?

2. MDA5 and type IFN and known effects on memory CD8+ T cells. A key finding in this paper is that the secondary CD8+ T cell response after boosting with BNT162b2 is dependent on MDA5 and type I IFN (Fig 7). The authors imply this is related to data in Fig 6 where they show that within a day of immunization, vaccine mRNA is present in macrophage and DC subsets in the dLN and associated with a type I IFN/MDA5/ISG response (Fig 6 and S10). There are several issues that confound this conclusion: (a) In Fig 7, the authors examine the CD8+ T cell response at day 42 and not at day 21 (as in Fig 2a); based on their hypothesis and data in Fig 7d showing low IFNα levels within one day of primary immunization in Mda5-/- mice, shouldn't primary CD8+ T cell responses be affected? (b) The data on anamnestic response is problematic because of reported effects of both MDA5 and type I IFN on memory CD8+ T cell responses (Welsh et al., 2012). The Colonna laboratory showed that in mice lacking MDA5, the majority of CD8+ T cells do not survive after primary immunization with poly I:C and antigen, impairing memory response to subsequent Ag challenge (Wang et al., 2010) [not cited]. Similarly, Murali-Krishna showed a lack of direct CD8+ T cell contact with type I IFN abrogates the generation memory cells due to poor survival during the antigen-driven proliferation phase (Kolumam et al., 2005) [cited]. Thus, the poor anamnestic CD8+ T cell responses seen after BNT162b2 boosting could be due to poor survival of memory CD8+ T cells rather than the observed defects in innate immune activation. To address this issue, the authors need to examine the CD8+ T cell response (including memory cells) at day 21 and prior to boosting in Mda5-/- mice. If the induction of memory is compromised, how does this affect their mechanistic interpretation?

3. B cell response analysis. In Fig 1, the authors provide a reasonably detailed analysis of B cell response generated by the BNT162b2 vaccine including spike-binding antibodies, functional neutralization, and flow-based analysis of cellular subsets. However, in their mechanistic studies with KO animals in Fig 7, S5, S6, S7, S8, and S9, they only perform spike-binding IgG assays. It is possible that binding is not the entire story, and differences in neutralizing titers or GC B reactions might occur in the absence of particular innate immune molecules. Indeed recent papers suggesting the LNP component itself is immunostimulatory and relies on IL-6 (and not on MAVS or MyD88) (Alameh et al.), which is induced soon after BNT162b2 immunization (Fig 3e).

4. Lung antigen-specific CD8+ T cells after vaccination. It is remarkable that 21 days after an intramuscular boost with BNT162b2, >60% of the lung CD8+ T cells show antigen-specificity as judged by IFNγ production (Fig 2b), especially given a complete absence of resident memory T cells (Fig 2d). How do the authors explain this observation? Did they perfuse the lung tissue extensively to remove circulating cells? Is this unique to the mRNA

vaccination platform? Why are there greater frequencies that in lymphoid tissues even though presumably there is no antigen or inflammation driving them there? What about another parenchymal tissue (e.g., liver or kidney)? The authors make a comment about this in the Discussion (lines 311-312) but provide no additional explanation or supporting data from the literature. Is anything similar seen in humans or NHPs?

5. In Fig 6f and S10, the authors suggest that the spike mRNA is associated with MDA5-dependent innate immune cell activation and innate immune response-related transcriptional modules. What would MDA5 be recognizing? – presumably double stranded elements of the spike mRNA? Can the authors confirm that in the absence of MDA5 (KO mice), these same myeloid cells that have vaccine mRNA lack these innate immune response modules? Or could this response be due to an adjuvanting effect of the LNP, and the viral RNA is a surrogate for cells that bound and internalized the vaccine.

Minor Comments

1. Statistical analysis. While most of the statistical analysis was done correctly, a few panels need updates. Fig 3c-d – as these are representative experiments, the statistical analysis should be removed. Alternatively, the data can be pooled, and analysis performed as was done elsewhere; Fig 3e needs some type of ANOVA to account for multiple data points; Fig 5b – does this need an ANOVA?

2. Throughout the paper, the authors show their flow cytometry as percentages of a given total. The authors should add [especially Fig 1, 2, 5e, 7a-b, 7g, S1, and S5-S9) the absolute number of cells, as percentages can be skewed by other populations.

3. Line 111-112. Is it surprising that the GC B response in the dLN drops off so quickly relative to that seen in humans (Turner et al., 2021)? Did they examine this at later time points either during primary or secondary responses? Did the authors considering measuring long-lived bone marrow derived plasma cells?

4. Fig 3a and elsewhere – did the authors look at other markers of activation (class II MHC, CD80, CD69)?

5. For consistency, consider using CXC nomenclature throughout for chemokines.

6. In several places, data is referred to as not shown – either show the data or delete the reference to it. Also, a paper in revision is referred to (line 171). Can this be posted online on a pre-print server if it is not yet accepted?

7. Fig 4f and S3d. The authors show the transcript differences as scaled values. How do these correlate with actual transcript levels – it is not clear. Also, how do these differences compare with earlier human mRNA vaccine studies.

8. Fig 5a. There was a broad range in serum IFNγ levels at day 22. Did these correlate in any way with the magnitude of the boosted B or T cell response?

9. Line 244-245 and Fig 6c. Could the cells have migrated due to chemokine gradients even if they did not have vaccine mRNA?

10. Lines 303-304. How do the experiments with Batf3-/- mice (which lack cDC1s and

presumably are deficient in antigen cross-presentation) support the conclusions about innate (IFN) immunity and CD8+ T cell responses? Why are there reduced antibody titers in these mice?

11. Fig 7a. The FACS data in lung shows 6.66% in panel A for Mda5-/- mice. The adjacent graph has all values below 3% -- how can this be?

12. Fig 7d. Did the authors check serum levels of IFNγ as well in Mda5-/- mice? If low, does it affect their interpretation?

13. Line 513. The authors' state that remnant BNT162b2 vaccine material was used for the study. Do they have IRB or manufacturer's approval given that the material was not available for direct purchase when the studies were conducted? Was the remnant clinical material provided under any type of clinical or research agreement or label license? This informations should be clearly stated in the Methods.

14. Fig S10 should be cited in the text.

LITERATURE CITED.

Alameh, M.-G., Tombácz, I., Bettini, E., Lederer, K., Sittplangkoon, C., Wilmore, J.R., Gaudette, B.T., Soliman, O.Y., Pine, M., Hicks, P., et al. (2021) Lipid nanoparticles enhance the efficacy of mRNA and protein subunit vaccines by inducing robust T follicular helper cell and humoral responses. Immunity.

Arunachalam, P.S., Scott, M.K.D., Hagan, T., Li, C., Feng, Y., Wimmers, F., Grigoryan, L., Trisal, M., Edara, V.V., Lai, L., et al. (2021). Systems vaccinology of the BNT162b2 mRNA vaccine in humans. Nature 596, 410-416.

Kolumam, G.A., Thomas, S., Thompson, L.J., Sprent, J., and Murali-Krishna, K. (2005). Type I interferons act directly on CD8 T cells to allow clonal expansion and memory formation in response to viral infection. J Exp Med 202, 637-650.

Turner, J.S., O'Halloran, J.A., Kalaidina, E., Kim, W., Schmitz, A.J., Zhou, J.Q., Lei, T., Thapa, M., Chen, R.E., Case, J.B., et al. (2021). SARS-CoV-2 mRNA vaccines induce persistent human germinal centre responses. Nature 596, 109-113.

Wang, Y., Cella, M., Gilfillan, S., and Colonna, M. (2010). Cutting edge: polyinosinic:polycytidylic acid boosts the generation of memory CD8 T cells through melanoma differentiation-associated protein 5 expressed in stromal cells. J Immunol 184, 2751-2755.

Welsh, R.M., Bahl, K., Marshall, H.D., and Urban, S.L. (2012). Type 1 interferons and antiviral CD8 T-cell responses. PLoS Pathog 8, e1002352.

Author Rebuttal to Initial comments

We thank both reviewers for their helpful comments. Below, we provide a point-by-point response to their comments.

Reviewer #1

(Remarks to the Author)
Chunfeng Li and colleagues performed an extensive analysis of the mechanisms of innate and adaptive immunity to the Pfizer-biontech BNT162b2 vaccine. They combined various techniques including flow cytometry, measurement of chemokines and cytokines, viral neutralization tests, single cell transcriptomic analysis, use of KO mice lacking various immune sensors, to provide a large overview of the impact of the Pfizer vaccine on the activation and role of the main immune cell subsets. It is shown that induction of antibody and T cell responses to BNT162b2 was not dependent on signaling via TLRs 2, 3 ,4 ,5, inflammasome activation, necroptosis or pyroptosis. CD8 T cell responses are shown to be dependent on type I IFN-dependent MDA5 signaling. This is an excellent work with important information regarding the function of mRNA-based vaccines.

We thank the reviewer for their encouraging comments.

Main concerns

1. Vaccine dose. The authors used a dose of 5 µg per mouse. In humans, the vaccine dose is 30 µg. A mouse weights approximatively 20 g and a human weights 60 kg. The authors thus injected in their mice about 500 times more mRNA/kg than the vaccine dose in humans. This high concentration may generate innate and inflammatory responses that are not relevant to humans. Did the authors try lower doses of vaccine? This should be tested or at least discussed as a limitation of the study.

Yes, we did use lower doses (up to 0.2 µg/mouse) of the vaccine, which is human-equivalent dose of mRNA vaccine in mice based on body weight[1, 2]. We had included some of these data in the original manuscript (**Fig. S1a-e in our revised manuscript**). Additionally, we have now included the cytokine responses in mice immunized with 0.2 µg (**Fig. S1f in our revised manuscript**) and described the results in pages 4-5 of the revised manuscript (yellow highlights). In summary, with the lower dose of vaccine certain key elements of the response (e.g. enhanced antigen specific T cells and Abs following secondary vaccination) are similar, but other elements (e.g. enhanced IFNγ in sera) are less obvious than with the high dose.

2. No viral challenge was performed in the different KO mice. This should be discussed as another limitation of the study. Some SARs-CoV-2 variants (beta and gamma variants for instance) have been shown to naturally infect mice, without the need of expressing the human ACE2 receptor, which may facilitate the use of various KO mice in future studies. Other teams have performed similar but less extensive studies in mice which included viral challenge. For instance, Iwasaki's team recently studied the adaptive immune determinants of viral clearance and protection in mouse models of SARS-CoV-2 (Science immunology). It is interesting to see that in this recent article, the vaccine dose was only 1 µg.

The recent literature should be discussed.
We discussed this and cited the relevant reference (first paragraph of page 12 in the revised manuscript).

Reviewer #2

(Remarks to the Author)
Review of Li et al

This paper from the Pulendran laboratory follows their elegant systems-based studies over the past several years evaluating the immunological correlates of responses against influenza, SARS-CoV-2, and yellow fever vaccines or viral infections. Their recent study of human responses to BNT162b2 published in Nature showed that booster vaccination stimulated an enhanced innate immune response as compared to primary vaccination, with a greater frequency of CD14+CD16+ inflammatory monocytes, a higher concentration of plasma IFNγ, and a transcripstional signature of innate antiviral immunity. In the current study, they performed analogous immunization studies in mice with the same (remnant) vaccine to determine the mechanistic basis for these observations as well as to evaluate immune responses in key tissues (e.g., draining lymph node [dLN], spleen, and lung). In addition to showing robust B and T cell responses (which has been seen by others), they report several potentially interesting observations: (a) high levels of antigen-specific CD8+ T cells in the lung after intramuscular boosting that appear dependent on MDA5 and type I IFN signaling; (b) rapid activation of specific myeloid cell subsets, some which contain vaccine mRNA in the dLN at early time points; (c) enhanced early serum cytokine/chemokine responses including IFNγ, which was important for innate immune cell activation; and (d) the unanticipated dispensability of many pathogen sensors (TLRs, NLR, etc.) for vaccine-mediated induction of B and T cell responses. The authors conclude that their study provides new insights into how BNT162b2 stimulates immune responses in vivo.

There are many strengths to this paper including the important question it addresses, the generally high-quality data, the clarity in writing, the rigor of design, the concordance of some of the findings (IFNγ induction and transcriptional patterns of activation of myeloid cell subsets) with published human studies, the analysis of multiple tissues, and the remarkable attempt to identify a key sensor that sets of the inflammatory process. Notwithstanding this, and despite a large body of careful work, there are some weaknesses (detailed below) that must be addressed to provide greater mechanistic clarity. For example, despite finding elevated levels of IFNγ in mice and humans, and showing it modulates myeloid cell activation, the impact of this cytokine on primary or secondary B and T cell responses was never tested. Moreover, the potential impact of MDA5 and type I IFN signaling on survival of memory CD8+ T cells has been largely passed over, which could affect their conclusion regarding the innate impact of these molecules/pathway on anamnestic CD8+ T cell responses after BNT162b2 boosting. The mouse studies were performed to provide new mechanistic insight as to why BNT162b2 induces such robust adaptive immunity. Beyond showing that the vaccine rapidly activates innate immune myeloid cells, which they already demonstrated in humans (Arunachalam et al., 2021), the main novel mechanistic take-aways require further delineation.

We are grateful for the reviewer's insightful and constructive suggestions and have tried our very best to address all her/his comments.

Major Comments

1. IFNγ and lack of direct linkage to B and T cell phenotypes. (a) In their recent analysis of mRNA vaccine responses in humans, the same authors showed that BNT162b2 induced a much greater innate immune response after boosting than after primary vaccination, and this was associated with increased plasma levels of IFNγ, enhanced transcriptional signatures of innate immunity, and antiviral immunity in myeloid cells (Arunachalam et al., 2021). In the current mouse paper, the authors demonstrate a similar augmented IFNγ response occurs soon after boosting (Fig 5a), determine which cells produce it (NK/T), and link this to activation (CD86 expression) of myeloid cells. However, a key advantage of performing studies in mice is the ability to test the significance of the IFNγ response for adaptive B and T cell responses. The authors should use their neutralizing anti-IFNγ antibody to test the functional impact of IFNγ on the primary or secondary B and T cell responses induced by BNT162b2. If there were no major impact, what is the significance of the IFNγ induction beyond myeloid cell activation?

Thank you for raising this important point. To-address this issue, we measured T cell and antibody responses in BNT162b2-immunized mice after IFNγ blockade as the reviewer suggested. We administered mice with a neutralizing anti-IFNγ receptor antibody on days 19-21 prior to boosting, and measured spike-specific T cell and antibody responses on day 42. We found that the antigen-specific CD4 and CD8 T cell responses did not differ significantly in the lung; nor was a there a difference in antibody response (**Fig. 1 for reviewer**). However, there was a ~2-fold reduction in the spike-specific CD8 T cells producing IFNγ in the spleen (**Fig. 1a for reviewer**). Thus, blockade of IFNγ activity does not appear to have a major impact on the generation of antigen specific CD8 T cells producing IFNγ. However, whether it does affect the generation of CD8 T cell memory etc remains to be studied. Thus, the major impact of the heightened IFNγ following secondary immunization appears to be on enhanced innate antiviral immunity during the first few days or weeks of vaccination, a period during which antigen specific T and B cell responses are still being generated. In line with this concept, we (**Wimmers et al. Cell 2021**) recently showed that vaccination with H5N1+AS03 induces epigenetic changes in monocytes and myeloid DCs associated with enhanced IRF accessibility and heightened resistance to infection with unrelated blood-borne viruses, such as dengue virus and Zika virus[3]. It is therefore conceivable that a similar mechanism caused by the enhanced production of early IFNγ leads to a heightened capacity to resist viral infection for a period before the T- and B-cell mediated mechanisms kick in. We have

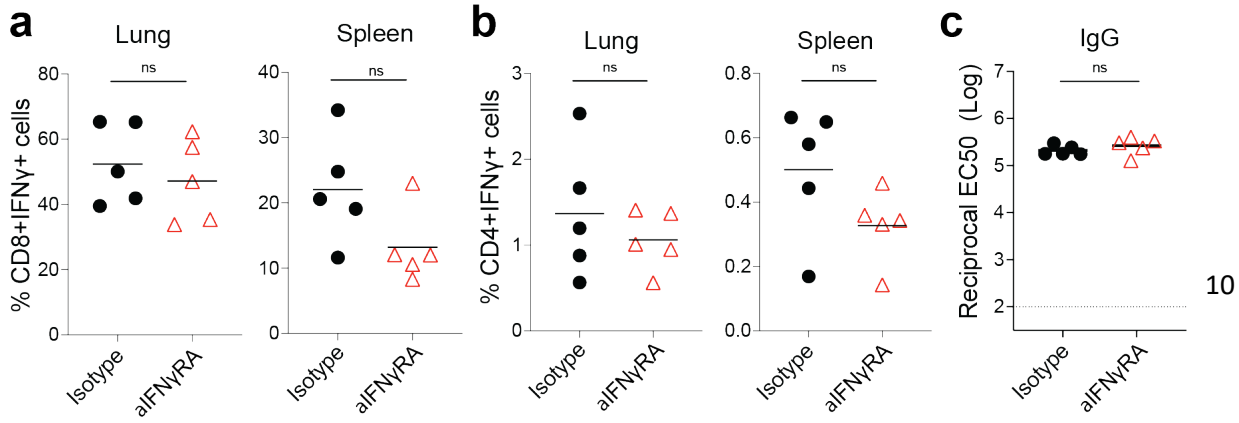


Figure 1 for reviewer. CD8+ and CD4+ T cell responses, and IgG titer at day 42 after blocking of IFNγ receptor. Mice were treated with IFNγ receptor neutralizing antibody or isotype control before boost at day 21. P-values were determined using Student's t-tests (two-tailed).

discussed in the revised text (Page 11).

(b) While they show in Fig 5e clearly that both NK and T cells are sources of IFNγ, it is not clear which is more important for the increased innate immune response seen after boosting – given that NK produced IFNγ is present in both primary and secondary responses, it would seem that T cell-derived IFNγ mediates this – could immune cell depletion studies confirm this?

We depleted NK or T cells (CD4 and CD8 T cells) prior to booster immunization using NK1.1 or CD4/CD8 depletion antibodies. Depletion of T cells, but not NK cells abrogated serum IFNγ on day 22 (**Figure 2a for reviewer; also Fig. S4c, in the revised manuscript**), 1 day after the boost demonstrating that the CD4 and CD8 T cells were the primary source of circulating IFNγ as the reviewer speculated. Consistent with this, the activation of innate immune cells measured by CD86 MFI was more substantially reduced in T cell-depleted mice compare to that in the naïve mice or mice depleted of NK cells. (**Figure 2b for reviewer; Fig. S4d in revised manuscript**).

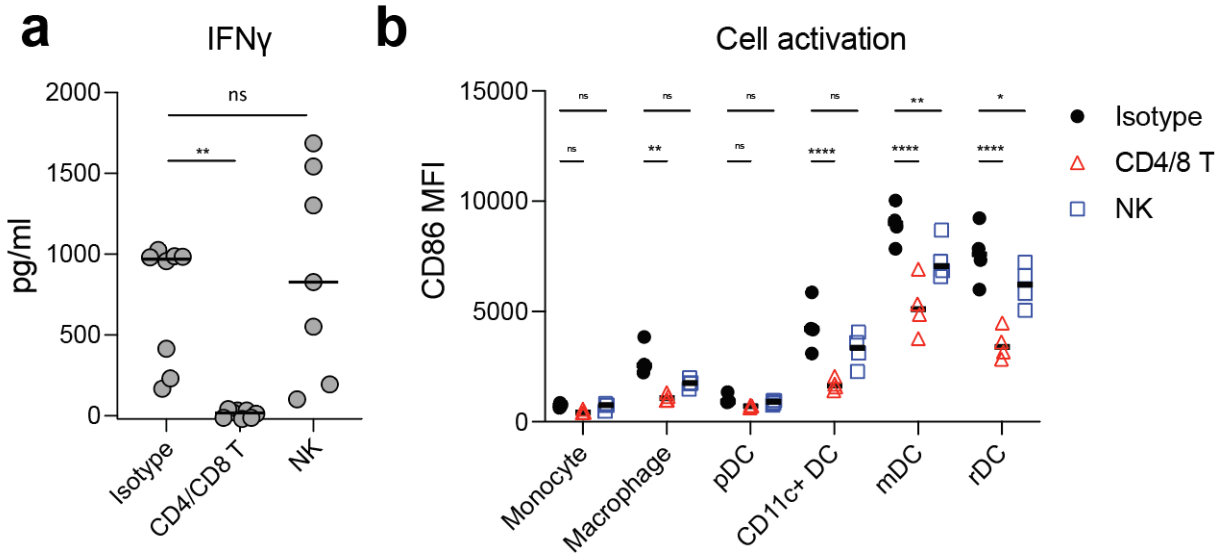


Figure 2 for reviewer. a, Serum IFNγ level at day 22 (1 day after boost) after T cells (CD4 and CD8 T cells) or NK cells depletion. b, Innate cell activation in spleen at 1 day post boost after T cells or NK cells depletion. P-values were determined using One-Way ANOVA (a), or Two-way ANOVA (b). *p<0.05, **p<0.01, ***p<0.001, ****p<0.0001.

2. MDA5 and type IFN and known effects on memory CD8+ T cells. A key finding in this paper is that the secondary CD8+ T cell response after boosting with BNT162b2 is dependent on MDA5 and type I IFN (Fig 7). The authors imply this is related to data in Fig 6 where they show that within a day of immunization, vaccine mRNA is present in macrophage and DC subsets in the dLN and associated with a type I IFN/MDA5/ISG response (Fig 6 and S10). There are several issues that confound this conclusion: (a) In Fig 7, the authors examine the CD8+ T cell response at day 42 and not at day 21 (as in Fig 2a); based on their hypothesis and data in Fig 7d showing low IFNa levels within one day of primary immunization in Mda5-/- mice, shouldn't primary CD8+ T cell responses be affected? (b) The data on anamnestic response is problematic because of reported effects of both MDA5 and type I IFN on memory CD8+ T cell responses (Welsh et al., 2012). The Colonna laboratory showed that in mice lacking MDA5, the majority of CD8+ T cells do not survive after primary immunization with poly I:C and antigen, impairing memory response to subsequent Ag challenge (Wang et al., 2010) [not cited]. Similarly, Murali-Krishna showed a lack of direct CD8+ T cell contact with type I IFN abrogates the generation memory cells due to poor survival during the antigen-driven proliferation phase (Kolumam et al., 2005) [cited]. Thus, the poor anamnestic CD8+ T cell responses seen after BNT162b2 boosting could be due to poor survival of memory CD8+ T cells rather than the observed defects in innate immune activation. To address this issue, the authors need to examine the CD8+ T cell response (including memory cells) at day 21 and prior to boosting in Mda5-/- mice. If the induction of memory is compromised, how does this affect their mechanistic interpretation?

Thanks for this insightful question. As suggested by the reviewer, we measured CD8 T cells after primary vaccination in MDA5-/- mice to demonstrate this experimentally. As indicated in **Figure 3 for reviewer (Figure S9 in the revised manuscript)**, indeed we observed a significant reduction in the antigen-specific CD8 T cell response after primary immunization. There was ~3-fold reduction in both tetramer+ T cell and IFNγ producing CD8 T cell frequencies, respectively, on day 7 after immunization. By day 21, the responses declined to near baseline levels in both groups. The assay is not sensitive enough to pick up a difference at that time point; however, we cannot exclude the possibility of impaired generation of memory CD8 T cells in MDA5-/- mice. This data is now included in the paper. Our interpretation of this data is as follows:

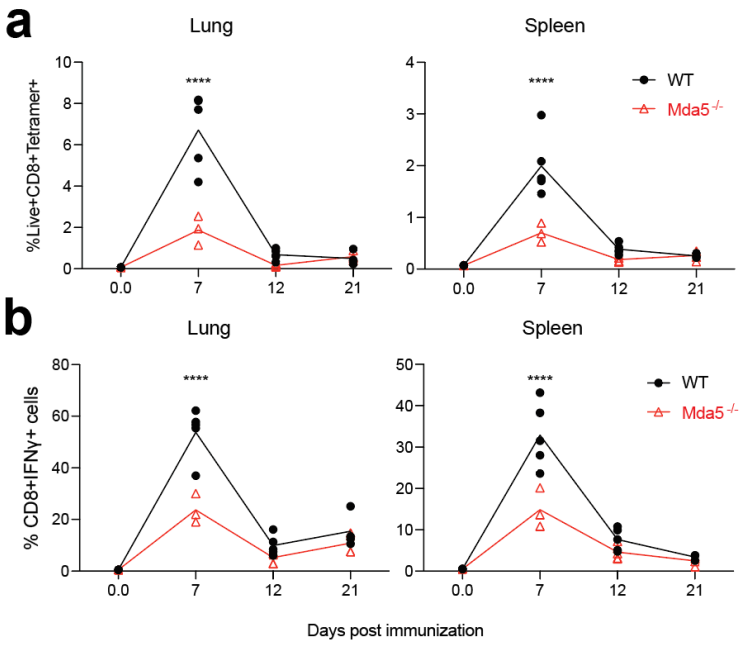


Figure 3 for reviewer. Role of MDA5 in BNT162b2-induced T cell response after prime. a-b, CD8+ T cell response in WT and Mda5$^{-/-}$ mice after prime. P-values were determined using two-way ANOVA followed by Tukey's test. ****p<0.0001.

1. MDA5 deficiency results in impaired IFNα response to BNT162b2 immunization.
2. The IFNα deficiency results in a significantly reduced clonal expansion of antigen-specific CD8 T cells

after primary immunization, which could potentially result in reduced precursor frequencies and functional capacity of antigen-specific memory T cells.

3. Following secondary vaccination, the clonal expansion of antigen specific CD8 T cells is substantially reduced because of (i) an abrogated type I interferon response, and (ii) a reduced memory T cell frequency.

These results are consistent with the results in the papers cited by the reviewer. Wang et al. showed that MDA5 deficiency resulted in a modest impairment in antigen-specific CD8 T cell response following OVA + polyI:C immunization at day 7[4]; however, there was a more pronounced defect in the antigen-specific CD8 T cell response following secondary immunization. This is consistent with the data reported in the present paper, but the more modest effect on the primary immune response observed by Wang et al may be related to differences in how poly I:C (which is a ligand for both TLR3 and MDA5) is sensed by the innate immune system, in contrast to BNT162b2 which clearly does not depend on TLR3 for its immunogenicity (**Fig. S5b-c in our revised manuscript**). Furthermore, our data is consistent with the results reported by Kolumam et al. 2005 who demonstrate that type I IFN acts directly on CD8 T cells to allow clonal expansion[5]. Consistent with this, IFNAR-/- mice show the same phenotype as MDA5-/- mice in our study showing that BNT162b2 targets the MDA5-IFNα-IFNAR axis to stimulate CD8 T cell responses. We have discussed this issue on **Page10.**

3. B cell response analysis. In Fig 1, the authors provide a reasonably detailed analysis of B cell response generated by the BNT162b2 vaccine including spike-binding antibodies, functional neutralization, and flow-based analysis of cellular subsets. However, in their mechanistic studies with KO animals in Fig 7, S5, S6, S7, S8, and S9, they only perform spike-binding IgG assays. It is possible that binding is not the entire story, and differences in neutralizing titers or GC B reactions might occur in the absence of particular innate immune molecules. Indeed recent papers suggesting the LNP component itself is immunostimulatory and relies on IL-6 (and not on MAVS or MyD88) (Alameh et al.), which is induced soon after BNT162b2 immunization (Fig 3e).

We agree that there are other aspects of B cell responses including but not limited to GC formation, GC longevity, the number of GC centroblasts, the number of GC centrocytes, somatic hypermutation, etc. that could be impaired in some of these mice. While we can delineate the effect of innate signaling on each of these parameters using various KO animals we used in our study, what matters the most eventually is the magnitude of binding and neutralizing antibodies. More importantly, our goal in these series of experiments was to determine the primary innate sensor of the magnitude of BNT162b2-induced antibody responses. Therefore, we measured, in addition to binding antibodies, the neutralization antibody titers in Tlr3-/-, Tlr7-/-, and Mda5-/- mice. There was a very modest reduction of nAb in these mice, consistent with the data on the binding antibody titers. We have included these results in the revised manuscript (**Figure 4-5 for reviewer; Fig. S5a, right panel; Fig. 7b in the revised manuscript**).

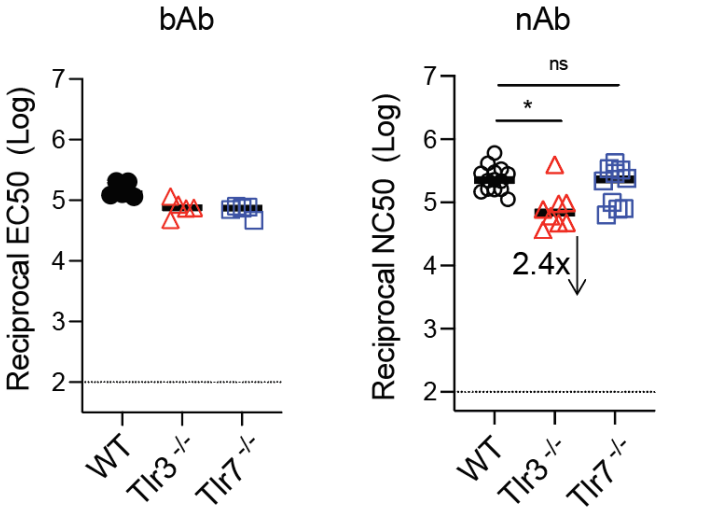


Figure 4 for reviewer. Binding antibody and neutralizing antibody titers of WT and Tlr3-/-, Tlr7-/- mice at day 42. One-Way ANOVA followed by Tukey's test was applied. *p<0.05.

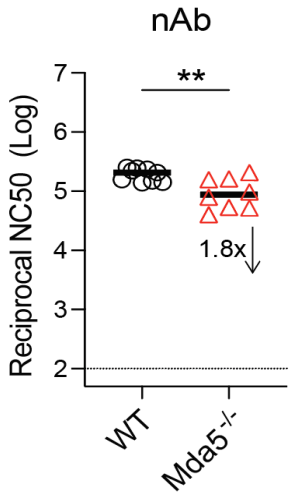


Figure 5 for reviewer. Neutralizing antibody titers of WT and Mda5-/- mice at day 42. P-values was determined using Student's t-tests (two-tailed). **p<0.01.

Lung antigen-specific CD8+ T cells after vaccination. It is remarkable that 21 days after an intramuscular boost with BNT162b2, >60% of the lung CD8+ T cells show antigen-specificity as judged by IFNγ production (Fig 2b), especially given a complete absence of resident memory T cells (Fig 2d). How do the authors explain this observation? Did they perfuse the lung tissue extensively to remove circulating cells? Is this unique to the mRNA vaccination platform? Why are there greater frequencies that in lymphoid tissues even though presumably there is no antigen or inflammation driving them there? What about another parenchymal tissue (e.g., liver or kidney)? The authors make a comment about this in the Discussion (lines 311-312) but provide no additional explanation or supporting data from the literature. Is anything similar seen in humans or NHPs?

We are surprised (as the reviewer is) with the high magnitude of Ag specific T cells in the lung. However, this is not unique to mRNA vaccine since we have previously observed higher magnitude of T cell

response in lung than that in spleen with MF59 and Addavax adjuvanted vaccines[6], and with the yellow fever vaccine YF-17D[7] and we cited these papers and discussed in the revised manuscript (last paragraph of Page 10). The detailed mechanism underlying this observation needs to be further studied.

The reviewer asks whether we perfuse the lung extensively to remove circulating cells. We did do this.

5. In Fig 6f and S10, the authors suggest that the spike mRNA is associated with MDA5-dependent innate immune cell activation and innate immune response-related transcriptional modules. What would MDA5 be recognizing? – presumably double stranded elements of the spike mRNA?

mRNA is known to spontaneously form dsRNA structures, and it is likely that this is what is being recognized by MDA5[8]. We have discussed this in the text (first paragraph of Page 12).

Can the authors confirm that in the absence of MDA5 (KO mice), these same myeloid cells that have vaccine mRNA lack these innate immune response modules? Or could this response be due to an adjuvanting effect of the LNP, and the viral RNA is a surrogate for cells that bound and internalized the vaccine.

These are interesting questions. However, addressing these experimentally will take a considerable amount of time, and we feel that it is beyond the scope of this paper.

MinorComments

1. Statistical analysis. While most of the statistical analysis was done correctly, a few panels need updates. Fig 3c-d – as these are representative experiments, the statistical analysis should be removed. Alternatively, the data can be pooled, and analysis performed as was done elsewhere; Fig 3e needs some type of ANOVA to account for multiple data points; Fig 5b – does this need an ANOVA? For Fig 3c-d, we think the statistical analysis is appropriate (n=5/group). Even though this figure represents the data from one representative experiment, we did have 5 mice in the knockout group and 5 mice in the control group. Therefore showing statistical significance between the two groups, each containing 5 mice, is entirely consistent with standard statistical practice.

We changed to one-way ANOVA for **Fig. 3e**. For **Fig. 5b**, we only compared the difference between day 1 and day 22. The *t* test is appropriate for this comparison.

2. Throughout the paper, the authors show their flow cytometry as percentages of a given total. The authors should add [especially Fig 1, 2, 5e, 7a-b, 7g, S1, and S5-S9) the absolute number of cells, as percentages can be skewed by other populations.

The total number of GC B cells and TFH cells (**Figure 6 for reviewer**) correlated with proportion (**Fig. 1d-f in revised manuscript**). For the T cell responses presented in the rest of the figures, presenting data as a % of total CD4 or CD8 T cells is a common practice[9, 10]. Due to limitations in space, we would not include these data in the manuscript.

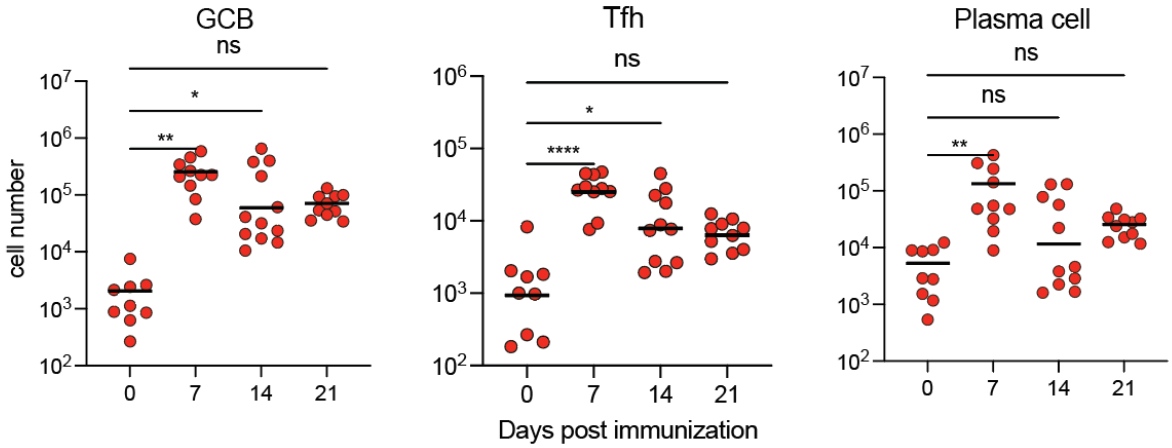


Figure 6 for reviewer. The cell numbers of GCB, TFH, and plasma cells after mRNA vaccination in draining lymph nodes. One-Way ANOVA followed by Tukey's test was applied. *p<0.05, **p<0.01, ****p<0.0001.

3. Line 111-112. Is it surprising that the GC B response in the dLN drops off so quickly relative to that seen in humans (Turner et al., 2021)? Did they examine this at later time points either during primary or secondary responses? Did the authors considering measuring long-lived bone marrow derived plasma cells?

Durability of GC responses and LLPCs (long lived plasma cells) is a key issue, but beyond the scope of

this already very extensive study (**7 multipart main figures with up to 8 sub-figures, and 11 multipart supplementary figures)**!

4. Fig 3a and elsewhere – did the authors look at other markers of activation (class II MHC, CD80, CD69)?
No, we did not look at other activation markers.

5. For consistency, consider using CXC nomenclature throughout for chemokines.

Thanks, we corrected this point.

6. In several places, data is referred to as not shown – either show the data or delete the reference to it. Also, a paper in revision is referred to (line 171). Can this be posted online on a pre-print server if it is not yet accepted?

We addressed this by adding new Luminex data from low dose (**Figure 7 for reviewer. Also Fig. S1f in the revised manuscript**). We removed the sentence "HEK293 reporter cells expressing these receptors also caused no activation of the reporter gene (data not shown).", since it does not affect other conclusions. The manuscript by Lee et al. is provisionally accepted in Nature Communication and will be online soon. We will update the citation as soon as it is online.

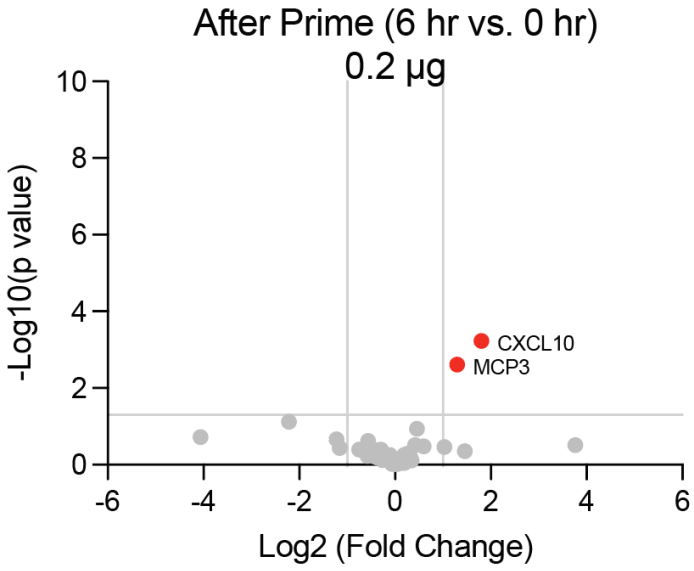


Figure 7 for reviewer. Cytokines/chemokines produced at 6 h post prime with low (0.2 µg/mouse) dose detected by Luminex assay. P-values was determined using Student's t-tests (two-tailed). The difference was significant if $p<0.05$.

7. Fig 4f and S3d. The authors show the transcript differences as scaled values. How do these correlate with actual transcript levels – it is not clear. Also, how do these differences compare with earlier human mRNA vaccine studies.

Many thanks for the question. We scaled the expression values in order to weight each gene equally in the clustering analysis. The scaled value is calculated by first centering each gene across all samples by subtracting the mean of the gene from each sample. The centered gene values are then scaled by taking the root-mean-square:

$$RSM = \sqrt{\sum_{m=1}^{N} \frac{x_m^2}{N}}$$

Where x_m is the mean-centered value of the gene for each sample and N is the number of samples.

Scaling has the advantages of (1) treating all genes equally when hierarchically clustering, as they are now on equivalent scales and (2) enabling easy visualization when plotting. A heatmap of unscaled, normalized transcript values results in a heatmap in which it is difficult to compare across genes and samples due to differences in transcript number between genes (**Figure 8 for reviewer**).

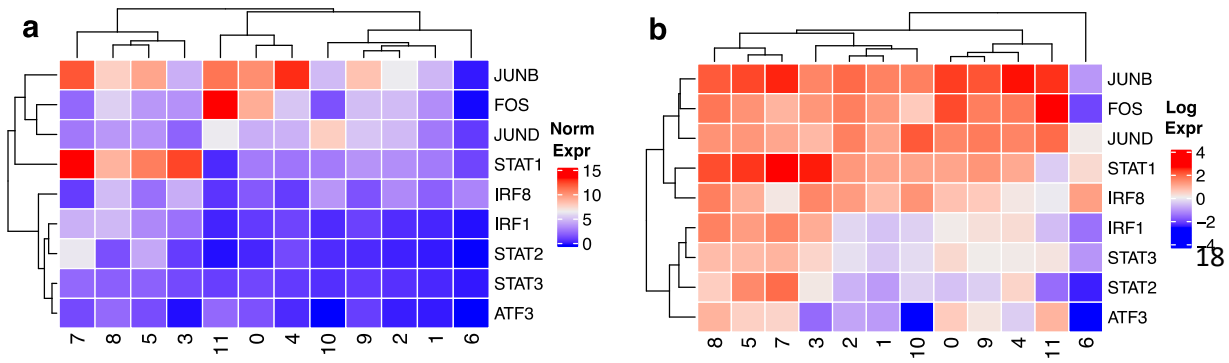


Figure 8 for reviewer. Heatmap of genes in figure 4f of the manuscript. (a) Normalized values of each gene are plotted. (b) Log-normalized values of each gene are plotted. Samples and genes are hierarchically clustered.

Further, as mentioned above, using normalized expression for hierarchical clustering has the distinct disadvantage of more heavily weighting genes that have a higher baseline transcript count. As average transcript count is not a metric of gene importance, this can skew sample clustering.

Using log transformed data is more visually interpretable but has the same clustering disadvantages as normalized expression (**Fig 8b**).

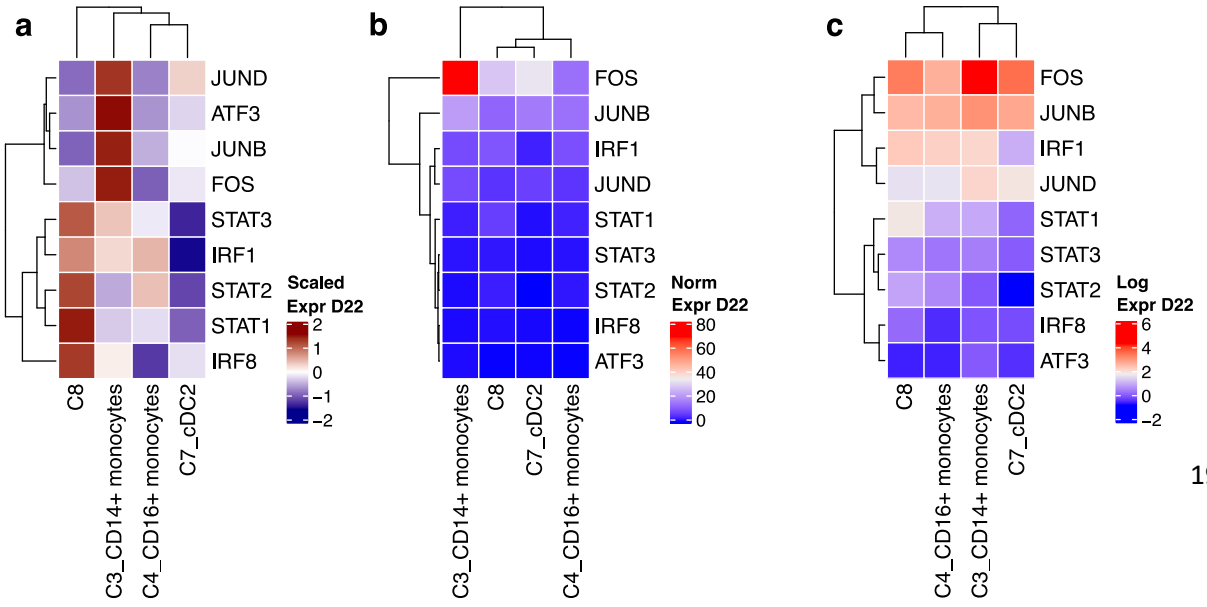


Figure 9 for reviewer. Reproduction of Figure 4g in Arunachalam et al. 2021 (by Pulendran and colleagues) with different scaling techniques. (a) centered and scaled transcript data. (b) normalized transcript data. (c) log transformed normalized data.

It is for these same reasons that we used scaled expression while investigating the effect of the novel BNT162b2 vaccine in human blood (**Figure 9 for reviewer**). Unscaled data is frankly misleading, as it implies connections between cell clusters that are simply due to transcript number and do not reflect true similarity (**Fig 9b,c**). Unscaled data also disempowers the reader from drawing conclusions about which cluster has the highest expression of the gene relative to the other clusters, a more important metric than absolute transcript count comparisons across clusters.

8. Fig 5a. There was a broad range in serum IFNγ levels at day 22. Did these correlate in any way with the magnitude of the boosted B or T cell response?

We did not follow these mice, so we did not do the correlation analysis.

9. Line 244-245 and Fig 6c. Could the cells have migrated due to chemokine gradients even if they did not have vaccine mRNA?

We changed the original statement "The frequency of these cells increased after vaccination (**Fig. 6c**), suggesting that they migrated to the dLNs following mRNA uptake." to "The frequency of these cells increased after vaccination (**Fig. 6c**)".

10. Lines 303-304. How do the experiments with Batf3-/- mice (which lack cDC1s and presumably are deficient in antigen cross-presentation) support the conclusions about innate (IFN) immunity and CD8+ T cell responses? Why are there reduced antibody titers in these mice?

Batf3-/- mice is known to be deficient in resident CD8α+ DCs[11], which are key for cross presentation of antigens to CD8 T cells. The reviewer implies in her question that the observed defect in immune responses in Batf3-/- mice is somehow is at odds with the *"(IFN) immunity and CD8+ T cell responses."* We are not sure why the phenotype in the Batf3-/- mice need to *"support the conclusions about innate (IFN) immunity and CD8+ T cell responses."* All the Batf3-/- data show is that CD8α+ DCs are required for generation of CD8+ T cell responses. All the IFNRα-/- mice data show is that IFNα is needed for the clonal expansion of CD8 T cells. These two events need not be mutually exclusive or contradictory.

As far as the reduction in antibody titers in Batf3-/- mice, this is negligible (<2.0-fold).

11. Fig 7a. The FACS data in lung shows 6.66% in panel A for Mda5-/- mice. The adjacent graph has all values below 3% -- how can this be?

Panel A showed the % of parent gating, panel B showed the % of live class I tetramer+ cells. Data in panel B should be lower than that in panel A.

12. Fig 7d. Did the authors check serum levels of IFNγ as well in Mda5-/- mice? If low, does it affect their interpretation?

Good question. We did not measure IFNγ in MDA5-/- mice. Given that the blockade of IFNγ activity does not appear to have a major impact on the generation of antigen specific CD8 T cells producing IFNγ, (Fig. 1 for reviewer), we believe that the MDA5-IFNα-IFNαR1 is the major signaling axis driving CD8 T cell response.

13. Line 513. The authors' state that remnant BNT162b2 vaccine material was used for the study. Do they have IRB or manufacturer's approval given that the material was not available for direct purchase when the studies were conducted? Was the remnant clinical material provided under any type of clinical or research agreement or label license? This informations should be clearly stated in the Methods.

We added the following information in revised manuscript (Page 17-18). "Discarded remnant material (Pfizer/BioNTech) was used within manufacturer's guidelines for stability at 50 µL of BNT162b2 mRNA vaccine (5 µg/mouse or 0.2 µg/mouse), as described in our previous study [12]. In addition, since this was

not available for purchase and since only remnant (otherwise to be discarded) material could be used at the time (since the product was approved for EUA only), we obtained approval from the Dean of Research at Stanford, Office for General Counsel at Stanford, and the FDA-CBER Vaccines Division)."

14. Fig S10 should be cited in the text.
We revised this.

LITERATURE CITED (From Reviewer#2).

Alameh, M.-G., Tombácz, I., Bettini, E., Lederer, K., Sittplangkoon, C., Wilmore, J.R., Gaudette, B.T., Soliman, O.Y., Pine, M., Hicks, P., et al. (2021) Lipid nanoparticles enhance the efficacy of mRNA and protein subunit vaccines by inducing robust T follicular helper cell and humoral responses. Immunity.

Arunachalam, P.S., Scott, M.K.D., Hagan, T., Li, C., Feng, Y., Wimmers, F., Grigoryan, L., Trisal, M., Edara, V.V., Lai, L., et al. (2021). Systems vaccinology of the BNT162b2 mRNA vaccine in humans. Nature 596, 410-416.

Kolumam, G.A., Thomas, S., Thompson, L.J., Sprent, J., and Murali-Krishna, K. (2005). Type I interferons act directly on CD8 T cells to allow clonal expansion and memory formation in response to viral infection. J Exp Med 202, 637-650.

Turner, J.S., O'Halloran, J.A., Kalaidina, E., Kim, W., Schmitz, A.J., Zhou, J.Q., Lei, T., Thapa, M., Chen, R.E., Case, J.B., et al. (2021). SARS-CoV-2 mRNA vaccines induce persistent human germinal centre responses. Nature 596, 109-113.

Wang, Y., Cella, M., Gilfillan, S., and Colonna, M. (2010). Cutting edge: polyinosinic:polycytidylic acid boosts the generation of memory CD8 T cells through melanoma differentiation-associated protein 5 expressed in stromal cells. J Immunol 184, 2751-2755.

Welsh, R.M., Bahl, K., Marshall, H.D., and Urban, S.L. (2012). Type 1 interferons and antiviral CD8 T-cell responses. PLoS Pathog 8, e1002352.

Reference for response letter:

1. Nair, A.B. & Jacob, S. A simple practice guide for dose conversion between animals and human. *J Basic Clin Pharm* **7**, 27-31 (2016).

2. Buschmann, M.D. *et al.* Nanomaterial Delivery Systems for mRNA Vaccines. *Vaccines (Basel)* **9** (2021).

3. Wimmers, F. *et al.* The single-cell epigenomic and transcriptional landscape of immunity to influenza vaccination. *Cell* **184**, 3915-3935 e3921 (2021).

4. Wang, Y., Cella, M., Gilfillan, S. & Colonna, M. Cutting edge: polyinosinic:polycytidylic acid boosts the generation of memory CD8 T cells through melanoma differentiation-associated protein 5 expressed in stromal cells. *J Immunol* **184**, 2751-2755 (2010).

5. Kolumam, G.A., Thomas, S., Thompson, L.J., Sprent, J. & Murali-Krishna, K. Type I interferons act directly on CD8 T cells to allow clonal expansion and memory formation in response to viral infection. *J Exp Med* **202**, 637-650 (2005).

6. Kim, E.H. *et al.* Squalene emulsion-based vaccine adjuvants stimulate CD8 T cell, but not antibody responses, through a RIPK3-dependent pathway. *Elife* **9** (2020).

7. Ravindran, R. *et al.* The amino acid sensor GCN2 controls gut inflammation by inhibiting inflammasome activation. *Nature* **531**, 523-527 (2016).

8. Wu, B. *et al.* Structural basis for dsRNA recognition, filament formation, and antiviral signal activation by MDA5. *Cell* **152**, 276-289 (2013).

9. Sahin, U. *et al.* COVID-19 vaccine BNT162b1 elicits human antibody and TH1 T cell responses. *Nature* **586**, 594-599 (2020).

10. Wieland, A. *et al.* Defining HPV-specific B cell responses in patients with head and neck cancer. *Nature* **597**, 274-278 (2021).

11. Hildner, K. *et al.* Batf3 deficiency reveals a critical role for CD8alpha+ dendritic cells in cytotoxic T cell immunity. *Science* **322**, 1097-1100 (2008).

12. Warren, C.M. *et al.* Assessment of Allergic and Anaphylactic Reactions to mRNA COVID-19 Vaccines With Confirmatory Testing in a US Regional Health System. *JAMA Netw Open* **4**, e2125524 (2021).

Decision Letter, first revision:

Subject: Your manuscript, NI-A33009A

Message: Our ref: NI-A33009A

20th Jan 2022

Dear Dr. Pulendran,

Thank you for your patience as we've prepared the guidelines for final submission of your Nature Immunology manuscript, "Mechanisms of innate and adaptive immunity to the Pfizer-BioNTech BNT162b2 vaccine" (NI-A33009A). Please carefully follow the step-by-step instructions provided in the attached file, and add a response in each row of the table to indicate the changes that you have made. Please also check and comment on any additional marked-up edits we have proposed within the text. Ensuring that each point is addressed will help to ensure that your revised manuscript can be swiftly handed over to our production team.

We would like to start working on your revised paper, with all of the requested files and forms, as soon as possible (preferably within two weeks). Please get in contact with us if you anticipate delays.

When you upload your final materials, please include a point-by-point response to any remaining reviewer comments and please make sure to upload your checklist.

If you have not done so already, please alert us to any related manuscripts from your group that are under consideration or in press at other journals, or are being written up for submission to other journals (see: https://www.nature.com/nature-research/editorial-policies/plagiarism#policy-on-duplicate-publication for details).

In recognition of the time and expertise our reviewers provide to Nature Immunology's editorial process, we would like to formally acknowledge their contribution to the external peer review of your manuscript entitled "Mechanisms of innate and adaptive immunity to the Pfizer-BioNTech BNT162b2 vaccine". For those reviewers who give their assent, we will be publishing their names alongside the published article.

Nature Immunology offers a Transparent Peer Review option for new original research manuscripts submitted after December 1st, 2019. As part of this initiative, we encourage our authors to support increased transparency into the peer review process by agreeing to have the reviewer comments, author rebuttal letters, and editorial decision letters published as a Supplementary item. When you submit your final files please clearly state in your cover letter whether or not you would like to participate in this initiative. Please note that failure to state your preference will result in delays in accepting your manuscript for publication.

Cover suggestions

As you prepare your final files we encourage you to consider whether you have any images or illustrations that may be appropriate for use on the cover of Nature Immunology.

Covers should be both aesthetically appealing and scientifically relevant, and should be supplied at the best quality available. Due to the prominence of these images, we do not generally select images featuring faces, children, text, graphs, schematic drawings, or collages on our covers.

We accept TIFF, JPEG, PNG or PSD file formats (a layered PSD file would be ideal), and the image should be at least 300ppi resolution (preferably 600-1200 ppi), in CMYK colour mode.

If your image is selected, we may also use it on the journal website as a banner image, and may need to make artistic alterations to fit our journal style.

Please submit your suggestions, clearly labeled, along with your final files. We'll be in touch if more information is needed.

Nature Immunology has now transitioned to a unified Rights Collection system which will allow our Author Services team to quickly and easily collect the rights and permissions required to publish your work. Approximately 10 days after your paper is formally accepted, you will receive an email in providing you with a link to complete the grant of rights. If your paper is eligible for Open Access, our Author Services team will also be in touch regarding any additional information that may be required to arrange payment for your article.

You will not receive your proofs until the publishing agreement has been received through our system.

Please note that Nature Immunology is a Transformative Journal (TJ). Authors may publish their research with us through the traditional subscription access route or make their paper immediately open access through payment of an article-processing charge (APC). Authors will not be required to make a final decision about access to their article until it has been accepted. Find out more about Transformative Journals.

If you have any questions about costs, Open Access requirements, or our legal forms, please contact ASJournals@springernature.com.

<B>Authors may need to take specific actions to achieve compliance with funder and institutional open access mandates. For submissions from January 2021, if your research is supported by a funder that requires immediate open access (e.g. according to Plan S principles) then you should select the gold OA route, and we will direct you to the

compliant route where possible. For authors selecting the subscription publication route our standard licensing terms will need to be accepted, including our self-archiving policies. Those standard licensing terms will supersede any other terms that the author or any third party may assert apply to any version of the manuscript.

Please use the following link for uploading these materials: [REDACTED]

If you have any further questions, please feel free to contact me.

Best regards,

Elle Morris
Senior Editorial Assistant
Nature Immunology
Phone: 212 726 9207
Fax: 212 696 9752
E-mail: immunology@us.nature.com

On behalf of

Nick Bernard, PhD
Senior Editor
Nature Immunology

Reviewer #1:
Remarks to the Author:
the authors have nicely addressed my concerns

Reviewer #2:
Remarks to the Author:
This revised paper from the Pulendran laboratory follows their recent study of human responses to BNT162b2, which showed that booster vaccination stimulated an enhanced innate immune response as compared to primary vaccination, with a greater frequency of inflammatory monocytes, a higher concentration of plasma IFNγ, and a transcriptional signature of innate antiviral immunity. In the current study, they performed analogous immunization studies in mice to determine the mechanistic basis for these observations as well as to evaluate immune responses in key tissues (e.g., draining lymph node [dLN], spleen, and lung). In addition to showing robust B and T cell responses (which has been seen by others), they report several potentially interesting observations: (a) high levels of antigen-specific CD8+ T cells in the lung after intramuscular boosting that appear dependent on MDA5 and type I IFN signaling; (b) rapid activation of specific myeloid cell subsets, some which contain vaccine mRNA in the dLN at early time points; (c) enhanced early serum cytokine/chemokine responses including IFNγ, which was important for innate

immune cell activation; and (d) the unanticipated dispensability of many pathogen sensors (TLRs, NLR, etc.) for vaccine-mediated induction of B and T cell responses.

The revision and rebuttal are well crafted, and this Reviewer appreciated the many new experiments that provide greater clarity and novelty to the paper. Thus, the paper is improved and will be an important contribution to the field. My only remaining issue is that the IFNγ blockade data and effects on vaccine immunity that was provided in the Rebuttal as Reviewer only (Fig 1 for reviewer). I think showing this data (no or small impact on B or T cell responses) as a Supplemental Figure and then discussing its implications and caveats (as they did in the rebuttal) is important and should be added to the current paper.

Author Rebuttal, first revision:

We thank both reviewers for their helpful comments. Below, we provide a point-by-point response to their comments.

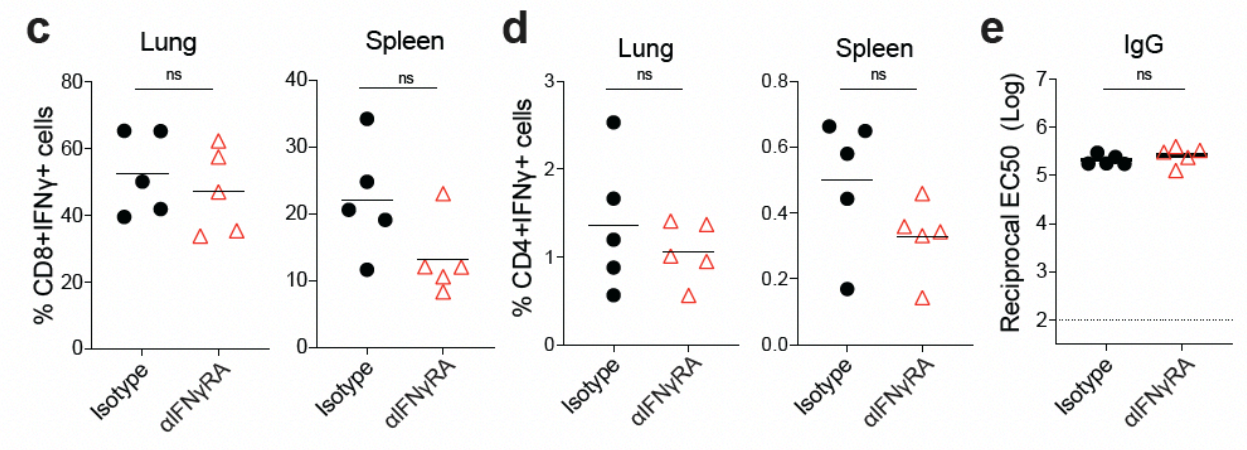
Reviewer #1:
Remarks to the Author:
the authors have nicely addressed my concerns
Thanks for the encouraging comments.

Reviewer #2:
Remarks to the Author:
This revised paper from the Pulendran laboratory follows their recent study of human responses to BNT162b2, which showed that booster vaccination stimulated an enhanced innate immune response as compared to primary vaccination, with a greater frequency of inflammatory monocytes, a higher concentration of plasma IFNγ, and a transcriptional signature of innate antiviral immunity. In the current study, they performed analogous immunization studies in mice to determine the mechanistic basis for these observations as well as to evaluate immune responses in key tissues (e.g., draining lymph node [dLN], spleen, and lung). In addition to showing robust B and T cell responses (which has been seen by others), they report several potentially interesting observations: (a) high levels of antigen-specific CD8+ T cells in the lung after intramuscular boosting that appear dependent on MDA5 and type I IFN signaling; (b) rapid activation of specific myeloid cell subsets, some which contain vaccine mRNA in the dLN at early time points; (c) enhanced early serum cytokine/chemokine responses including IFNγ, which was important for innate immune cell activation; and (d) the unanticipated dispensability of many pathogen sensors (TLRs, NLR, etc.) for vaccine-mediated induction of B and T cell responses.
Thanks for the encouraging comments.

The revision and rebuttal are well crafted, and this Reviewer appreciated the many new experiments that provide greater clarity and novelty to the paper. Thus, the paper is improved and will be an important contribution to the field. My only remaining issue is that the IFNg blockade data and effects on vaccine

immunity that was provided in the Rebuttal as Reviewer only (Fig 1 for reviewer). I think showing this data (no or small impact on B or T cell responses) as a Supplemental Figure and then discussing its implications and caveats (as they did in the rebuttal) is important and should be added to the current paper.

As suggested by the reviewer, we added Fig 1 for reviewer as Extended Data Fig. 4c-e, and discussed the implications in discussion of revised manuscript.



Extended Data Fig. 4c-e. CD8+ and CD4+ T cell responses, and IgG titer at day 42 after blocking of IFNγ receptor. Mice were treated with IFNγ receptor neutralizing antibody or isotype control before boost at day 21. P-values were determined using Student's t-tests (two-tailed).

Final Decision Letter:

Subject: Decision on Nature Immunology submission NI-A33009B

Message: In reply please quote: NI-A33009B

Dear Dr. Pulendran,

I am delighted to accept your manuscript entitled "Mechanisms of innate and adaptive immunity to the Pfizer-BioNTech BNT162b2 vaccine" for publication in an upcoming issue of Nature Immunology.

Over the next few weeks, your paper will be copyedited to ensure that it conforms to Nature Immunology style. Once your paper is typeset, you will receive an email with a link to choose the appropriate publishing options for your paper and our Author Services team will be in touch regarding any additional information that may be required.

After the grant of rights is completed, you will receive a link to your electronic proof via email with a request to make any corrections within 48 hours. If, when you receive your proof, you cannot meet this deadline, please inform us at

rjsproduction@springernature.com immediately.

You will not receive your proofs until the publishing agreement has been received through our system.

Due to the importance of these deadlines, we ask that you please let us know now whether you will be difficult to contact over the next month. If this is the case, we ask you provide us with the contact information (email, phone and fax) of someone who will be able to check the proofs on your behalf, and who will be available to address any last-minute problems.

Acceptance is conditional on the data in the manuscript not being published elsewhere, or announced in the print or electronic media, until the embargo/publication date. These restrictions are not intended to deter you from presenting your data at academic meetings and conferences, but any enquiries from the media about papers not yet scheduled for publication should be referred to us.

Please note that Nature Immunology is a Transformative Journal (TJ). Authors may publish their research with us through the traditional subscription access route or make their paper immediately open access through payment of an article-processing charge (APC). Authors will not be required to make a final decision about access to their article until it has been accepted. Find out more about Transformative Journals.

<B>Authors may need to take specific actions to achieve compliance with funder and institutional open access mandates. For submissions from January 2021, if your research is supported by a funder that requires immediate open access (e.g. according to Plan S principles) then you should select the gold OA route, and we will direct you to the compliant route where possible. For authors selecting the subscription publication route our standard licensing terms will need to be accepted, including our self-archiving policies. Those standard licensing terms will supersede any other terms that the author or any third party may assert apply to any version of the manuscript.

If you have any questions about our publishing options, costs, Open Access requirements, or our legal forms, please contact ASJournals@springernature.com

Your paper will be published online soon after we receive your corrections and will appear in print in the next available issue. Content is published online weekly on Mondays and Thursdays, and the embargo is set at 16:00 London time (GMT)/11:00 am US Eastern time (EST) on the day of publication. Now is the time to inform your Public Relations or Press Office about your paper, as they might be interested in promoting its publication. This will allow them time to prepare an accurate and satisfactory press release. Include your manuscript tracking number (NI-A33009B) and the name of the journal, which they will need when they contact our office.

About one week before your paper is published online, we shall be distributing a press release to news organizations worldwide, which may very well include details of your

work. We are happy for your institution or funding agency to prepare its own press release, but it must mention the embargo date and Nature Immunology. Our Press Office will contact you closer to the time of publication, but if you or your Press Office have any enquiries in the meantime, please contact press@nature.com.

Also, if you have any spectacular or outstanding figures or graphics associated with your manuscript - though not necessarily included with your submission - we'd be delighted to consider them as candidates for our cover. Simply send an electronic version (accompanied by a hard copy) to us with a possible cover caption enclosed.

To assist our authors in disseminating their research to the broader community, our SharedIt initiative provides you with a unique shareable link that will allow anyone (with or without a subscription) to read the published article. Recipients of the link with a subscription will also be able to download and print the PDF.

As soon as your article is published, you will receive an automated email with your shareable link.

You can now use a single sign-on for all your accounts, view the status of all your manuscript submissions and reviews, access usage statistics for your published articles and download a record of your refereeing activity for the Nature journals.

If you have not already done so, we strongly recommend that you upload the step-by-step protocols used in this manuscript to the Protocol Exchange. Protocol Exchange is an open online resource that allows researchers to share their detailed experimental know-how. All uploaded protocols are made freely available, assigned DOIs for ease of citation and fully searchable through nature.com. Protocols can be linked to any publications in which they are used and will be linked to from your article. You can also establish a dedicated page to collect all your lab Protocols. By uploading your Protocols to Protocol Exchange, you are enabling researchers to more readily reproduce or adapt the methodology you use, as well as increasing the visibility of your protocols and papers. Upload your Protocols at www.nature.com/protocolexchange/. Further information can be found at www.nature.com/protocolexchange/about .

Please note that we encourage the authors to self-archive their manuscript (the accepted version before copy editing) in their institutional repository, and in their funders' archives, six months after publication. Nature Research recognizes the efforts of funding bodies to increase access of the research they fund, and strongly encourages authors to participate in such efforts. For information about our editorial policy, including license agreement and author copyright, please visit www.nature.com/ni/about/ed_policies/index.html

An online order form for reprints of your paper is available at https://www.nature.com/reprints/author-reprints.html. Please let your coauthors and your institutions' public affairs office know that they are also welcome to order reprints by this method.

Sincerely,

Nick Bernard, PhD
Senior Editor
Nature Immunology